SUBSTRATE PROFILING OF HUMAN AND YEAST ARGININE METHYLTRANSFERASES USING CHEMICAL TOOLS

by

Michael Louis Langberg

A Dissertation

Presented to the Faculty of the Louis V. Gerstner, Jr.

Graduate School of Biomedical Sciences,

Memorial Sloan Kettering Cancer Center

in Partial Fulfillment of the Requirements for the Degree of

Doctor of Philosophy

New York, NY

February, 2019

_____ _____

Minkui Luo, Ph.D. Date
Dissertation Mentor

Abstract

Protein arginine methylation is a post-translational modification (PTM) that occurs on a similar level in the proteome as better known and studied PTMs such as phosphorylation and glycosylation, but far less is known about the role of arginine methylation in biology. Identification of arginine methylation in proteins is made difficult by the small size and lack of charge on methyl groups, making the development of methylarginine selective antibodies and identification through untargeted mass spectrometry challenging. The Luo group developed a technique known as biorthogonal profiling of protein methylation (BPPM) to bypass these challenges and unambiguously identify methylated proteins and determine which protein arginine methyltransferase (PRMT) is responsible for identified methylation events. BPPM relies on the pairing of semisynthetic PRMT substrate analogues containing clickable handles with PRMT mutants capable of accepting these substrates in an orthogonal manner to native substrates.

This work details the development of BPPM tools for and substrate profiling of two PRMTs in distinct model organisms: the human type II arginine methyltransferase PRMT5 and the yeast type I arginine methyltransferase Hmt1. The active sites of both enzymes were engineered to accept a synthetic analog of the cellular methyl donor SAM and the resulting biorthogonal enzyme-substrate pairs were used to conduct unbiased substrate profiling of both PRMT5 and Hmt1 using quantitative proteomics. These profiling experiments represent the first applications of biorthogonal profiling to a type II PRMT and the first such experiment performed in yeast cells, as well as the most extensive substrate screens ever performed of these two enzymes. In addition to recapitulating many of the known substrates and biological functions of both PRMT5 and

Hmt1, the results of these two profiling experiments suggest previously unknown roles for arginine methylation. Interestingly, regulators of translation initiation were overrepresented in both data sets although PRMTs have not previously been implicated in the regulation of translation. This may represent a previously unknown biological role for arginine methylation that is evolutionarily conserved across eukaryotes.

Contents

List of Tables

List of Figures

Chapter 1: Background and Introduction

1.1 The Importance of Post-Translational Protein Modification in Biology

The discovery of the three-dimensional DNA double helix structure in the 1950s led to the formulation of the central dogma of molecular biology. The central dogma states that DNA serves as a template for transcription into RNA, which is in turn translated by the ribosome into proteins which carry out the necessary functions of life, including DNA replication, and allow for the passage of genetic information from parent to daughter cells and organisms.[1] In its most basic form, the central dogma posits that the heritable base sequence of DNA contains all the necessary information to form fully functional proteins capable of carrying out cellular tasks. However, as the processes of transcription, translation, and the maturation and generation of functional proteins have come to be better understood, researchers discovered that many non-genetically encoded processes are necessary to produce them.

Proteolytic cleavage to generate functional polypeptides, protein folding chaperones, and post-translational modifications, the focus of this work, are examples of the processes that may be required for generation of a functioning polypeptide independent of the proper translation of its nucleotide sequence. Post-translational modifications (PTMs) are covalent, typically enzyme mediated, modifications on amino acids of a protein following its exit from the ribosome. A huge variety of PTMs have been described, such as protein phosphorylation, acylation, glycosylation, and methylation, and an equally large number of functions have been ascribed to these

PTMs.[2–5] Although all of these PTMs perform essential biological functions, the focus of this work will be on protein methylation.

1.2 Protein Methylation

Protein methylation consists of the transfer of a methyl group to a nitrogen atom on the side chain of either a lysine or arginine residue on a protein substrate. A class of enzymes known as protein methyltransferases (PMTs) are responsible for carrying out these reactions in the cell using the small molecule *S*-adenosyl methionine (SAM) as the methyl donor, or cofactor (figure 1).[6–8] Lysine and arginine methylation are carried out by unique classes of enzymes termed lysine methyltransferases (PKMTs) and arginine methyltransferases (PRMTs) respectively, with mutually exclusive activity toward their amino acid substrate of choice. PKMTs are the larger and more well studied of these enzyme families, with approximately 100 PKMTs described in humans. However, this work will focus on PRMTs, a smaller enzyme family with less well-studied functions.

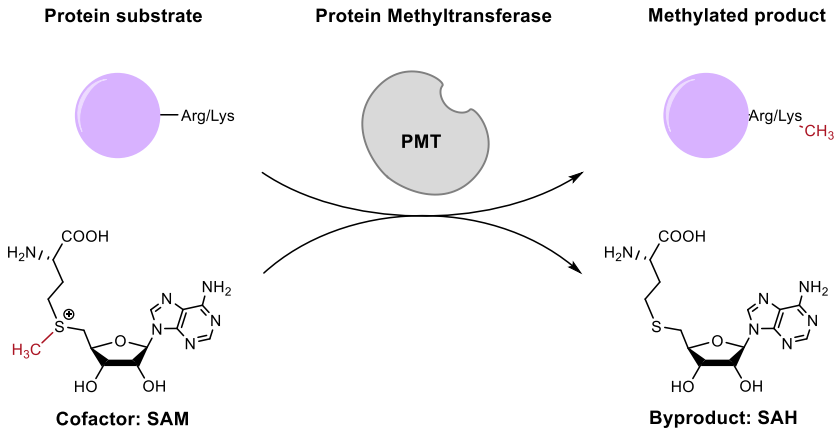

Figure 1: The protein methylation reaction

Protein methyltransferases effect the transfer of a methyl group from a sulfur atom on the cofactor *S*-adenosyl methionine to a nitrogen atom at the end of the side chain of either a lysine or arginine residue on a substrate protein. The products of this reaction are a molecule of *S*-adenosyl homocysteine (SAH) and a methylated protein substrate. A protein arginine methyltransferase is shown placing a methyl group on an arginine residue of a substrate protein in the schematic above.

1.3 PRMTs

There are 9 human PRMTs which can be grouped into 3 types based on their activity: type I PRMTs (PRMTs 1,2,3,4,6, and 8) can generate both monomethyl arginine (MMA) and asymmetric dimethylarginine (ADMA), type II PRMTs (PRMTs 5 and 9) can generate both MMA and symmetric dimethyl arginine (SDMA), while the lone type III PRMT (PRMT7) can generate only MMA (figure 2).[6–8] Notably, MMA and ADMA disrupt the symmetry of the guanidinium group of the arginine sidechain while SDMA preserves the symmetry of an unmethylated arginine sidechain.

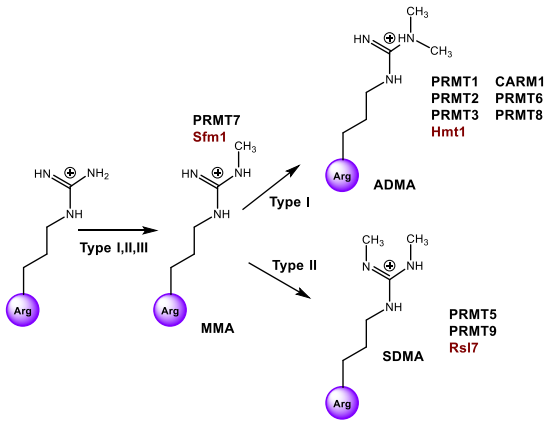

Figure 2: Arginine methylation types and the type I, II, and III arginine methyltransferases

The observed forms of arginine methylation are depicted from unmethylated arginine to mono, symmetric, and asymmetric dimethylarginine. The human

(black text) and *S. cerevisiae* (red text) PRMTs are placed next to the modification that they generate.

Arginine methylation is a common PTM, with at least 0.5% of arginine residues in human cells methylated, representing at least 3300 proteins subject to arginine methylation.[9,10] Despite the prevalence of arginine methylation and a great deal of research interest in its roles, its function is not particularly well-understood.

1.4 Molecular Functions of Arginine Methylation

Arginine commonly serves as a modulator of protein-protein interactions and protein-nucleic acid interactions independent of its methylation state. Arginine is unique in that it is positively charged at cellular pH but also exhibits a planar structure with delocalized π electrons, giving it preferential properties for interaction with nucleic acids. Arginine is capable of forming hydrogen bonds with the phosphoesters of nucleic acid backbones and with bases not involved in watson-crick base pairing. It can also interact with the aromatic rings of bases via cation-π interactions and disrupt π-π stacking through intercalation.[11–13] Given the variety of modes of interaction between arginine and nucleic acids, it is unsurprising that it is overrepresented among residues contributing to protein-nucleic acid interactions, particularly cation-π interactions.[13,14] Because they are positively charged amino acids, arginine residues often reside on the solvent facing surfaces of proteins where it is well positioned to mediate protein-protein interactions. Arginine very commonly participates in cation-π interactions with amino acid side chains containing aromatic rings and it is the most common participant in ionic salt bridges between amino acids.[15–18] Methylation does not significantly alter the physical properties

of arginine when compared to other PTMs such as phosphorylation or acetylation, which are far larger and alter the charge of modified residues. The relatively subtle change makes it difficult to understand the molecular effects of arginine methylation on its interaction with other biomolecules.

On a molecular level, there are two models to describe the potential roles of arginine methylation on protein function: arginine methylation as a signaling mark for recognition by reader domains or arginine methylation at specific residues of a protein directly perturbing protein-protein/protein-nucleic acid interactions.

Methyllysine and methylarginine can be specifically recognized by tudor domain containing proteins, of which there are 36 in humans.[9] The tudor domains functions as readers for methylated lysine and arginine residues using an aromatic cage to recognize methylated residues through cation-π interactions. This aromatic cage recognition is capable of differentiating between methyllysine and methylarginine, with eight known tudor domain containing proteins; SMN, SPF30, TDRD1, TDRD2, TDRD3, TDRD6, TDRD9, and TDRD11 known to interact specifically with methylarginine.[9,19] Of these eight, SMN, SPF30, and TDRD6 specifically recognize SDMA with the other five recognizing MMA or ADMA.[20–22] The existence of an arginine methylation recognition domain supports the model of arginine methylation as a signaling mark which can be recognized by a reader protein, triggering further events such as the assembly of a protein complex or recruitment of other PTM-placing enzymes. This model appears to be correct in the case for SMN, which specifically recognizes SDMA on sm proteins with its tudor domain, recruiting them to begin assembly of the spliceosome.[20,21,23,24]

A model in which a reader domain specifically recognizes methylarginine, distinguishing between SDMA and ADMA, and then recruits appropriate partner proteins to perform its function is easy to generalize across all PRMT substrates to predict and study function. It also suggests a mechanism through which a competition model between SDMA and ADMA might function, as PRMT1 and PRMT5 have been known to modify the same residue on substrate proteins as in the case of H4R3.[25,26] However, the reader model of arginine methylation function is unlikely to apply in all cases as there are 8 known methylarginine interacting tudor proteins and over 3300 arginine methylated proteins in human cells.[9,10] While it is possible that some tudor domains might function as scaffolds to bring different methylarginine containing proteins together with binding partners in a context dependent manner, it is unlikely that the known tudor proteins are able to mediate every possible downstream function of arginine methylation. It is possible that there is an unidentified domain with poor sequence homology that recognizes a larger portion of cellular methylarginine than the tudor proteins, but it is also possible that the functional effect of most arginine methylation events occurs by direct modulation of protein-protein and/or protein-nucleic acid interactions without the assistance of a specific reader domain.

Methylation slightly increases the size and hydrophobicity of arginine and can limit its ability to serve as a hydrogen bond donor but does not change the charge of the side chain or its ability to serve as a hydrogen bond acceptor. This points to relatively subtle roles for arginine methylation in interactions with proteins and nucleic acids. The fact that methylation does not change arginine's charge means that it cannot disrupt existing cation-π interacts or ionic salt bridges, two obvious means by which significant structural

remodeling of proteins or disruption of protein-protein interactions can occur. Disruption of hydrogen bonds is likely the highest energy interaction that can be altered by arginine methylation, although no examples of this phenomenon have been reported in either protein-protein or protein-nucleic acid interactions. The increased hydrophobicity and size of methylated vs unmethylated arginine could increase its ability to form van der Waals interactions with hydrophobic residues and its ability to participate in π-stacking interactions with aromatic amino acid side chains and nucleobases. In fact, the most well-characterized alteration in the physical properties of arginine upon methylation is an increased binding affinity for the aromatic amino acid side chain of tryptophan.[27] This methylarginine-tryptophan interaction forms the aromatic cage that allows tudor domains to specifically recognize methylarginine, and may in fact mediate a number of other methylarginine specific interactions outside of the context of a structured domain detectable by homology.

The differences between arginine and methylarginine are subtle and therefore most of the functional changes arginine methylation can effect on a substrate are likely to be subtle as well. Detection of subtle changes is difficult and outside of tudor domain-mediated protein-protein interactions, few examples of arginine methylation dependent interactions have been described at the molecular level. The molecular role of arginine methylation on protein function remains an open field.

1.5 Roles of Arginine Methylation in Normal Biology and Disease

PRMTs first attracted interest from researchers when it was discovered that arginine methylation of histone tails is capable of regulating transcription.[28] The concept of a "histone code" of combinatorial covalent histone tail modifications capable of

transcriptional regulation and heritable epigenetic changes in chromatin structure led to extensive investigations of the PTMs on histone tails and the enzymes that place them.[29,30] Most human PRMTs methylate histone tails, the only PRMTs that have not been demonstrated to have methyltransferase activity against histone tails on at least one site are PRMT3, PRMT8 and PRMT9.[9] PRMT1 and CARM1 (PRMT4) generally function as transcriptional coactivators while PRMT5 and PRMT6 function as transcriptional repressors. However these roles are not absolute, as PRMT5 and PRMT6 have been reported to activate transcription by methylating H3R2 and H3R42, respectively.[31,32] While PRMTs methylate many non-histone proteins, the bulk of known PRMT biology is attributable to transcriptional regulation through histone tail methylation. PRMTs also methylate thousands of non-histone substrates which perform a variety of cellular roles, perhaps most notably RNA binding and ribosomal component proteins are often found to be heavily methylated.[9,33] The non-histone substrates of the PRMTs studied in this work will be discussed in their respective chapters.

The biological function of PRMTs 1-5 and 7 have been investigated through mouse germline genetic knockouts. PRMT1 and PRMT5 knockouts are both early embryonic lethal, with both enzymes shown to be important for proliferation of embryonic stem cells.[34–36] CARM1 knockout mice survive until birth but die soon afterwards. Interestingly, studies have shown CARM1 to be necessary for pluripotency due to its methylation of histones at the pluripotency factors Sox2, Nanog, and Oct4, making the observation that CARM1 knockout mice complete embryonic development somewhat surprising. [37,38] PRMT7-null mice are viable but suffer delayed embryonic development, early aging, and adult obesity. The latter two of these phenotypes are

caused by premature senescence due to increased levels of the CDK inhibitor p21 in muscle cells where PRMT7 is normally highly expressed.[39] PRMT2-null mice are develop normally and display reduced obesity rates and lower leptin levels compared to WT mice, attributable to alterations in JAK/STAT signaling caused by PRMT2 mediated methylation of STAT3.[40] Similary to PRMT7 knockouts, PRMT3-null mice display delayed embryonic development but reach normal size by birth, attributable to loss of RPS2 methylation.[41]

To gain an understanding of the tissue specific roles of PRMTs in development, tissue specific mouse knockouts have also been generated for many PRMTs, shedding more light on the context-specific roles these enzymes play. Central nervous system-specific PRMT knockouts have shown important roles for multiple PRMT family members. PRMT1, CARM1, PRMT7, and PRMT8 are all required for the development of various neural lineages.[42–45] PRMT5 is required for neural stem cell renewal and survival, rather than a single neural lineage decision. Brain-specific PRMT5 depletion is lethal within two weeks of birth in mice. Interestingly this is due to a loss of splicing fidelity caused by depletion of SDMA on sm proteins rather than transcriptional alteration.[46] These studies clearly demonstrate essential roles for PRMTs during neurodevelopment, although it remains unknown what role they play in adult tissues where they are still expressed.

Multiple bone marrow or hematopoietic stem cell specific PRMT knockouts have been developed, resulting in the discovery of essential roles for multiple PRMTs in immunity and hematopoiesis. PRMT, CARM1, PRMT5, and PRMT7 have all been shown to be necessary for cell proliferation and differentiation in both the erythroid and

lymphoid lineages both through histone methylation to modulate transcription and direct methylation of proteins responsible for cell fate decisions.[47–52] Similar to the case of neurodevelopment, specific PRMTs appear to function as regulators of specific cell states. Since hematopoiesis occurs throughout an organism's lifetime, there is a clear role for PRMTs in the hematopoietic system into adulthood.

In addition to their roles in normal development and tissue function, PRMTs have been implicated in a variety of disease states. PRMTs are commonly upregulated in cancer, most frequently serving as drivers of oncogenesis and tumor growth with the exception of PRMT8, which appears to function as a tumor suppressor in the context of glioblastoma.[7,44,53] PRMTs have also been implicated in multiple neurodegenerative diseases. Mutations in the protein FUS, a highly expressed nucleic acid binding protein important for transcription and RNA export, cause it to aggregate in the cytoplasm and form toxic aggregates in ALS. When PRMT1 is depleted in cells mutant FUS loses the ability to form these toxic aggregates, making PRMT1 a potential drug target for ALS.[54] PRMT5 may function as a negative regulator of amyloid-β induced apoptosis in the context of Alzheimer's disease as well as in the context of Huntington's disease where mutant huntingtin protein reduces PRMT5-mediated SDMA.[55,56] Finally, PRMT6 acts as a positive regulator of a family of neurodegenerative diseases caused by polyglutamine expansion mutations in the androgen receptor (AR) through its role as an AR coactivator. PRMT6's catalytic activity is necessary for its AR coactivator function, making it a potential drug target in this context.[57] As small molecule binding enzymes that appear to largely function as positive regulators of disease states with often poor survival rates, PRMTs are attractive drug targets in the fields of cancer and neurodegenerative disease.

Multiple PRMT inhibitors have been developed and are beginning to make their way into the clinic, primarily as cancer treatments although notably a selective PRMT1 inhibitor has not been reported.[58,59]

Arginine methylation is indispensable for mammalian life, with PRMTs performing a variety of biological roles. Despite its importance and prevalence, arginine methylation is relatively poorly understood. The small size and subtle physical perturbation caused by arginine methylation makes it difficult to detect and study. The inherent difficulty of identifying methylarginine makes it a challenge to define the function of an individual PRMT in terms of its substrates, particularly its non-histone substrates. The next sections focus on innovative chemical biology methods that have been developed to identify novel PRMT substrates

1.6 The Use of Chemical Biology to Study Post-Translational Modifications

Detecting PTMs in an unbiased manner is difficult using the conventional tools of molecular biology and genetics. It is challenging for many reasons, for example: antibodies specific to a PTM often also recognize flanking amino acids which prevents them from being used in unbiased screening experiments, and many enzymes that place PTMs have a large number of substrates and redundancy within enzyme families, which makes mapping a modified substrate to the modifying enzyme a challenge. Tracking PTMs in a cellular context to study their roles and phenotypes is often impossible without high quality reagents capable of differentiating complex modification states or even modified versus unmodified substrates.[60,61]

The shortcomings of biological techniques in identifying and characterizing PTMs has resulted in the development of chemical methods to circumvent the difficulties

encountered when trying to study PTMs. Two such techniques are used in this work: "bump-hole" enzyme engineering and enzyme mediated labeling with biorthogonal chemical reporters.

The "bump-hole" approach to enzyme engineering was developed to study the functions of individual protein kinases before the development of selective kinase inhibitors. Staurosporine, a promiscuous ATP-competitive kinase inhibitor, was modified to include a bulky hydrophobic moiety (the "bump") preventing it from binding to the active sites of wildtype kinases. The active site of a protein kinase of interest was engineered using site directed mutagenesis to convert a bulky hydrophobic residue into a less bulky residue, introducing a "hole" in the enzyme active site which could accommodate the bulky staurosporine derivative.[62] The resulting engineered enzyme-selective inhibitor pair relies on a non-natural enzyme paired with an inhibitor with no natural biological targets resulting in an entirely biorthogonal platform that can be easily translated to any system (figure 3).[63]

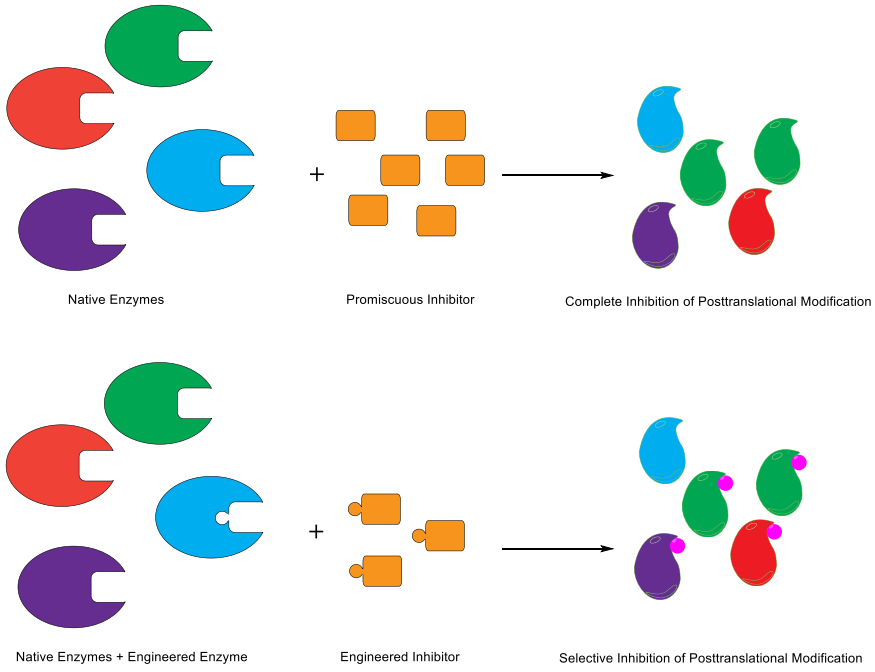

Figure 3: Enzyme engineering using the "bump-hole" approach

To identify the substrates of an enzyme of interest in the absence of a specific inhibitor, one can engineer the active site of the enzyme using site-directed mutagenesis and pair this engineered enzyme with a complementary chemically modified inhibitor. Substituting this engineered enzyme for the native enzyme in a cellular context followed by addition of it complementary inhibitor results in selective depletion of PTMs generated by the enzyme of interest allowing them to be identified and the role of their modification to be interrogated.

The biorthogonal nature of the "bump-hole" approach makes identifying the enzyme responsible for any PTMS found using it trivial and greatly simplifies the development of enzyme-specific tools, but it does not address the inherent difficulty of identifying and tracking PTMs on unknown substrates, which can be achieved using enzyme mediated labeling with biorthogonal chemical reporters. This technique relies on the use of a non-native cofactors which can be used by an enzyme of interest to modify

substrates, yielding a substrate modified by a non-natural PTM which contains some chemical functionality that can be identified and tracked in a cellular context.[64–66] Many trackable moieties, such as fluorescent molecules or short peptides or other biomolecules for which high quality commercially available antibodies exist, are simply too large to fit in the active site of an enzyme of interest even if the site is expanded using enzyme engineering.[64] To circumvent the problem presented by the size of most trackable molecules one can instead install a smaller molecular handle which is not found in the cellular environment and introduce an additional reactant appended to the reporter of interest capable of reacting selectively with each other in a cellular milieu. These reactants must be absent from the normal cellular environment as well as inert to it, recognizing only each other and ignoring all other components of the cellular environment and making the reaction bio-orthogonal. This bio-orthogonal reaction should ideally proceed quickly in an aqueous environment without generating toxic byproducts. Reactions that meet these criteria are commonly known as "click chemistry" reactions.[64,65,67] The copper(I) catalyzed [3+2] cycloaddition between a terminal alkyne and an azide (CUAAC) is a well-characterized and commonly used click reaction that tolerates a wide-variety of substrates and satisfies the criteria of bio-orthogonality, fast kinetics in a cellular environment at temperatures that sustain life, and a lack of toxic byproducts (figure 4).

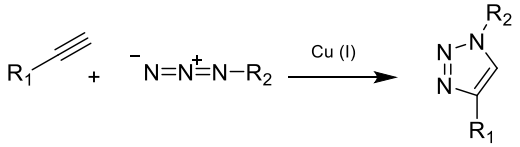

Figure 4: The copper (I) catalyzed alkyne-azide cycloaddition (CUAAC) reaction

The CUAAC reaction results in the formation of a covalent adduct between a terminal alkyne and an azide. This reaction proceeds rapidly in aqueous environments at moderate temperates in the presence of catalytic Cu (I) and displays no cross-reactivity with molecules found in a normal cell environment. These properties make the CUAAC an excellent reaction for conjugation of markers to biomolecules in the context of bio-orthogonal labeling systems.

The CUAAC reaction is an ideal reaction due to its ease of use and the commercial availability of a broad range of both alkyne and azide conjugated tracking and enrichment moieties such as fluorescent molecules, biotin, and high molecular weight PEG groups to detect mass shifts.[67] The small size of both terminal alkynes and azides allows them to be taken up by some native enzymes and, in cases where native enzymes cannot make use of alkyne/azide containing cofactors, their active sites can be readily engineered to become compatible with these functionalities.[66,68] The combination of non-native cofactors containing "clickable" moieties with marker groups containing suitable "clickable" reaction partners allows the substrates of an enzyme of interest to be easily visualized or enriched in an unbiased manner (figure 5). This work exclusively uses the CUAAC to conjugate fluorescent or biotin markers to potential PRMT substrates of interest in order to validate bio-orthogonal systems and identify novel enzyme substrates identified by these systems.

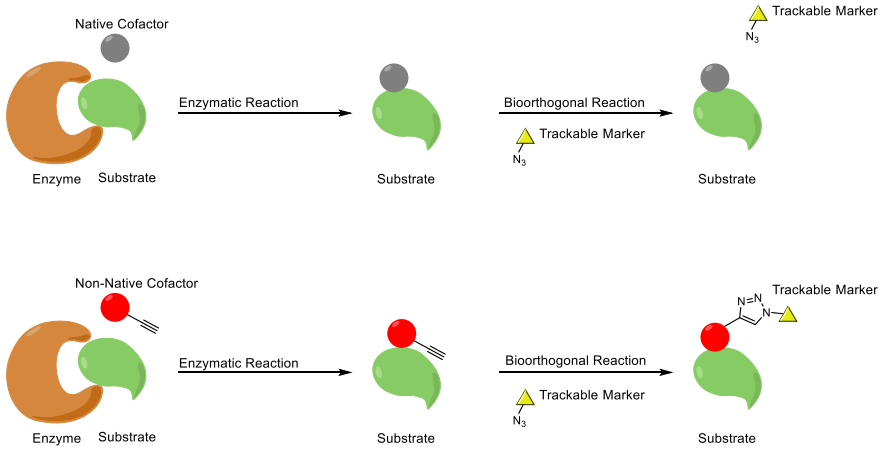

Figure 5: Enzyme-mediated substrate labeling with a bio-orthogonal chemical reporter

Non-native cofactors containing a chemical handle for biorthogonal reactions which are capable of being used by an enzyme of interest to label substrates can be introduced to the cellular environment, resulting in labeling of the enzyme's substrates with a biorthogonal chemical handle. Following a bio-orthogonal chemical reaction with an appropriate reagent containing a trackable marker, labeled substrates can be enriched for identification or visualized in the native cellular environment.

This technique was pioneered in the study of glycosyltransferases, which can produce complex multimeric branched chains on their protein substrates that are difficult to identify and map to functionality in a cellular context. To track glycans of interest, semi-synthetic variants containing azide functionalities were introduced into cells followed by reaction with a fluorophore containing alkyne allowing the cellular location of the glycan of interest to be tracked using fluorescence microscopy. Glycosyltransferases are promiscuous enough in their glycan preference that native enzymes are capable of using azido-sugars as substrates.[69] A SAM variant developed by the Luo group called propargylic *Se*-adenosyl-L-selenomethionine (Pro-SeAM) can be used to similar effect by PMTs in order to track and identify methylated proteins.

However there are over 100 human PMTs, many of which have seemingly contradictory roles in human disease, making the functional role of a particular methylation difficult to study without knowledge of the enzyme which placed it.[7,70] The Luo group has developed a system known as bio-orthogonal profiling of protein methylation (BPPM) that combines "bump-hole" enzyme engineering with bio-orthogonal substrate reporters to create a platform capable of identifying novel methylation events and mapping them to the PMT responsible for placing them.

1.7 Bio-orthogonal Profiling of Protein Methylation

There have been over 3300 proteins found to be subject to arginine methylation in human cells.[10] Given that there are 9 known PRMTs in humans, one can estimate that each PRMT is likely to methylate hundreds, if not thousands of cellular proteins. Given the known capacity of PRMTs for redundant methylation and the challenge of identifying arginine methylation in the context of proteome-wide mass spectrometry experiments, traditional biological approaches based on genetic knockouts or immunoprecipitation followed by MS analysis would be unlikely to efficiently identify the substrate scope of a specific PRMT.[61,71] A chemical biology approach to identifying novel PRMT substrates based on a combination of the approaches employed to study kinases and glycosyltransferases would allow for enzyme specific targeting of chemical probes and enzyme mediated substrate labeling with an easily trackable chemical moiety. This approach circumvents the two major issues associated with the study of PRMTs: identifying which enzyme is responsible for a methylation event and the difficulty of tracking methylation in a cellular context, making it a highly desirable tool for the advancing the study of PRMTs.

Although the "bump-hole" approach was used to develop selective kinase inhibitors in order to study the function of individual kinases, an inhibition-based approach is not tenable in the context of PMTs due to the large number of substrates modified by each individual PMT, the difficulty of detecting methylation in a proteomic context (compounded by the fact that in the context of inhibitor vs vehicle treatment experiments a positive result would be loss of methylation in the inhibitor treated group, which presents an even greater detection challenge), and the lack of a clear phenotype attributable to a single substrate in the context of PMT inhibition. Rather than generating the "bump" in the "bump-hole" pair from a non-specific inhibitor as in the case of kinases, semi-synthetic analogs of the native methyl donor SAM were used with the S-methyl group replaced by bulky alkyl groups. The additional steric bulk of the S-alkyl groups in synthetic SAM analogs prevents them from being used as substrates by native methyltransferases, conferring selectivity for a non-native enzyme that can be introduced.[72] The placement of the bulky synthetic moiety at the site of methyl transfer from SAM to substrate in native systems allows the synthetic moiety to be transferred to substrates.[68,73,74] One can take advantage of this transfer by placing a terminal alkyne or azide group on the bulky moiety, allowing proteins modified by a synthetic SAM analog to be tracked by subjecting them to CUAAC with a marker that can be easily visualized or enriched.

The "hole" was engineered similarly to the kinase method through site-directed mutagenesis of a bulky hydrophobic residue (e.g. methionine or phenylalanine) in the cofactor binding pocket of the PMT of interest to a residue with a smaller sidechain (e.g. glycine or alanine) without altering the relative charge in the area of interest or

introducing hydrogen bond donors or receivers.[75,76] This combination of engineered enzymes with expanded cofactor binding pockets and SAM analogs containing alkyl moieties that are too sterically bulky to be used in methylation reactions by wild type PMTs yields a bio-orthogonal enzyme-cofactor pair that can be used in a cellular environment to identify the substrates of a PMT of interest and study their function (figure 6).

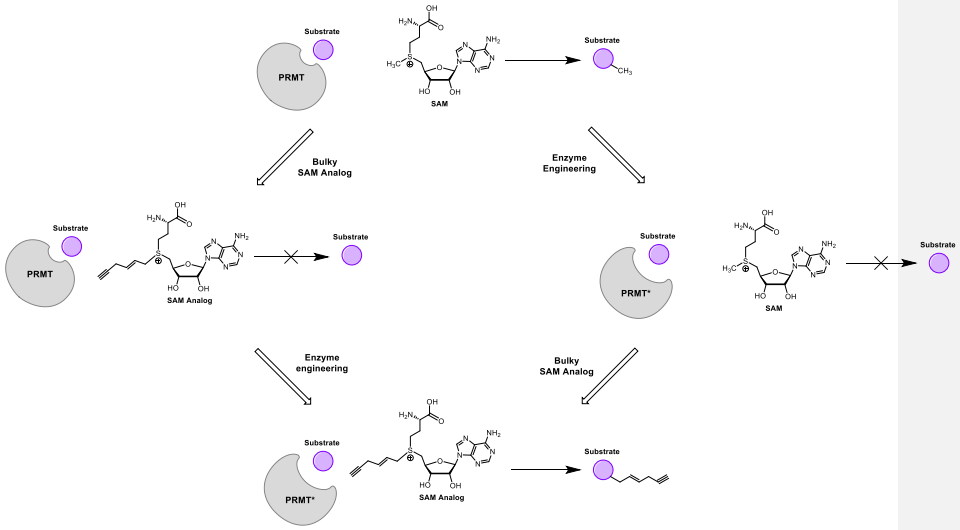

Figure 6: A bio-orthogonal enzyme-cofactor pair is required for BPPM

Engineered enzymes are deficient in ordinary methyltransferase activity, resulting in decreased cellular substrate methylation while bulky synthetic cofactors cannot be used by native PMTs to modify their substrates. Only in combination is an enzyme-cofactor pair capable of modifying substrates with a clickable chemical group, resulting in labeling system orthogonal to native cellular protein methylation.

The BPPM system allows for direct mapping of substrate methylation events to responsible methyltransferases, a difficult process in the absence of a bio-orthogonal platform. Redundancy and substrate scavenging among PMTs can prevent detection of

disappearing methyl marks in the context of PMT genetic knockout or RNAi models regardless of the detection method used to identify methylation.[71] BPPM circumvents this issue by placing a novel bio-orthogonal mark that is not subject to false negative signal due to PRMT redundancy and does not require back-validation of a detected methyl group to the enzyme responsible for placing it.

BPPM has been used to perform substrate profiling of both lysine and arginine methyltransferases in a cellular context.[75–77] The process of enzyme engineering is dependent on the individual enzyme of interest, although sequence and structural homology are both of use when attempting to engineer multiple enzymes from closely related families. Many SAM analogs were synthesized to pair with engineered enzymes, all containing extended alkyl chains to increases the steric bulk of the cofactor and a terminal handle to allow for tracking via click chemistry. Of the cofactors synthesized (E)-hex-2-en-5-ynyl-SAM (Hey-SAM) and 4-propargyloxy-but-2-enyl-SAM (Pob-SAM) are preferred for BPPM studies in a cellular context due to their lack of reactivity toward native human PMTs (figure 7).[72]

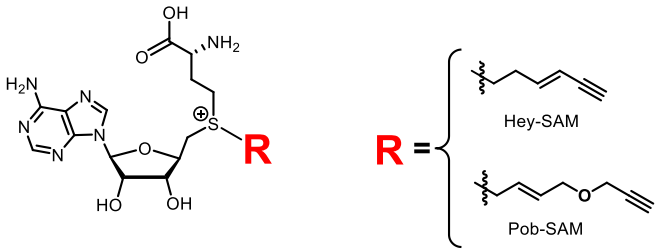

Figure 7: The synthetic SAM analogs Hey-SAM and Pob-SAM

The structures of Hey-SAM and Pob-SAM, the most commonly used cofactors for BPPM are shown here. Both contain long alkyl chains to create additional steric bulk, preventing them from occupying the cofactor binding pocket of native PMTs in a position favorable for an alkyl transfer reaction.

The physical properties of the methyl donor molecule SAM present significant difficulties to performing BPPM in living cells and organisms. As a positively charged amino acid, SAM has limited ability to diffuse across cell membranes and mammalian cells do not contain transporter proteins capable of carrying SAM across cell membranes.[78] Due to this cell permeability problem BPPM cofactor cannot be directly introduced into cells for substrate profiling. The Luo group has developed a complementary enzyme engineering system allowing cells to be treated with permeable methionine analogs which are then converted into the corresponding SAM analogs using an engineered exogenously expressed methionine adenosyltransferase enzyme alongside an engineered PMT, forming a functional cofactor-enzyme pair inside a living cell capable of labeling substrates.[79] Although effective, this additional engineering step is technically challenging and therefore an *ex cellulo* approach labeling whole cell lysates is preferred for most applications. Although working in cell lysate has the disadvantage of not preserving the localization and compartmentalization of cellular components and can result in the disruption of necessary interactions and structures to observe some methylation marks, it has proven successful in the past for the identification of a vast number of PMT substrates. Additionally, it is necessary to validate any substrate discovered by BPPM using native enzymes and the number of novel putative substrates observed in typical BPPM experiments makes false positives a greater concern than an insufficient number of novel hits.

In the *ex cellulo* labeling approach cells are transfected with engineered PMT constructs and then lysed. The fresh lysate contains active engineered PMTs and is incubated with SAM analogs, allowing enzyme mediated substrate labeling to take place

in the context of a cell lysate. Only after labeling has occurred in the lysate are the proteins precipitated and excess SAM analog washed out followed by CUAAC of labeled proteins to an appropriate reagent for either visualization or profiling of substrates (figure 8).

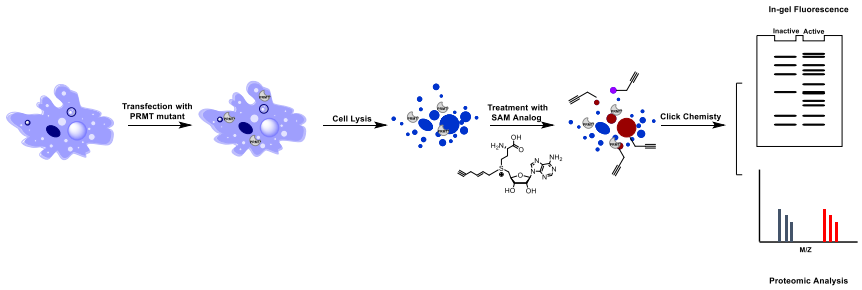

Figure 8: Schematic representation of bio-orthogonal PMT substrate labeling in whole cell lysates

Living cells are transfected with engineered enzymes, lysed, and then incubated with appropriate synthetic cofactors to allow enzymatic substrate labeling. Labeled substrates are reacted with appropriate azide-conjugated reagents for either fluorescent visualization or proteomic analysis of substrates.

When validating an enzyme-cofactor pair in a cellular context, CUAAC of labeled lysates to a fluorescent azide for visualization of total labeling efficiency is the preferred method. This is the preferred validation method because it requires a small amount of protein and synthetic cofactor (50-100 µg protein and approximately 10-20 µg cofactor) and is quick and easy to perform, yielding an interpretable result within days rather than the weeks or months required for a profiling experiment. It is essential to always perform in-gel fluorescence assays with a paired control BPPM inactive enzyme due to the significant background labeling which occurs when using cofactors in the context of cell lysates. The source of this background is a combination of non-enzymatic labeling of reactive

cysteine residues on cellular proteins and trace activity toward cofactors by native enzymes present in the cell lysate (figure 9).

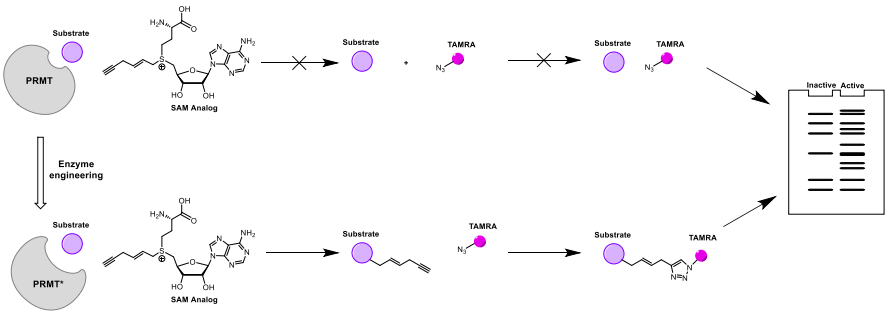

Figure 9: In-Gel fluorescence assay to assess bio-orthogonal enzyme-cofactor pair efficacy in a cellular context

Following enzymatic substrate labeling of cell lysates, lysates are subjected to CUAAC with a fluorescently labeled azide and substrates are visualized using a fluorescence scanner to identify fluorescent bands dependent on the presence of a BPPM pair. Note the presence of bands both in the presence and absence of a BPPM active enzyme. This is due to the presence of relatively high background signal in this assay system which makes paired controls of active and inactive enzymes necessary.

After validating a BPPM enzyme-cofactor pair in a cellular context using in-gel fluorescence, a similar approach is used to perform proteomic experiments to profile the substrates of a PMT of interest. Lysates that have been labeled with synthetic cofactors are subjected to a click reaction with an azide conjugated to a biotin molecule by a cleavable linker group. Biotinylating substrate proteins allows them to be enriched with streptavidin beads and the presence of a linker allows them to then be easily cleaved off the beads once they are isolated from whole cell lysate. These enriched proteins can then be identified by mass spectrometry (figure 10). Performing profiling experiments requires a large amount of material (5-10 mg protein per sample, several hundred µg cofactor per sample) and an investment of weeks to months between beginning an

experiment and obtaining a list of candidate substrates. Due to the effort involved in performing a profiling experiment and the inherent background of the BPPM technique in cellular contexts it is essential to perform paired experiments with lysates expressing BPPM active mutants and lysates not expressing BPPM active mutants. These active BPPM mutant and inactive control samples are then analyzed using a quantitative mass spectrometry technique such as SILAC or tandem mass tagging (TMT) to prevent the inherent background of BPPM from preventing the identification of as many novel PMT substrates as possible.[80,81]

The ability to biotinylate substrates, enrich them using streptavidin beads, and then identify all proteins enriched in the presence of a BPPM active mutant using paired mass spectrometry allows for facile identification of novel candidate PMT substrates in an unbiased manner in the context of a whole cellular proteome. Traditional techniques that rely on either enrichment with methyllysine or arginine antibodies or identification of methylated peptides can suffer from bias due to the recognition sites of the antibodies used and the inherent difficulty of accurately detecting methylation in a proteomic experiment. The use of a bio-orthogonal platform to enrich proteins allows for any protein found in an MS study to be considered, rather than only peptides containing methylarginine, which are relatively difficult to detect in large scale experiments. The major disadvantage to the use of BPPM is that while it is easier to detect methylated proteins using BPPM than non-bio-orthogonal techniques, it is easier to map the methylation sites of a protein of interest using other techniques.

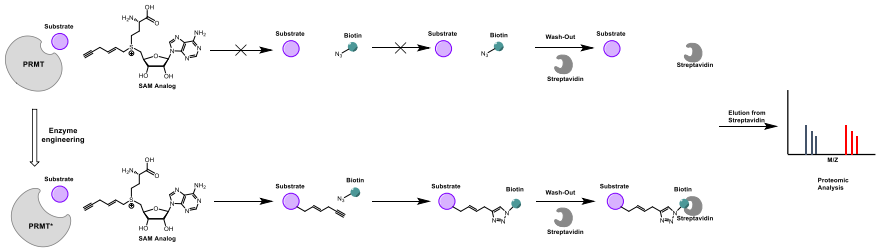

Figure 10: Biotin pulldown assay to perform PMT substrate profiling with proteomic analysis

Following enzymatic substrate labeling of cell lysates, lysates are subjected to CUAAC with a biotin-conjugated azide, biotinylated substrates are enriched by streptavidin pulldown, and proteins are cleaved from streptavidin and analyzed by mass spectrometry to identify novel substrates of the enzyme of interest.

BPPM has proven itself to be a powerful technology for the identification of novel PMT substrates, but the process of engineering a methyltransferase of interest, validating a novel enzyme-cofactor pair in a cellular context, and performing substrate profiling MS experiments represents a significant commitment of both time and resources. Therefore, it is imperative to identify PMTs for which substrate profiling will contribute both to the understanding of basic methyltransferase biology and human disease.

1.8 Rationale for Work

The BPPM platform has been used to perform substrate profiling of multiple human type I PRMTs previously, this work seeks to expand the scope of enzyme types studied using BPPM and the systems in which it can be employed.[76,77] PRMT5, the major human type II PRMT is essential for mammalian life and has been implicated in a number of cancer types.[7,82–84] Adapting the BPPM platform to PRMT5 therefore both expands the utility of the technique to a new enzyme type with distinct biochemistry and

is likely to highlight potential mechanisms through which PRMT5 plays a role in disease, pointing to new applications for existing PRMT5 inhibitors.

BPPM has previously been applied only to mammalian PMTs. While this is advantageous for directly studying the role of protein methylation in human biology and disease, BPPM is challenging in living cells and applying the technique to living multicellular organisms is entirely out of reach at this point. The major type I PRMT in *S. cerevisiae* (generally referred to as yeast in this work), Hmt1, is a promising target to expand the scope of BPPM to a non-mammalian model organism. As yeast is a unicellular eukaryote, the use of BPPM in living yeast cells would constitute the first fully *in vivo* application of the technology. Additionally, the potential overlap and divergence in yeast and human PRMT substrates could lend insight into the evolutionary conservation and development of PRMT function from simple to complex eukaryotes.

1.9 References

1. Crick, F. On protein synthesis. *Symp Soc Exp Biol.* (1958). doi:10.1038/227561a0
2. Krebs, E. G. & Beavo, J. A. Phosphorylation-Dephosphorylation of Enzymes. *Annu. Rev. Biochem.* (1979). doi:10.1146/annurev.bi.48.070179.004423
3. Moremen, K. W., Tiemeyer, M. & Nairn, A. V. Vertebrate protein glycosylation: Diversity, synthesis and function. *Nature Reviews Molecular Cell Biology* (2012). doi:10.1038/nrm3383
4. Towler, D. A., Gordon, J. I., Adams, S. P. & Glaser, L. The biology and enzymology of eukaryotic protein acylation. *Annu. Rev. Biochem.* (1988). doi:10.1146/annurev.biochem.57.1.69
5. Deribe, Y. L., Pawson, T. & Dikic, I. Post-translational modifications in signal integration. *Nature Structural and Molecular Biology* (2010). doi:10.1038/nsmb.1842
6. Bedford, M. T. Arginine methylation at a glance. *J. Cell Sci.* (2007). doi:10.1242/jcs.019885
7. Yang, Y. & Bedford, M. T. Protein arginine methyltransferases and cancer. *Nature*

Reviews Cancer (2013). doi:10.1038/nrc3409

8. Yang, Y. *et al.* PRMT9 is a Type II methyltransferase that methylates the splicing factor SAP145. *Nat. Commun.* (2015). doi:10.1038/ncomms7428

9. Gayatri, S. & Bedford, M. T. Readers of histone methylarginine marks. *Biochimica et Biophysica Acta - Gene Regulatory Mechanisms* (2014). doi:10.1016/j.bbagrm.2014.02.015

10. Larsen, S. C. *et al.* Proteome-wide analysis of arginine monomethylation reveals widespread occurrence in human cells. *Sci. Signal.* (2016). doi:10.1126/scisignal.aaf7329

11. Allers, J. & Shamoo, Y. Structure-based analysis of protein-RNA interactions using the program ENTANGLE. *J. Mol. Biol.* (2001). doi:10.1006/jmbi.2001.4857

12. Luscombe, N. M. Amino acid-base interactions: a three-dimensional analysis of protein-DNA interactions at an atomic level. *Nucleic Acids Res.* (2001). doi:10.1093/nar/29.13.2860

13. Wintjens, R., Lievin, J., Rooman, M., Buisine, E. & Liévin, J. Contribution of cation-pi interactions to the stability of protein-DNA complexes. *J. Mol. Biol.* (2000). doi:10.1006/jmbi.2000.4040

14. Sathyapriya, R., Vijayabaskar, M. S. & Vishveshwara, S. Insights into protein-DNA interactions through structure network analysis. *PLoS Comput. Biol.* (2008). doi:10.1371/journal.pcbi.1000170

15. Gallivan, J. P. & Dougherty, D. A. Cation-pi interactions in structural biology. *Proc. Natl. Acad. Sci.* (1999). doi:10.1073/pnas.96.17.9459

16. Gallivan, J. P. & Dougherty, D. A. A computational study of cation-π interactions vs salt bridges in aqueous media: Implications for protein engineering. *J. Am. Chem. Soc.* (2000). doi:10.1021/ja991755c

17. Gowri Shankar, B. A. *et al.* Ion pairs in non-redundant protein structures. *J. Biosci.* (2007). doi:10.1007/s12038-007-0069-1

18. Magalhaes, A., Maigret, B., Hoflack, J., Gomes, J. N. F. & Scheraga, H. A. Contribution of unusual Arginine-Arginine short-range interactions to stabilization and recognition in proteins. *J. Protein Chem.* (1994). doi:10.1007/BF01891978

19. Blanc, R. S. & phane Richard, S. Arginine Methylation: The Coming of Age. *Mol. Cell* (2017). doi:10.1016/j.molcel.2016.11.003

20. Côté, J. & Richard, S. Tudor domains bind symmetrical dimethylated arginines. *J. Biol. Chem.* (2005). doi:10.1074/jbc.M414328200

21. Tripsianes, K. *et al.* Structural basis for dimethylarginine recognition by the Tudor domains of human SMN and SPF30 proteins. *Nat. Struct. Mol. Biol.* (2011).

doi:10.1038/nsmb.2185

22. Friesen, W. J., Massenet, S., Paushkin, S., Wyce, A. & Dreyfuss, G. SMN, the product of the spinal muscular atrophy gene, binds preferentially to dimethylarginine-containing protein targets. *Mol. Cell* (2001). doi:10.1016/S1097-2765(01)00244-1

23. Friesen, W. J. *et al.* The Methylosome, a 20S Complex Containing JBP1 and pICln, Produces Dimethylarginine-Modified Sm Proteins. *Mol. Cell. Biol.* (2001). doi:10.1128/MCB.21.24.8289-8300.2001

24. Meister, G. *et al.* Methylation of Sm proteins by a complex containing PRMT5 and the putative U snRNP assembly factor pICln. *Curr. Biol.* (2001). doi:10.1016/S0960-9822(01)00592-9

25. Strahl, B. D. *et al.* Methylation of histone H4 at arginine 3 occurs in vivo and is mediated by the nuclear receptor coactivator PRMT1. *Curr. Biol.* (2001). doi:10.1016/S0960-9822(01)00294-9

26. Deng, X. *et al.* Protein arginine methyltransferase 5 functions as an epigenetic activator of the androgen receptor to promote prostate cancer cell growth. *Oncogene* (2017). doi:10.1038/onc.2016.287

27. Hughes, R. M. & Waters, M. L. Arginine methylation in a ??-hairpin peptide: Implications for Arg-?? interactions, ??Cp??, and the cold denatured state. *J. Am. Chem. Soc.* (2006). doi:10.1021/ja061656g

28. Chen, D. *et al.* Regulation of transcription by a protein methyltransferase. *Science (80-.).* (1999). doi:10.1126/science.284.5423.2174

29. Jenuwein, T. & Allis, C. D. Translating the histone code. *Science* (2001). doi:10.1126/science.1063127

30. Strahl, B. D. & Allis, C. D. The language of covalent histone modifications. *Nature* (2000). doi:10.1038/47412

31. Migliori, V. *et al.* Symmetric dimethylation of H3R2 is a newly identified histone mark that supports euchromatin maintenance. *Nat. Struct. Mol. Biol.* (2012). doi:10.1038/nsmb.2209

32. Casadio, F. *et al.* H3R42me2a is a histone modification with positive transcriptional effects. *Proc. Natl. Acad. Sci.* (2013). doi:10.1073/pnas.1312925110

33. Wei, H., Mundade, R., Lange, K. C. & Lu, T. Protein arginine methylation of non-histone proteins and its role in diseases. *Cell Cycle* (2014). doi:10.4161/cc.27353

34. Pawlak, M. R., Scherer, C. A., Chen, J., Roshon, M. J. & Ruley, H. E. Arginine N-methyltransferase 1 is required for early postimplantation mouse development, but cells deficient in the enzyme are viable. *Mol. Cell. Biol.* (2000).

doi:10.2139/ssrn.2577329

35. Tee, W. W. *et al.* Prmt5 is essential for early mouse development and acts in the cytoplasm to maintain ES cell pluripotency. *Genes Dev.* (2010). doi:10.1101/gad.606110

36. Yu, Z., Chen, T., Hebert, J., Li, E. & Richard, S. A Mouse PRMT1 Null Allele Defines an Essential Role for Arginine Methylation in Genome Maintenance and Cell Proliferation. *Mol. Cell. Biol.* (2009). doi:10.1128/MCB.00042-09

37. Torres-Padilla, M. E., Parfitt, D. E., Kouzarides, T. & Zernicka-Goetz, M. Histone arginine methylation regulates pluripotency in the early mouse embryo. *Nature* (2007). doi:10.1038/nature05458

38. Wu, Q. *et al.* CARM1 is required in embryonic stem cells to maintain pluripotency and resist differentiation. *Stem Cells* (2009). doi:10.1002/stem.131

39. Blanc, R. S., Vogel, G., Chen, T., Crist, C. & Richard, S. PRMT7 Preserves Satellite Cell Regenerative Capacity. *Cell Rep.* (2016). doi:10.1016/j.celrep.2016.01.022

40. Iwasaki, H. *et al.* Disruption of protein arginine N-methyltransferase 2 regulates leptin signaling and produces leanness in vivo through loss of STAT3 methylation. *Circ. Res.* (2010). doi:10.1161/CIRCRESAHA.110.225326

41. Swiercz, R., Cheng, D., Kim, D. & Bedford, M. T. Ribosomal protein rpS2 is hypomethylated in PRMT3-deficient mice. *J. Biol. Chem.* (2007). doi:10.1074/jbc.M609778200

42. Hashimoto, M. *et al.* Severe hypomyelination and developmental defects are caused in mice lacking protein arginine methyltransferase 1 (PRMT1) in the central nervous system. *J. Biol. Chem.* (2016). doi:10.1074/jbc.M115.684514

43. Selvi, B. R. *et al.* CARM1 regulates astroglial lineage through transcriptional regulation of Nanog and posttranscriptional regulation by miR92a. *Mol. Biol. Cell* (2015). doi:10.1091/mbc.E14-01-0019

44. Simandi, Z. *et al.* PRMT1 and PRMT8 regulate retinoic acid-dependent neuronal differentiation with implications to neuropathology. *Stem Cells* (2015). doi:10.1002/stem.1894

45. Dhar, S. S. *et al.* Trans-tail regulation of MLL4-catalyzed H3K4 methylation by H4R3 symmetric dimethylation is mediated by a tandem PHD of MLL4. *Genes Dev.* (2012). doi:10.1101/gad.203356.112

46. Bezzi, M. *et al.* Regulation of constitutive and alternative splicing by PRMT5 reveals a role for Mdm4 pre-mRNA in sensing defects in the spliceosomal machinery. *Genes Dev.* (2013). doi:10.1101/gad.219899.113

47. Hua, W. K. *et al.* Protein Arginine Methyltransferase 1 Interacts with and

Activates p38α to Facilitate Erythroid Differentiation. *PLoS One* (2013). doi:10.1371/journal.pone.0056715

48. Infantino, S. *et al.* Arginine methylation of the B cell antigen receptor promotes differentiation. *J. Exp. Med.* (2010). doi:10.1084/jem.20091303

49. Streubel, G. *et al.* PRMT4 Is a Novel Coactivator of c-Myb-Dependent Transcription in Haematopoietic Cell Lines. *PLoS Genet.* (2013). doi:10.1371/journal.pgen.1003343

50. Li, J. *et al.* Coactivator-Associated Arginine Methyltransferase 1 Regulates Fetal Hematopoiesis and Thymocyte Development. *J. Immunol.* (2013). doi:10.4049/jimmunol.1102513

51. Liu, F. *et al.* Arginine methyltransferase PRMT5 is essential for sustaining normal adult hematopoiesis. *J. Clin. Invest.* (2015). doi:10.1172/JCI81749

52. Ying, Z. *et al.* Histone Arginine Methylation by PRMT7 Controls Germinal Center Formation via Regulating *Bcl6* Transcription. *J. Immunol.* (2015). doi:10.4049/jimmunol.1500224

53. Greenblatt, S. M., Liu, F. & Nimer, S. D. Arginine methyltransferases in normal and malignant hematopoiesis. *Experimental Hematology* (2016). doi:10.1016/j.exphem.2016.03.009

54. Tradewell, M. L. *et al.* Arginine methylation by prmt1 regulates nuclear-cytoplasmic localization and toxicity of FUS/TLS harbouring ALS-linked mutations. *Hum. Mol. Genet.* (2012). doi:10.1093/hmg/ddr448

55. Quan, X. *et al.* The protein arginine methyltransferase PRMT5 regulates Aβ-induced toxicity in human cells and Caenorhabditis elegans models of Alzheimer's disease. *J. Neurochem.* (2015). doi:10.1111/jnc.13191

56. Ratovitski, T., Arbez, N., Stewart, J. C., Chighladze, E. & Ross, C. A. PRMT5-mediated symmetric arginine dimethylation is attenuated by mutant huntingtin and is impaired in Huntington's disease (HD). *Cell Cycle* (2015). doi:10.1080/15384101.2015.1033595

57. Scaramuzzino, C. *et al.* Protein Arginine Methyltransferase 6 Enhances Polyglutamine-Expanded Androgen Receptor Function and Toxicity in Spinal and Bulbar Muscular Atrophy. *Neuron* (2015). doi:10.1016/j.neuron.2014.12.031

58. Chan-Penebre, E. *et al.* A selective inhibitor of PRMT5 with in vivo and in vitro potency in MCL models. *Nat. Chem. Biol.* (2015). doi:10.1038/nchembio.1810

59. Eram, M. S. *et al.* A Potent, Selective, and Cell-Active Inhibitor of Human Type i Protein Arginine Methyltransferases. *ACS Chem. Biol.* (2016). doi:10.1021/acschembio.5b00839

60. Levy, D. *et al.* A proteomic approach for the identification of novel lysine

methyltransferase substrates. *Epigenetics and Chromatin* (2011). doi:10.1186/1756-8935-4-19

61. Egelhofer, T. A. *et al.* An assessment of histone-modification antibody quality. *Nat. Struct. Mol. Biol.* (2011). doi:10.1038/nsmb.1972

62. Bishop, A. C. *et al.* A chemical switch for inhibitor-sensitive alleles of any protein kinase. *Nature* (2000). doi:10.1038/35030148

63. Blethrow, J., Zhang, C., Shokat, K. M. & Weiss, E. L. Design and use of analog-sensitive protein kinases. *Curr Protoc Mol Biol* (2004). doi:10.1002/0471142727.mb1811s66

64. Prescher, J. A. & Bertozzi, C. R. Chemistry in Living Systems. *Nature Chemical Biology* (2005). doi:10.1038/nchembio0605-13

65. Sletten, E. M. & Bertozzi, C. R. Bioorthogonal chemistry: Fishing for selectivity in a sea of functionality. *Angewandte Chemie - International Edition* (2009). doi:10.1002/anie.200900942

66. Laughlin, S. T. *et al.* Metabolic Labeling of Glycans with Azido Sugars for Visualization and Glycoproteomics. *Methods in Enzymology* (2006). doi:10.1016/S0076-6879(06)15015-6

67. Kolb, H. C. & Sharpless, K. B. The growing impact of click chemistry on drug discovery. *Drug Discovery Today* (2003). doi:10.1016/S1359-6446(03)02933-7

68. Wang, R. & Luo, M. A journey toward bioorthogonal profiling of protein methylation inside living cells. *Current Opinion in Chemical Biology* (2013). doi:10.1016/j.cbpa.2013.08.007

69. Hang, H. C., Yu, C., Kato, D. L. & Bertozzi, C. R. A metabolic labeling approach toward proteomic analysis of mucin-type O-linked glycosylation. *Proc. Natl. Acad. Sci.* (2003). doi:10.1073/pnas.2335201100

70. Hamamoto, R., Saloura, V. & Nakamura, Y. Critical roles of non-histone protein lysine methylation in human tumorigenesis. *Nature Reviews Cancer* (2015). doi:10.1038/nrc3884

71. Dhar, S. *et al.* Loss of the major type i arginine methyltransferase PRMT1 causes substrate scavenging by other PRMTs. *Sci. Rep.* (2013). doi:10.1038/srep01311

72. Wang, R. *et al.* Formulating a fluorogenic assay to evaluate S-adenosyl-L-methionine analogues as protein methyltransferase cofactors. *Mol. Biosyst.* (2011). doi:10.1039/c1mb05230f

73. Blum, G., Islam, K. & Luo, M. Using Azido Analogue of S-Adenosyl-L-methionine for Bioorthogonal Profiling of Protein Methylation (BPPM). *Curr Protoc Chem Biol.* (2013). doi:10.1002/9780470559277.ch120240.Using

74. Blum, G., Bothwell, I. R., Islam, K. & Luo, M. Profiling protein methylation with cofactor analog containing terminal alkyne functionality. *Curr. Protoc. Chem. Biol.* (2013). doi:10.1080/13691058.2015.1018949

75. Islam, K., Zheng, W., Yu, H., Deng, H. & Luo, M. Expanding cofactor repertoire of protein lysine methyltransferase for substrate labeling. *ACS Chem. Biol.* (2011). doi:10.1021/cb2000567

76. Wang, R., Zheng, W., Yu, H., Deng, H. & Luo, M. Labeling substrates of protein arginine methyltransferase with engineered enzymes and matched S-adenosyl-l-methionine analogues. *J. Am. Chem. Soc.* (2011). doi:10.1021/ja2006719

77. Guo, H. *et al.* Profiling Substrates of Protein Arginine *N* -Methyltransferase 3 with *S* -Adenosyl- l -methionine Analogues. *ACS Chem. Biol.* (2014). doi:10.1021/cb4008259

78. Zhang, J. & Zheng, Y. G. SAM/SAH Analogs as Versatile Tools for SAM-Dependent Methyltransferases. *ACS Chemical Biology* (2016). doi:10.1021/acschembio.5b00812

79. Wang, R. *et al.* Profiling genome-wide chromatin methylation with engineered posttranslation apparatus within living cells. *J. Am. Chem. Soc.* (2013). doi:10.1021/ja309412s

80. Ong, S.-E. & Mann, M. Stable isotope labeling by amino acids in cell culture for quantitative proteomics. *Methods Mol. Biol.* (2007). doi:10.1007/978-1-59745-255-7_3

81. Thompson, A. *et al.* Tandem mass tags: A novel quantification strategy for comparative analysis of complex protein mixtures by MS/MS. *Anal. Chem.* (2003). doi:10.1021/ac0262560

82. Stopa, N., Krebs, J. E. & Shechter, D. The PRMT5 arginine methyltransferase: Many roles in development, cancer and beyond. *Cellular and Molecular Life Sciences* (2015). doi:10.1007/s00018-015-1847-9

83. Kryukov, G. V. *et al.* MTAP deletion confers enhanced dependency on the PRMT5 arginine methyltransferase in cancer cells. *Science (80-.).* (2016). doi:10.1126/science.aad5214

84. Mavrakis, K. J. *et al.* Disordered methionine metabolism in MTAP/CDKN2A-deleted cancers leads to dependence on PRMT5. *Science (80-.).* (2016). doi:10.1126/science.aad5944

Chapter 2: Bioorthogonal Profiling of PRMT5 in Human Cells

2.1 Introduction

There are nine mammalian protein arginine methyltransferases (PRMTs) with demonstrated activity *in vivo* or *in vitro*. All members of the PRMT family catalyze the addition of one or more methyl groups onto an ω-nitrogen of the guanidino group of an arginine residue using S-adenosyl methionine (SAM) as a methyl donating cofactor. PRMTs can be further subdivided into type I, II, or III. Type I PRMTs (PRMTs 1-4, 6, and 8) primarily generate asymmetric dimethyl arginine (ADMA) but can also generate monomethyl arginine (MMA). Type II PRMTs (PRMTs 5 and 9) generate symmetric dimethyl arginine (SDMA) as well as MMA. Type III PRMTs (PRMT7) generate only monomethyl arginine.[1–3,10,11] Type I PRMTs are the largest and most well studied PRMT class and have been found to function as both positive and negative regulators of transcription in addition to many other cellular processes.[4–8] PRMT5 is the major mammalian Type II PRMT. It was initially discovered as a binding partner of the kinase Jak2 in a yeast two-hybrid assay and was found to exhibit methyltransferase activity against the histones H2A and H4 *in vitro*.[9] PRMT5 was subsequently determined to be a type II arginine methyltransferase and to function as a transcriptional repressor of the *cyclin E1* gene. PRMT5 knockout is embryonic lethal in mice, causing death at day 6.5 in development.[12,13] Recombinant PRMT5 purified from *E. coli* displays no *in vitro* activity; in order to demonstrate activity against histone tail peptides or full length histone *in vitro*, PRMT5 must associate with its binding partner MEP50, which is believed to facilitate substrate recognition.[14–16]

PRMT5 is known to regulate transcription by methylating histone tails. PRMT5 has been found to associate with the SWI/SNF complex to symmetrically dimethylate H3R8 and H4R3, which serves to repress transcription.[17,18] While PRMT5's histone modifying activity is generally associated with transcriptional repression, PRMT5-mediated H3R2me2s specifically recruits WDR5-associated coactivator complexes and maintains euchromatin at modified loci.[19] PRMT5 also modulates transcription through methylation of non-histone targets. PRMT5 methylation of the transcription factor Spt5 results in decreased transcriptional elongation while methylation of the p65 subunit of Nuclear Factor (NF)-κB promotes promoter binding and expression of NF-κB target genes, PRMT5 methylation of RNA polymerase II promotes proper transcriptional termination.[20–23] Finally, PRMT5 association with the proteins SNAIL and AJUBA is necessary for repression of *E-cadherin*, although it is unclear whether PRMT5 methylates histones at the *E-cadherin* promoter, AJUBA directly, or another target. *E-cadherin* repression is thought to be a key step in epithelial to mesenchymal transition and cancer metastasis.[24]

PRMT5 also possesses many functions unrelated to transcriptional regulation. Some of the first discovered and most well-characterized non-histone targets of PRMT5 to be discovered were the Sm proteins, which are subunits of snRNPs. Sm protein methylation increases association with the SMN protein, which serves as a chaperone when loading Sm proteins onto snRNA.[25,26] PRMT5 inducible knockout mice display aberrant snRNP maturation and defects in splicing.[27] PRMT5 has been show to modulate ERK signaling through methylation of both EGFR and CRAF, increasing phosphatase recruitment to EGFR and stability of CRAF, attenuating signal amplitude in both

cases.[28,29] p53 is a substrate of PRMT5 and this methylation event seems to promote p53-mediated cell cycle arrest over apoptosis.[30] PRMT5 also promotes ribosome biogenesis through methylation of the ribosomal protein S10 and proper Golgi apparatus structure through methylation of GM130.[31,32] Overall, PRMT5 regulates a wide array of cellular processes through interaction with a constantly growing list of identified substrates, with promotion of cell growth and survival and modulation of protein-nucleic acid interactions emerging as common tenets of PRMT5 activity.

PRMT5 is highly expressed in a number of cancer types including melanoma, ovarian cancer, lung cancer, glioma, and lymphoma, where it has been shown to repress transcription of *RB* genes.[33–40] This expression often correlates with poor prognosis. Interestingly while high expression generally signifies poor outcome, subcellular localization differs between cancer type, indicating that the precise oncogenic role played by PRMT5 may be cancer type specific.[41]

There have also been several studies which provide a direct mechanistic role for PRMT5 in cancers. In JAK2 mutant driven leukemia cell lines and mouse models, phosphorylation of PRMT5 by JAK2 decreases association of PRMT5 with MEP50, reducing its activity. This phosphorylation event was shown to promote leukemia cell proliferation, implying that PRMT5 functions as a tumor suppressor in JAK2 mutant driven malignancies.[42] In lymphoma models driven by Cyclin D1T286A increased CDK4 phosphorylation of MEP50 promotes PRMT5 methyltransferase activity which promotes cell proliferation through *CUL4* repression leading to increased levels of the replication licensing protein CDT1 as well as repression of pro-apoptotic p53 target genes, presumably through increased methylation of p53 by PRMT5.[43,44] A great deal of

interest has been generated in PRMT5 as a therapeutic target because of the discovery that the deletion of the MTAP gene dramatically increases sensitivity to PRMT5 inhibition in a variety of cancers. This MTAP deletion occurs as a "passenger" deletion due to the gene's proximity to the commonly deleted tumor suppressor CDKN2A. The increased sensitivity of cells to PRMT5 inhibitors is the result of partial inhibition of PRMT5 activity by the MTAP substrate methylthioadenosine, which happens to selectively inhibit PRMT5 over other methyltransferases and accumulates at high levels in MTAP deficient cells. The effects of this "passenger" deletion make PRMT5 a potential therapeutic target in a number of tumor types in which PRMT5 has not been previously implicated.[45–47] It is unclear which downstream PRMT5 effects or which PRMT5 substrates are responsible for the dependency on PRMT5 in MTAP deficient cancers and these downstream effects and substrates may very well vary depending on tumor type. Selective inhibitors of PRMT5 have been developed and are currently undergoing a phase I trial in patients with solid tumors and non-Hodgkin's lymphoma (NCT02783300).[48]

PRMT5 is an essential protein for human survival which plays a role in many cancer types and modifies a broad range of substrates with many different biological roles. It is also the major type II PRMT in mammalian cells and generates the vast majority of SDMA in humans, giving it a largely non-redundant chemical function in human cells unlike type I PRMTs. We decided to engineer PRMT5 for BPPM analysis and substrate profiling for both of these reasons. We have previously engineered both PKMTs and type I PRMTs but PRMT5 would afford us an opportunity to expand our BPPM technology to type II PRMTs. We hypothesized that there are a number of

PRMT5 substrates that have not yet been reported, possibly even a majority of them, and a systematic profiling experiment would help to define the substrate scope of PRMT5 and highlight areas of biological importance in which it plays an important role. A stronger sense of its substrate scope would also be useful for identifying the unknown molecular mechanisms through which PRMT5 plays a role in many of the cancers in which its activity is essential.

2.2 Results and Discussion

2.2.1 Constructing a BPPM Active PRMT5 Mutant-Cofactor Pair

We sought to generate a set of PRMT5 mutants likely to accept our synthetic SAM analogs using both published PRMT5 crystal structures and sequence-based alignment to other PRMTs profiled by the Luo lab. A crystal structure of a tertiary complex of PRMT5 bound to both a SAM-competitive inhibitor and a peptide substrate shows that a phenylalanine residue at position 327 (F327) sits at the interface between the SAM-competitive inhibitor and the peptide substrate, representing a likely site to generate steric space for a bulky synthetic SAM analog.[49] Sequence alignment to PRMT1 and PRMT3 showed that F327 aligned with a conserved methionine residue in the type I PRMTs which has been successfully mutated for BPPM profiling (figure 11).[50,51]

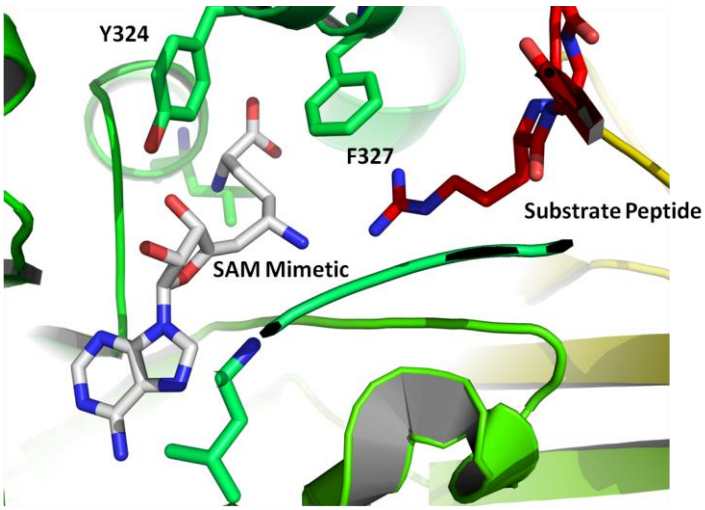

PRMT5	TYEVFEKDPIKYSQYQQAIYKC
PRMT1	IHEEMLKDEVRTLTYRNSMFH
PRMT3	IHEEMLKDKIRTESYRDFIYQN

Figure 11: Crystal structure of the active site of PRMT5 and alignment to PRMT1 and PRMT3

Residues Y324 and F327 are proximal to the SAM binding site in PRMT5 and F327 aligns to a conserved methionine in type I PRMTs.

We generated mutations of several bulky hydrophobic PRMT5 residues located near the SAM-binding site (L315, Y324, and F327) based on the published crystal structure and overexpressed these mutants in HEK 293T cells (figure 12). After establishing that our mutants expressed well, we performed in-gel fluorescence experiments with the mutants to determine their ability to selectively label 293T cell lysates with either Hey-SAM or Pob-SAM (figure 13). We observed that our PRMT5 F327G overexpressing cells appeared to have a faint band not present in other mutants or PRMT5 WT overexpressing cells, which may correspond to a selective labeling of 293T cell lysate.

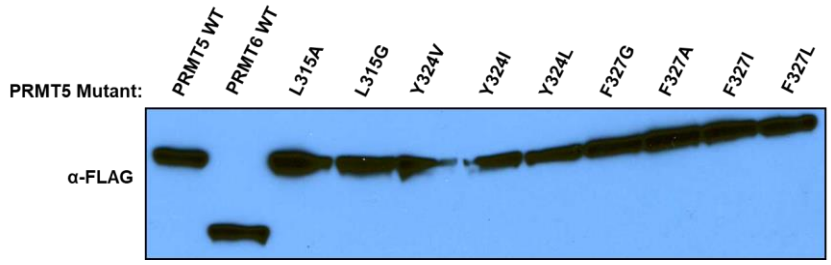

Figure 12: Western blot showing overexpression of FLAG-tagged PRMT5 constructs

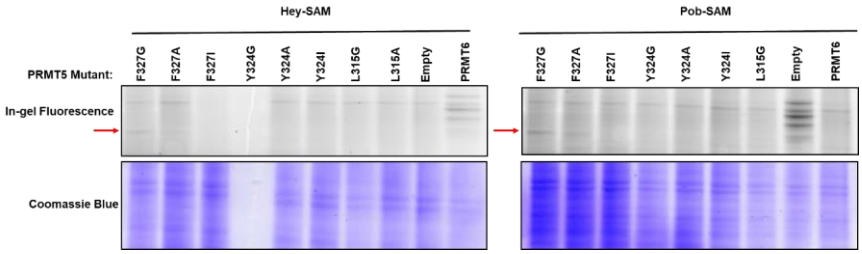

Figure 13: Western blot showing overexpression of FLAG-tagged PRMT5 constructs

We observed a faint band in the F327G expressing mutants (red arrow) corresponding to selective labeling of cell lysates.

We reasoned that the faintness of the band in our in-gel fluorescence contrasted with the robust overexpression of our PRMT5 mutants could be due to insufficient expression of the PRMT5 binding partner MEP50 rendering most of the exogenous FLAG-PRMT5 inactive. To test the effect of MEP50 level on our PRMT5 mutant activity we performed in-gel fluorescence experiments comparing PRMT5 mutants with and without MEP50 co-transfection. We observed enhanced signal in PRMT5 F327G expressing 293T cells when co-transfected with MEP50 (figure 14). This observation provides probable validation to our hypothesis that additional MEP50 is required to complex with exogenously overexpressed PRMT5 and generate an active complex.

Notably we did not observe increased levels of FLAG-PRMT5 upon transfection of MEP50, lending credence to our hypothesis (figure 15). Based on these results we included cotransfection of MEP50 with all experiments involving PRMT5 overexpression performed throughout the work detailed.

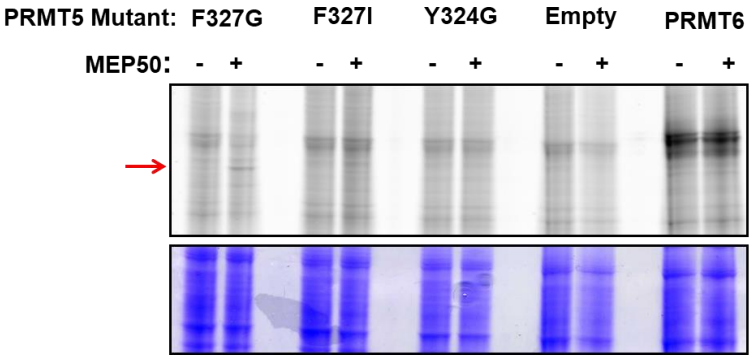

Figure 14: In-gel fluorescence of PRMT5 mutants with and without co-transfection of MEP50

A distinct band indicated by a red arrow can be observed in the PRMT5 F327G and F327I mutants exclusively in the case of MEP50 overexpression. Notably background signal is not notably different in PRMT5 mutants compared to empty vector control.

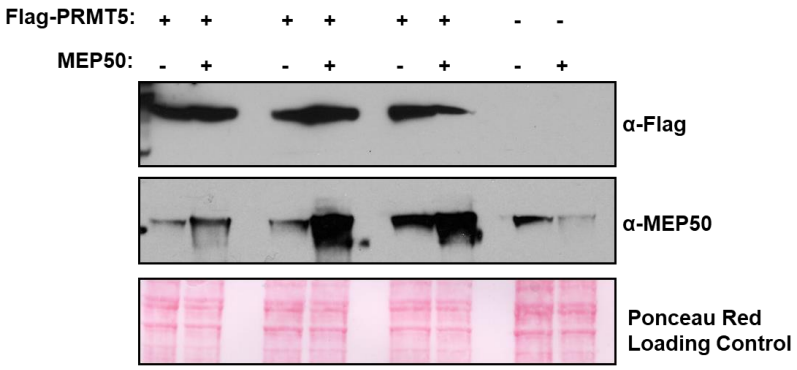

Figure 15: Western blot of expression levels of FLAG-PRMT5 and MEP50 with and without cotranfection

Groups have increased levels of MEP50 transfection from left to right in the MEP50 + samples. We observe that cotransfection of MEP50 and FLAG-PRMT5

leads to an increase of MEP50 levels but not FLAG-PRMT5 levels. Interestingly attempts to overexpress MEP50 in the absence of exogenous PRMT5 overexpression fail, possibly indicating that MEP50 is not stable when not in complex with PRMT5.

We were satisfied that our PRMT5 F327G mutant was capable of using synthetic SAM analogs to modify proteins in 293T cell lysate but in order to perform substrate profiling in the context of total cellular protein we required a negative control to ensure that any modified proteins we observed were quantifiable. An empty vector control was unsuitable for this purpose as we had no way to ensure that substrates we observed were not the results of changes in gene expression caused by overexpression of PRMT5 in our positive condition that would not occur in the empty vector sample. We also rejected overexpression of PRMT5 WT as a negative control for our BPPM experiments because of the strong potential for false negatives due to either residual activity of PRMT5 toward our SAM analogs or its ability to modify native substrates with endogenous SAM when overexpressed, reducing their ability to be pulled down for quantitative proteomics. We instead generated a PRMT5 G367A/R368A double mutant which has been previously reported to lack methyltransferase activity.[9,52] We reasoned that a catalytically defective PRMT5 construct would preserve any functions unrelated to methyltransferase activity while minimizing methylation events and allowing us to gain maximal signal from our PRMT5 F327G mutant. We compared the PRMT5 F327G and G367A/R368A mutants side by side in an in-gel fluorescence experiment and determined that our active mutant labeled cell lysates more efficiently than the inactive mutant (figure 16). We determined that the active PRMT5 F327G and inactive PRMT5 G368A/R368A pair was suitable for use in proteomic substrate profiling experiments.

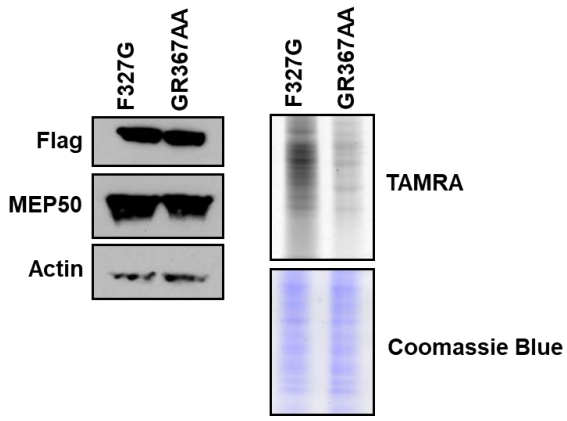

Figure 16: In-gel fluorescence experiment in 293T cells of PRMT5 F327G and G367A/R368A

Western blot analysis shows that PRMT5 and MEP50 expression levels are comparable in the F327G and G367A/R368A mutants. In-gel fluorescence results show substantial labeling in the F327G sample not present in the G367A/R368A sample which cannot be ascribed to a discrepancy in protein levels.

2.2.2 Substrate Profiling of PRMT5 using SILAC and BPPM

With an effective PRMT5 mutant SAM analog pair and a suitable negative control mutant in hand we felt prepared to perform substrate profiling of PRMT5 using our BPPM technique and proteomic analysis. We elected to use SILAC (stable isotope labeling of amino acids in living cells) to generate samples that could be paired for quantitative proteomic analysis. SILAC allows for quantitative analysis of two or more protein samples through mass spectrometry by growing the cells for the sample of interest in culture media supplemented entirely with heavy stable isotope containing amino acids. This allows unambiguous resolution of proteins peaks by sample of origin through a corresponding mass shift. These resolved peaks can then be quantified within a single mass spectrometry experiment (figure 17).[53] We considered a quantitative mass

spectrometry technique necessary to identify candidate substrates with any degree of certainty due to the high background noise evident in our in-gel fluorescence experiments.

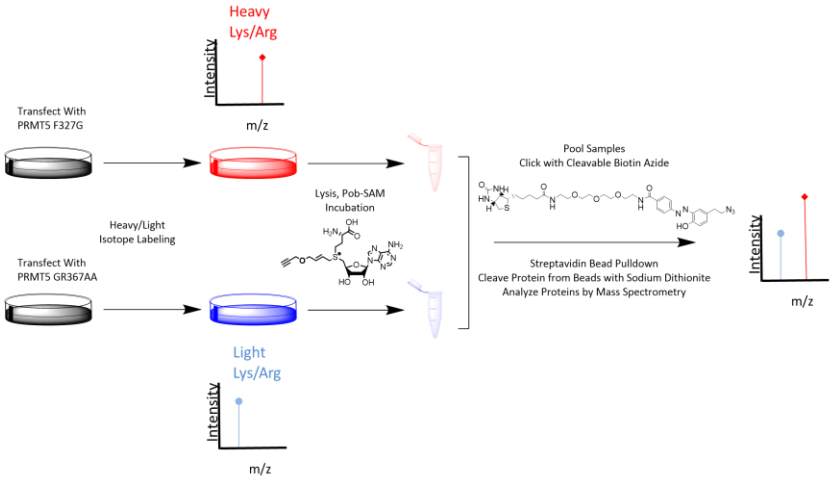

Figure 17: Schematic representation of the SILAC BPPM workflow

Cells are transfected with either active or inactive PRMT5 mutants and grown in media with either light or heavy amino acids. Cells are then harvested, lysed, and incubated with Pob-SAM. Soluble lysate proteins are precipitated, resuspended, and the heavy and light samples are mixed together and subjected to CuAAC with Biotin Azide containing a cleavable di-azo linker. Proteins are then pulled down on strepatavidin beads, chemically cleaved, and subjected to quantitative mass spectrometry analysis to identify proteins present only in the active PRMT5 mutant containing (heavy) sample.

We performed a small-scale pilot SILAC experiment to ascertain that we could achieve resolution of heavy and light labeled proteins to capture both known and previously unknown PRMT5 substrates before committing to the use of time and reagents required to perform a large-scale triplicate SILAC analysis. Our pilot experiment yielded 177 proteins enriched at least 1.5-fold in our active PRMT5 mutant over the inactive PRMT5 mutant. 8 of the enriched proteins had been previously identified as

PRMT5 substrates (figure 18). Interestingly, of the 177 enriched proteins, 127 are associated with RNA metabolism based on a gene ontology search reinforcing the known functions of PRMT5 in the regulation of transcription and splicing. An overview of the most highly enriched proteins in our pilot experiment shows a mix of proteins of known and unknown function including several known substrates of PRMT5 and a number of proteins involved in RNA metabolism (figure 19). The results of our pilot experiment demonstrate that SILAC BPPM can identify both known substrates and novel candidate substrates of PRMT5 that potentially linked to previously unknown biological roles for arginine methylation.

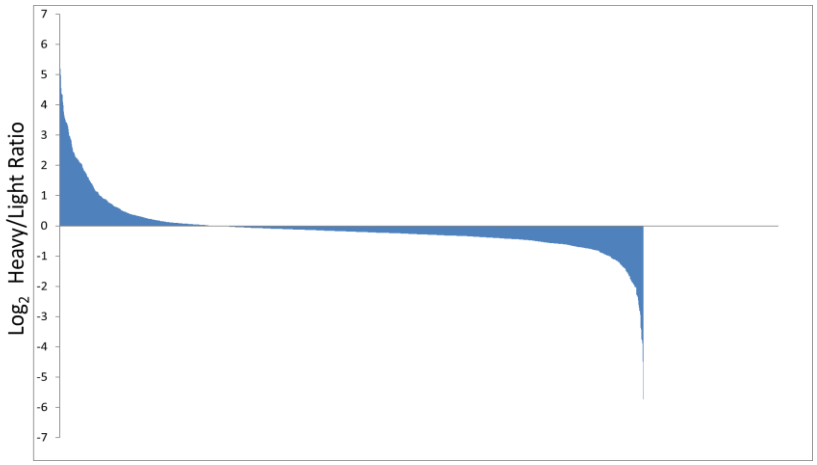

Figure 18: Waterfall plot of all proteins identified in pilot PRMT5 SILAC BPPM experiment

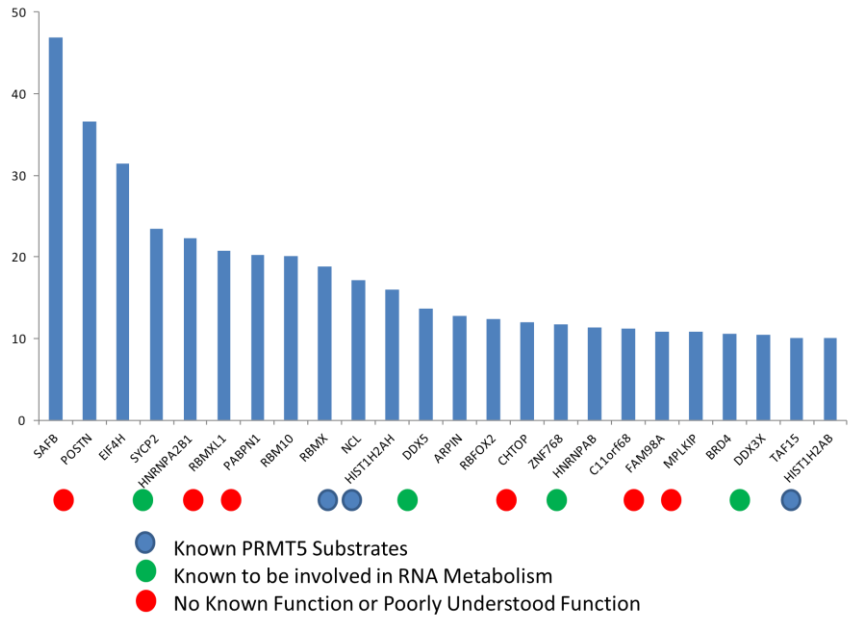

Figure 19: Overview of the most highly enriched proteins in pilot BPPM-SILAC experiment

Among the top proteins are 3 known substrates, 2 histones and 1 non-histone substrate, as well as a number of proteins known as RNA binders, poorly characterized proteins, and proteins with known functions unrelated to RNA binding and metabolism.

The success of our pilot experiment convinced us to perform a large scale SILAC-BPPM analysis in triplicate to allow for statistical analysis of our enriched proteins. Our triplicate BPPM-SILAC was completed at a large scale (10 mg protein per sample in each replicate) and contained a total of 1353 proteins present in all 3 replicates with 478 of these proteins possessing a mean enrichment greater than 0 (figure 20). We wanted to determine if the enrichment we observed was generally consistent across different replicates, as this would give us a general sense of the ability of our technique to return consistent results rather than results which had a tendency to vary wildly between

replicates. We correlated each of our replicates against the other two and were pleased to observe a strong and consistent correlation across replicates, making us confident in the consistency and validity of our BPPM technique (figure 21).

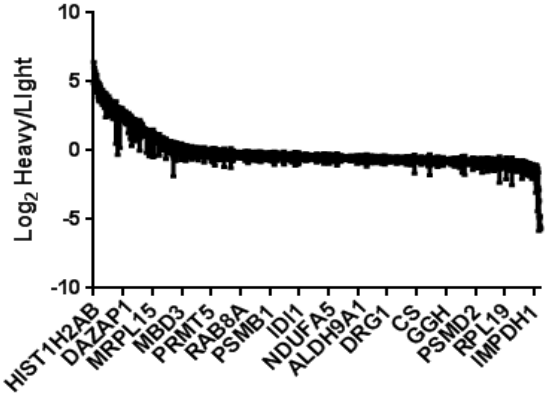

Figure 20: Waterfall plot of all proteins present in all 3 members of triplicate SILAC-BPPM experiment

A total of 1353 proteins were present in all 3 replicates with 478 possessing a mean Log_2 Heavy/Light ratio > 0.

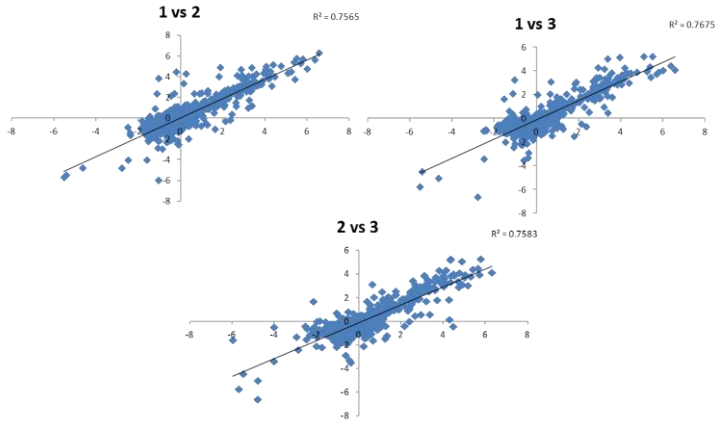

Figure 21: Inter-replicate correlation of enrichment of shared proteins

The high degree of correlation in enrichment scores across proteins indicates that our PRMT5 BPPM technique is consistent and reduces the likelihood of

highly enriched proteins being the result of anomalous high enrichment scores in a single replicate with little or no enrichment in the other two.

We calculated p-values for our heavy/light ratios and constructed a volcano plot to visualize highly significant and enriched proteins to provide a direction for further investigation of PRMT5 biology (figure 22). The most highly enriched hits that cleared a significance threshold are included in (table 1) below. Although we observed a number of highly enriched hits, none appeared to be clear choices above all other targets so we chose to perform further analysis of our data set by hand.

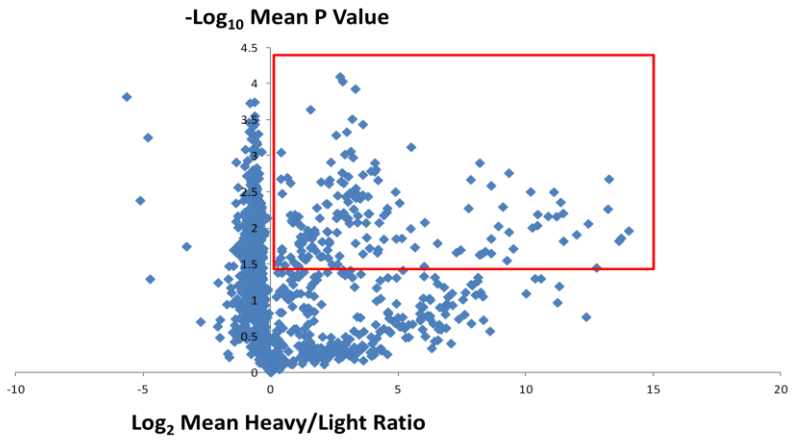

Figure 22: Volcano plot of PRMT5 SILAC-BPPM triplicate

Proteins inside the red box were annotated by hand for potential follow-up experiments.

Gene Name	Mean Enrichment	Log p-value
DAZAP1	2.71839	4.09848
SNRPE	2.820056667	4.03269
LEMD3	3.31841	3.92961
FMR1	1.557566667	3.64356
RPS19	3.194896667	3.51289
FAM98B	3.614176667	3.43842
PSPC1	2.981386667	3.33285
RAB5A	2.564846667	3.2889
EIF4H	5.504466667	3.12424

RPS19	3.138896667	3.06475
FOXRED1	0.407052667	3.05037
HNRNPUL1	2.905686667	3.02304
PABPN1	3.22713	2.97925
RBM8A	2.35674	2.91517
BYSL	4.084846667	2.90514
MAGED2	8.193153333	2.90379
TOP2B	4.124313333	2.81636
RAB5C	3.931196667	2.79186
UTP3	4.072963333	2.78387
PDCD4	2.799073333	2.76907
SPEN	9.336733333	2.76489
G3BP1	3.613623333	2.73996
NTHL1	3.04281	2.71563
TARDBP	0.397995333	2.68341
HMGA1	13.26413333	2.68112
TMEM214	7.842166667	2.67373
TP53BP1	2.311186667	2.67046
HNRNPA0	4.204346667	2.66541
RRP1	2.758053333	2.64964
EWSR1	1.970353333	2.64171
POLD1	0.776287	2.62771
DDX3X	2.85802	2.62452
SMARCA5	2.28214	2.61585
GTF2F1	8.642246667	2.59029
NCL	3.33578	2.55329
NDNL2	10.18923	2.50542
C19orf43	4.889426667	2.50369
GEMIN6	11.10125333	2.50217
SFPQ	3.103606667	2.49195
PDS5B	3.352106667	2.48579
EIF4G1	3.60544	2.46247
FUBP3	2.623423333	2.45301
HNRNPA1	3.81277	2.44042
CPSF6	2.939306667	2.43799
C1orf174	3.313003333	2.42602
API5	3.352326667	2.42207
EEFSEC	3.504783333	2.40967
LMNA	3.027856667	2.3657
ARFGEF1	11.36933333	2.36008

Table 1: Top 50 PRMT5 SILAC-BPPM hits ranked by p value

The full list of enriched and unenriched proteins from the SILAC-BPPM experiment is present in appendix I.

We chose a somewhat arbitrary $-Log_{10}$ p-value of 1.5 and annotated all 192 of the enriched hits above this cut-off by hand with the rationale that above this significance it was likely that we would be able to observe methylation by PRMT5 and a lower total enrichment could be the result of these proteins being less abundant or accessible and therefore receiving less methylation in our experiments. We discarded proteins with no known function and proteins which showed a high enrichment in one replicate but which were more enriched in the inactive sample in the other two. We curated a list of 124 proteins, which we still considered too many proteins to individually validate. We performed a gene set enrichment analysis on our list of proteins using consensus pathway database to identify enriched biological pathways in our data set and gain a holistic view of novel roles for PRMT5 which our data set points us towards (table 2). The majority of the enriched pathways we observed in our enrichment analysis recapitulate known PRMT5 functions such as RNA processing and metabolism, splicing, and transcription.[18,25–27,39,42,54] We also observed enrichment in the pathways of translation, ribosomal subunit assembly, and cap-dependent translation initiation. PRMT5 has previously been shown to methylate ribosomal component proteins and PRMT5 deficient cells have been shown to have some defects in proper ribosome assembly.[31] PRMT5 has not been implicated in the regulation of translation initiation, however, and we felt this was a promising area for further investigation as PRMT5 has a tendency to associate with RNA binding and modifying proteins and PRMTs have not previously been shown to play a significant role in the biology of cap-dependent translation initiation.

GO Term	Log p-value	Total Genes	Genes in Data Set
Metabolism of RNA	12.64	586	43
Metabolism of proteins	8.73	2008	30
Processing of Capped Pre-mRNA	8.43	240	29

mRNA Splicing	7.83	186	27
Gene expression (Transcription)	6.62	1372	23
RNA Polymerase II Transcription	6.02	1235	21
Spliceosome	5.42	134	19
mRNA Processing	5.42	127	19
Signal Transduction	4.52	2643	16
Translation	4.21	310	15
Cell Cycle	3.91	561	14
Immune System	3.61	1840	13
Post-translational protein modification	3.31	1383	12
RNA transport	3.31	171	12
EGFR1	3.01	455	11
Innate Immune System	2.71	1077	10
mRNA surveillance pathway	2.71	91	10
Generic Transcription Pathway	2.71	1106	10
Metabolism	2.71	1966	10
Cleavage of Growing Transcript in the Termination Region	2.71	67	10
RNA Polymerase II Transcription Termination	2.71	67	10
miR-targeted genes in lymphocytes	2.41	483	9
Cell Cycle Checkpoints	2.41	249	9
Cap-dependent Translation Initiation	2.41	133	9
mRNA binding to 43S ribosomal subunit	2.11	69	8
L13a-mediated translational silencing of Ceruloplasmin expression	2.11	125	8
GTP hydrolysis and joining of the 60S ribosomal subunit	2.11	126	8
Nonsense-Mediated Decay (NMD)	2.11	118	8
DNA Repair	2.11	320	8

Table 2: Top biological pathways enrichments of PRMT5 candidate substrates

2.2.3 Validation of PRMT5 Candidate Substrates Identified by SILAC-BPPM Profiling

We wished to directly validate the ability of PRMT5 to methylate some of our candidate substrates in a cellular context. We chose a variation on our BPPM technique

as our primary validation assay using a western blot for the substrate of interest as our readout. Briefly, we labeled cell lysate proteins with our SAM analogs and performed CuAAC with a biotin-azide. We then enriched our biotin labeled proteins with a streptavidin pulldown before cleaving protein from the streptavidin beads using sodium dithionite and immunoblotting for enrichment of the protein of interest in samples expressing active PRMT5 mutant (figure 23).

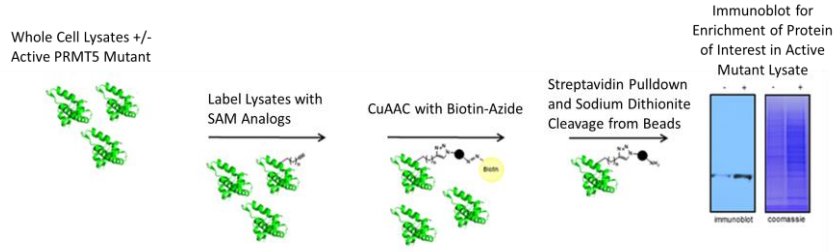

Figure 23: Schematic of BPPM-western blot validation technique for candidate substrates

Cell lysates with or without active PRMT5 mutant are labeled with SAM analogs followed by CuAAC with biotin-azide, streptavidin pulldown and cleavage of proteins from beads and western blotting for enrichment of proteins of interest.

We initially chose a combination of proteins previously known to be PRMT5 substrate proteins belonging to families known to be heavily methylated by PRMTs, and proteins of interest. We observed selective enrichment from our BPPM-western blot analysis on the known PRMT5 substrates histone 4, hnRNP-A1, and the splicing factor SmD3, as well in the novel substrates DDX3 and DDX5 (members of the DEAD-box RNA helicase family), which we have previously observed to be substrates of other PRMTs in studies yet to be published (figure 24).[38,54,62]

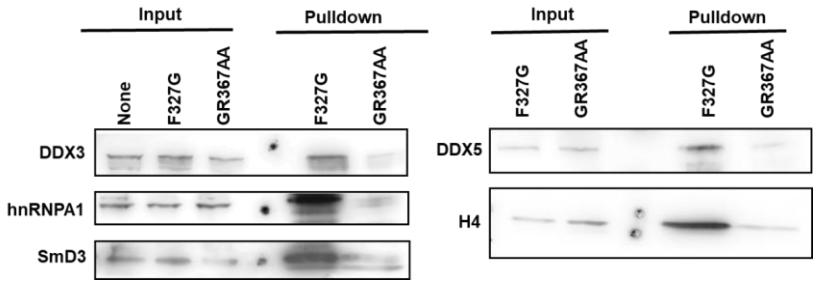

Figure 24: BPPM- western blot enrichment of known and novel PRMT5 substrates

Selective enrichment following PRMT5-activity dependent pulldowns is evident in all five proteins tested when comparing the SAM analog active PRMT5 F327G expressing cells to the SAM analog inactive PRMT5 G367A/R368A expressing cells following pulldown.

We next performed our BPPM-western blot enrichment assay on two other candidates substrates, hnRNPA2/B1 and BRD4 as well as histone 3 and p53, two known PRMT5 substrates which we did not identify in our BPPM-SILAC profiling.[18,30] We observed enrichment in hnRNPA2/B1, but not in BRD4 or the known PRMT5 substrates histone 3 or p53 (figure 25). These results suggest an inherent limitation to our use of BPPM as a validation technique and suggest it may not be capable of fully recapitulating the substrate scope of WT PRMT5. It is not clear whether this is merely a dosage issue due to the use of PRMT5 overexpression in our experiments or a change in substrate scope caused by our F327G mutant. Regardless, the inability to validate known PRMT5 substrates through BPPM-western demonstrates the necessity of orthogonal validation methods for substrates of interest prior to more involved investigations of the role of PRMT5 on their cellular function.

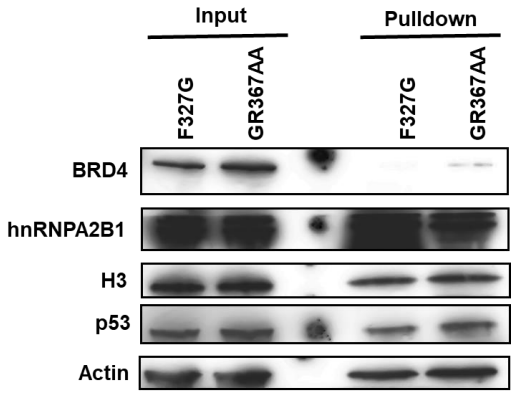

Figure 25: BPPM-western blot analysis of candidate and known PRMT5 substrates

Enrichment of the candidate substrate hnRNPA2/B1 but not the candidate substrate BRD4 or the known PRMT5 substrates H3 and p53 was observed. A discussion of possible reasons for the failure of our BPPM based technique to generate H3 and p53 enrichment is present in the main text.

Since it exists within the realm of possibility that our BPPM-western blot validation is capable of generating false negative results and BRD4 is a protein of significant interest both as a master transcriptional regulator essential for superenhancer formation in many contexts and as a therapeutic target we attempted to validate it as a substrate using orthogonal techniques to BPPM.[63–66] We immunoprecipitated endogenous BRD4 from Hek293T cells treated with inhibitors of type I PRMTs and PRMT5 alone and in combination along with overexpressed PRMT5 WT.[48,67] We then performed a western blot on the immunoprecipitated BRD4 for SDMA to identify PRMT5 mediated methylation. We observed faint bands corresponding to the molecular weight of BRD4 in our immunoprecipitated samples in the presence of MS023 and PRMT5 overexpression, but not in untreated cells or cells treated with a PRMT5 inhibitor (figure 26). Our results indicate that PRMT5 appears to be capable of weakly

methylating BRD4, although the extent of this methylation is unclear as it does not appear to be detectable under normal conditions. The ability of MS023 treatment to induce detectable SDMA in our BRD4 immunoprecipitates hints at possible competition between PRMT5 and a type I PRMT for modification of BRD4 with the type I PRMT predominating under standard conditions.

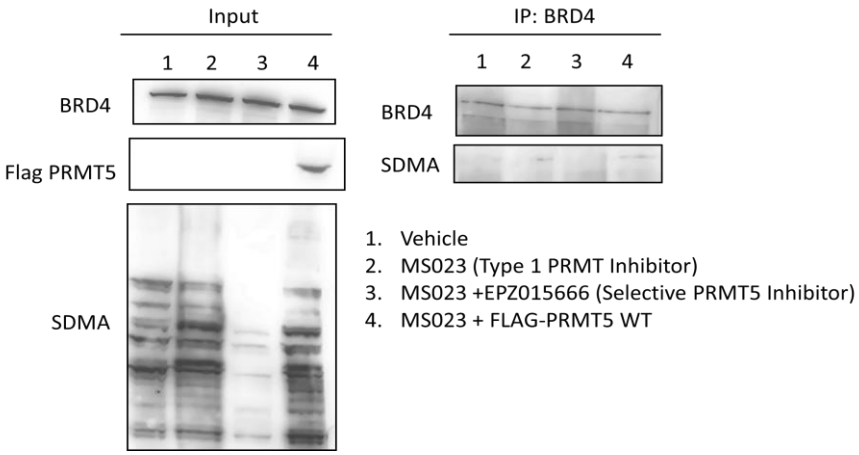

Figure 26: Detection of BRD4 symmetric dimethylation by immunoprecipitation followed by western blot analysis

Our attempts to use BPPM-western blot analysis demonstrated both the utility of the technique in identifying PRMT5 substrates and its limitations due to our observation of false negatives. Although our BPPM technique provides a powerful platform for methyltransferase substrate profiling and can be useful as a validation tool, it is important to understand its limitations. The reliance of BPPM on a methyltransferase with an engineered active site is an inherent limitation of the technique which can alter the substrate specificity of the engineered enzyme. It is therefore essential to validate any candidate substrate of interest discovered in a BPPM profiling experiment with at least

one orthogonal technique that uses a wildtype methyltransferase, preferably at its native expression level in a cellular context, before moving on to investigations of the biological role of methylation of this candidate substrate.

2.2.4 Validation and Functional Investigation of Methylation of the Translation Initiation Regulator 4EBP1

We searched our BPPM-SILAC data set for all proteins associated with cap-dependent translation initiation in both the enriched and unenriched members of the set. We found a total of 22 proteins which are known to be constituents of the cap-dependent translation initiation machinery distributed evenly between our enriched and unenriched hits (table 3). We were surprised to find eIF4A1 and eIF4E were not enriched in our data. eIF4A1 is a member of the DEAD box RNA helicase family, members of which are often methylated by PRMTs based on both our PRMT5 BPPM-SILAC experiment and similar experiments performed using other PRMTs in the Luo lab.[55] eIF4E is the member of the cap-dependent translation initiation eIF4F which directly binds the m^7GTP cap of mature mRNA molecules to bring them to ribosomes for translation.[56] We reasoned that it was probable that arginine methylation may be able to modulate the ability of an RNA-binding protein to engage RNA molecules as these contacts are commonly mediated by arginine residues, however our data indicates that this is likely not the case for eIF4E.[57,58]

When examining the set of translation initiation factors that we found to be enriched, two proteins stood out as likely candidates for further examination: eIF4E2 and 4EBP1. eIF4E2 is an m^7GTP cap binding protein related to eIF4E that has been reported as both a negative regulator of translation initiation through competition with eIF4E and

as a specialized regulator of cap-dependent translation initiation of hypoxia-specific mRNAs.[59,60] Since eIF4E2 possesses cap-binding activity we applied the same rationale as we would have for eIF4E to justify our prioritization of it as a target. 4EBP1 is a negative regulator of cap-dependent translation initiation that binds eIF4E competitively with the scaffold protein eIF4G1 and is a substrate of the kinase mTOR, which inhibits eIF4E-4EBP1 binding when it phosphorylates 4EBP1.[61] We focused our efforts on 4EBP1 because it is a well-studied protein with known relevance to human disease. Validation of 4EBP1 as a substrate of PRMT5 would link PRMT5 activity to both translation regulation and mTOR signaling.

Gene Name	Mean Enrichment
EIF4E2	6.629581357
EIF4H	5.504463734
EIF4G2	4.986199415
EIF4G1	3.605440006
EIF3H	3.259320828
EIF2B3	1.653544547
EIF3D	1.240553293
EIF4B	1.196590409
EIF4EBP1	0.780505737
EIF3F	-0.303414782
EIF2S1	-0.317999748
EIF1AY	-0.374985969
EIF3L	-0.439117515
EIF4A1	-0.445217557
EIF5A	-0.557477948
EIF3K	-0.560795389
EIF6	-0.664352331
EIF2S3	-0.67335665
EIF1AD	-0.727770552
EIF3G	-0.737820337
EIF2B1	-0.821093383
EIF4E	-0.436796277

Table 3: Translation initiation factors observed in BPPM-SILAC data set

We first sought to validate 4EBP1 as a PRMT5 substrate in a cellular context using our BPPM-western blot technique to show 4EBP1 enrichment in Pob-SAM active PRMT5 F327G expressing Hek293T lysates over Pob-SAM inactive PRMT5 G367A/R368A lysates. We incubated both active and inactive PRMT5 containing lysates with Pob-SAM and performed CuAAC with biotin-azide to generate biotinylated PRMT5 substrates which we then separated out from total cellular protein using streptavidin labeled beads. We analyzed our biotinylated PRMT5 substrate proteins by western blot for 4EBP1 to observe enrichment in our active PRMT5 lysates over our inactive PRMT5 lysates (figure 27). We observed enrichment in our active PRMT5 F327G expressing sample after adjusting the exposure time of our western blots (middle panel) to account for the strength of our 4EBP1 antibody which led to saturation at higher exposure times (upper panel) making the enrichment difficult to observe by eye.

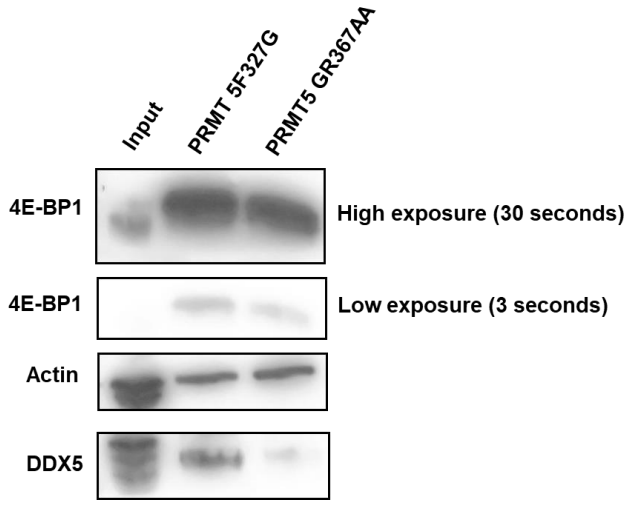

Figure 27: 4EBP1 is enriched in active PRMT5 BPPM biotin pulldown experiments

Hek293T lysates collected from cells overexpressing either PRMT5 F327G (active mutant) or PRMT5 G367A/R368A (inactive mutant) were incubated overnight with Pob-SAM followed by protein precipitation, CuAAC with biotin azide and pulldown with streptavidin beads. Protein bound to beads was cleaved and desalted before 4EBP1 levels in bound protein from active mutant and inactive mutant lysates were determined by western blot for 4EBP1.

We were pleased to see enrichment in our BPPM western blot validation of 4EBP1 as a PRMT5 substrate, however we also wished to validate PRMT5 mediated 4EBP1 methylation using a technique that is independent of our BPPM platform using WT PRMT5 to demonstrate that our observed enrichment is not an artifact arising from our PRMT5 mutant or synthetic cofactor. We elected to perform *in vitro* validation of 4EBP1 as a substrate of PRMT5 by autoradiography. As PRMT5 and PRMT1 can often modify the same substrates, we chose to perform *in vitro* methylation reactions for both enzymes. We incubated recombinant full length 4EBP1 with SAM containing a tritiated methyl group ("hot" SAM) and either recombinant PRMT5, PRMT1, or no methyltransferase and then analyzed the methylation status of 4EBP1 by autoradiograph (figure 28). We confirmed that 4EBP1 is modified by both WT PRMT5 and PRMT1 *in vitro*, although this finding provided no information about the methylation site or the functional consequences of 4EBP1 methylation.

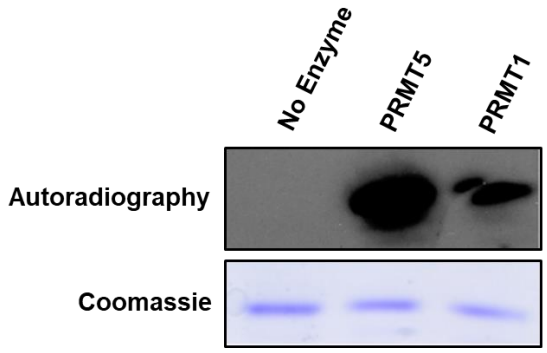

Figure 28: 4EBP1 is methylated in vitro by PRMT5 and PRMT1

Recombinant 4EBP1 was incubated overnight with SAM containing a tritiated S-methyl group, the SAH metabolizing enzyme MTAN, and PRMT5, PRMT1, or in the absence of PRMT. These reaction mixtures were quenched with SDS buffer and equal 4EBP1 content was confirmed by coomassie blue stain. Following coomassie staining samples were exposed to radiography film for 72 hours and developed to determine whether recombinant 4EBP1 could be methylated by tritiated SAM in a PRMT5 or PRMT1 dependent manner.

We consulted the phosphosite plus database to identify any previously reported methylation sites of 4EBP1. We found a single known site, R63, arising from a proteome-wide study of cellular arginine monomethylation.[72] R63 is proximal to the well-studied 4EBP1 phosphorylation site S65 known to be involved in the modulation of 4EBP1's binding affinity to eIF4E and accompanying regulation of translation initiation.[73] We hypothesized that the proximity of R63 to S65 could indicate some form of crosstalk between the two post-translation modifications, namely that PRMT5 or PRMT1 mediated methylation might stimulate phosphorylation of 4EBP1 at S65, promoting dissociation from eIF4E and translational elongation. We explored this hypothesis by treating Hek293T cells wither DMSO, the ATP competitive mTOR inhibitor MLN0128 (MLN), the PRMT5 inhibitor EPZ, or the pan-type I PRMT inhibitor

MS followed by probing 4EBP1 phosphorylation states by western blot using phosphor-site specific antibodies. Our initial experiments showed that treatment of cells with MS phenocopied the phosphorylation level at S65 resulting from MLN treatment (figure 29). This result suggests that PRMT1 activity is necessary for 4EBP1 phosphorylation at the S65 position, although it does demonstrate that PRMT1 activity toward 4EBP1 is the cause of this PRMT1 dependency.

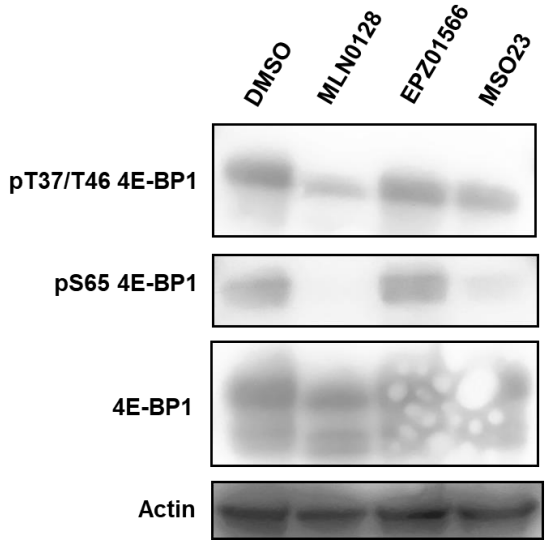

Figure 29: Treatment of Hek293T cells with type I PRMT inhibitors causes a reduction in 4EBP1 pS65 levels

Hek293T cells with either DMSO, the mTOR inhibitor MLN0128, the PRMT5 inhibitor EPZ01566, or the type I PRMT inhibitor MS023 until confluent. 4EBP1 phosphorylation levels were then measured by western blot using site specific anti-phospho antibodies.

We wished to study this relationship with greater depth and stringency since 4EBP1 phosphorylation has never been linked to PRMT activity before and this relationship would represent a significant alteration to the consensus understanding of

4EBP1 function. We repeated our drug treatment experiments adding in titrations of drug concentration as well as time courses and combinatorial treatment with EPZ and MS. We were unable to recapitulate the dramatic reduction of pS65 levels following MS treatment we observed in our initial experiments. We found that we could induce a far more modest reduction in pS65 levels after 72 hours with combined treatment with EPZ and MS (figure 30). This could indicate either that PRMT5 and type I PRMTs possess a redundant function promoting 4EBP S65 phosphorylation which can only be reduced by eliminating both activities or that the dual inhibition of PRMT5 and type I PRMTs over a prolonged period at high inhibitor concentrations induces cellular stress which may result in reduced mTOR signaling and therefore a decrease in 4EBP1 pS65 levels. Given the preponderance of previous studies into the role and regulation of mTOR signaling and the lack of prior evidence that PRMT activity plays a role in this activity, we are inclined to favor the second explanation: that our earlier positive result with MS treatment and our later result from dual inhibitor treatment were both due to non-specific cellular stress resulting in an alteration in mTOR signaling and not due to a mechanism arising from direct methylation of 4EBP1.[74]

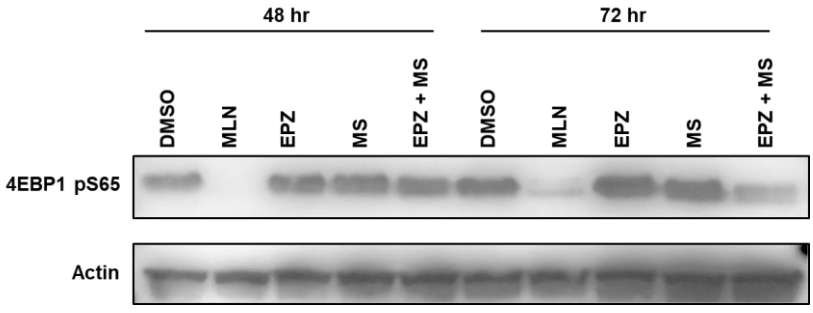

Figure 30: 4EBP1 pS65 levels are reduced reproducibly by MLN treatment and with combinatorial treatment with EPZ and MS at 72 hours

Hek293T cells were treated with DMSO, MLN, EPZ, MS, or a combination of EPZ and MS for either 48 or 72 hours. 4EBP1 pS65 levels were then detected by western blot using a site specific anti-phospho antibody with actin levels serving as a loading control.

Given our validation of arginine methylation of 4EBP1 *in vitro* and in tissue culture and our inability to find a strong link between PRMT activity and 4EBP1 phosphorylation, we wished to probe the potential role of PRMT mediated methylation of 4EBP1 using a functional readout of 4EBP1 activity. We took advantage of both the fact that 4EBP1 binds eIF4E competitively with eIF4G1 but not the m^7GTP cap of a mature mRNA and the fact that eIF4E recognizes only m^7GTP, not a full mRNA, allowing for the use of well-established pulldown assays using m^7GTP immobilized to sepharose beads to isolate eIF4E and all proteins bound to it. We can then measure relative levels of eIF4E associated 4EBP1 under various types of treatment that would interfere with the ability of PRMTs to methylate it to determine if this methylation has functional outcomes related to the ability of 4EBP1 to properly associate or dissociate from eIF4E and regulate cap-dependent translation.

Relative whole cell lysate levels of 4EBP1 and eIF4E and relative levels bound to m^7GTP resin were compared by western blot. Treatment with PRMT5 and type I PRMT inhibitors alone did affect the association of eIF4E or 4EBP1 to m^7GTP resin while the PRMT inhibitors combined resulted in a decrease of both eIF4E and 4EBP association to m^7GTP resin (figure 31). This is likely indicative of broad cellular stress resulting from dual inhibition leading to an overall reduction in cap-dependent translation. This reduction in translation levels probably functions through a mechanism that is either only partially dependent upon or wholly independent of PRMT activity toward 4EBP1 as stated previously.

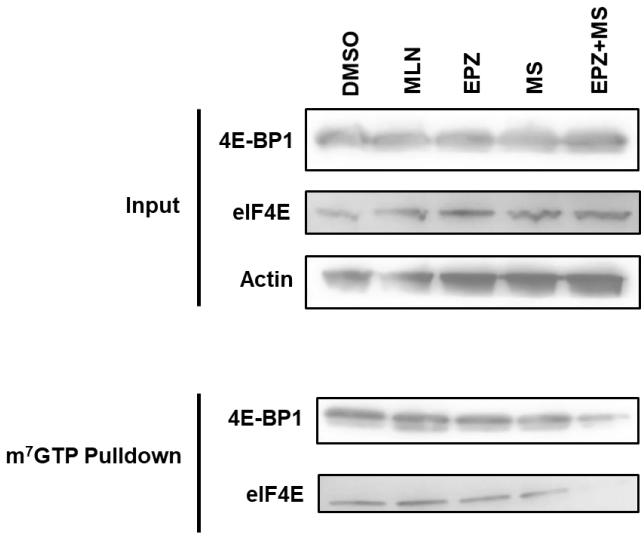

Figure 31: PRMT inhibition does not affect the association of 4EBP1 with the m7GTP cap independently of eIF4E

Hek293T cells were treated with mTOR inhibitor (MLN), PRMT5 inhibitor (EPZ), type I PRMT inhibitor (MS), or PRMT5 and type I PRMT inhibitors (EPZ+MS) for 72 hours and then incubated with m^7GTP-Sepharose resin and bound protein amounts compared by western blot.

Performing the m^7GTP pulldown assay using cells treated with PRMT inhibitors did not provide evidence of altered eIF4E association. While this could be because arginine methylation of 4EBP1 does not exhibit an effect on its activity, it could also be because basal levels of 4EBP1 methylation are too low for an observable effect from our inhibitors. It is also possible that other PRMT substrates exert effects because of inhibitor treatment that disrupted cellular function and altered eIF4E binding to the m^7GTP cap or mTOR signaling itself. To directly assess the ability of arginine methylation to affect 4EBP1 binding to eIF4E, we performed the m^7GTP pulldown assay using exogenously overexpressed HA-tagged 4EBP1 containing single R to K mutations at R51, R63, or

R73. We chose these residues due to their proximity to the 4EBP1 phosphorylation sites T46, S65, and T70 which are known to be important for eIF4E binding. We probed the m^7GTP bound protein using an HA-directed antibody in order to determine if elimination of potential PRMT substrates was sufficient to partially or fully eliminate 4EBP1 binding to eIF4E (figure 32). We observed no reduction in HA signal in our pulldown fractions for any mutant indicating that elimination of arginine methylation sites is not sufficient to eliminate or markedly reduce 4EBP1 association with m^7GTP bound eIF4E. The R-K HA-4EBP1 mutants are present in higher amounts in the pulldown than WT HA-4EBP1, but this enrichment is proportional to a higher expression level in the input that occurs reproducibly for unclear reasons. This result indicates that arginine methylation of 4EBP1 is not sufficient to alter its binding to eIF4E under normal growth conditions.

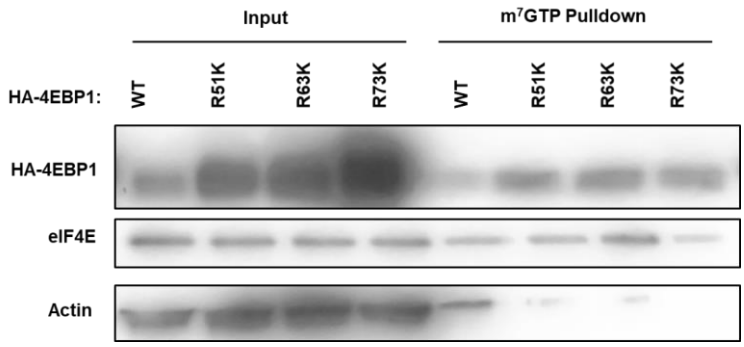

Figure 32: m7GTP-Sepharose Pulldown of HA-4EBP1 R to K mutants does not result in decreased cap association

Hek293T cells transfected with HA-4EBP1 mutants corresponding to arginine residues close to important phosphorylation sites were incubated with m^7GTP-Sepharose resin to isolate cap-associating proteins. These cap-associating proteins were compared to whole cell lysate inputs by western blotting for eIF4E as a positive control, actin as a negative control, and HA to measure the association of R to K HA-4EBP1 mutants to eIF4E. R to K mutants do not demonstrate decreased association to m^7GTP resin compared to WT by western blot.

We have validated 4EBP1 as a substrate of PRMT5 in a cellular context and as substrate of both PRMT5 and PRMT1 *in vitro*. Our efforts to identify alterations in the phosphorylation state and eIF4E association of 4EBP1 resulting from this arginine methylation were unsuccessful. It is possible that Hek293T cells are simply not sufficiently reliant on mTOR signaling to observe major changes in 4EBP1 phosphorylation and eIF4E binding and that the same experiments would result in a clear phenotype in a different model system. It is also possible that the role of 4EBP1 methylation is negligible under normal growth conditions and a clear role would only be found if the same assays were performed under conditions that would hinder normal cell growth and translation such as nutrient or serum deprivation. A final possibility is that arginine methylation of 4EBP1 alone has only a minimal effect on its activity and on cap-dependent translation rates. PRMT5 may affect translation by methylating multiple translation initiation factors and ribosomal proteins causing only minimal perturbation to the activity of each factor, with the summation of all these individually negligible effects resulting in biologically significant changes.

2.3 Materials and Methods

2.3.1 Tissue Culture

All cell-based experiments in this work were completed in Hek 293T cells grown in DMEM (Hyclone) supplemented with 10% FBS, Penicillin, and Streptomycin (Hyclone). Cells were grown at 37°C and 5% CO_2.

2.3.2 Plasmids and Mutagenesis

PRMT5 overexpression and mutagenesis was performed using a pCMV plasmid containing a PRMT5 WT sequence with a C-terminal Flag tag (sino biological). MEP50

overexpression was performed using a PCDNA.3 plasmid containing an untagged MEP50 WT sequence (sino biological).

All mutagenesis experiments were performed using the Stratagene Quikchange Lightning Site-Directed Mutagenesis kit (Agilent technologies) according to manufacturer's instructions. The following primers were used to generate the PRMT5 mutants used in the experiments detailed:

Mutation	Primer Sequence
F327A	gaatctcagacatatgaagtgGCTgaaaaggaccccatcaaat
F327G	gaatctcagacatatgaagtgGGCgaaaaggaccccatc
F327M	gaatctcagacatatgaagtgATGgaaaaggaccccatc
F327L	ctcagacatatgaagtgCTTgaaaaggaccccatc
F327I	ctcagacatatgaagtgATTgaaaaggaccccatc
Y324A	ggaatctcagacaGCTgaagtgtttg
Y324G	ggaatctcagacaGGCgaagtgtttg
Y324L	ggacaatctggaatctcagacaCTTgaagtgtttgaaaaggaccc
Y324I	ggacaatctggaatctcagacaATTgaagtgtttgaaaaggaccc
Y324V	ggacaatctggaatctcagacaGTTgaagtgtttgaaaaggaccc
K393A	gtatgctgtggagGCTaacccaaatg
K393G	gtatgctgtggagGGCaacccaaatg
K393L	gtatgctgtggagCTTaacccaaatg
K393V	gtatgctgtggagGTTaacccaaatg
D394A	gtatgctgtggagaaaGCTccaaatgcc
D394G	gtatgctgtggagaaaGGCcccaaatgcc
D394L	gtatgctgtggagaaaCTTccaaatgcc
D394V	gtatgctgtggagaaaGTTccaaatgcc
L315A	gcttcagccaGCTatggacaatctg
L315G	gcttcagccaGGCatggacaatctg
D419A	gaccgtagtctcatcaGCTatgagggaatgggtggctccag
D419G	gaccgtagtctcatcaGGCatgagggaatgggtggctccag
D419L	gtgaccgtagtctcatcaCTTatgagggaatgggtggc
D419V	gtgaccgtagtctcatcaGTTatgagggaatgggtggc
G367A/R368A	TGGTGCTGGGAGCAGCAGCAGGACCCCTGGTGAA

All mutants were confirmed by sanger sequencing.

2.3.3 Western Blotting and Antibodies

20 µg of total protein from cell lysate was separated by SDS-PAGE, transferred to a nitrocellulose membrane and blocked in 5% BSA for 1 hour at room temperature before overnight incubation with primary antibody at a 1:1000 dilution at 4°C. Membranes were washed 3x with PBST before a 1 hour incubation with HRP-conjugated secondary antibodies (1:5000 dilution). Following by an additional 3x washes with PBST membranes were treated with Luminata™ Crescendo Western HRP Substrate (Millipore) and protein bands detected using a Fujifilm X-A2 digital camera with a KwikQuant Imager attachment. The following antibodies were used in this study:

Antibody	Supplier	Catalog Number
Flag	Sigma Aldrich	F3165
Actin	Sigma Aldrich	A5441
BRD4	Abcam	128874
DDX3X	Sigma Aldrich	HPA005631
DDX5	Cell Signaling	4387S
hnRNPA1	Abcam	ab5832
SmD3	Sigma Aldrich	HPA001170
hnRNPA2B1	Abcam	ab6102
p53	Santa Cruz	SC-126
Histone 3	Millipore	07-690
Histone 4	Millipore	07-108
MEP50	Cell Signaling	2018S
SDMA	Cell Signaling	13222S
ADMA	Cell Signaling	13522S
MMA	Cell Signaling	8015S
Anti-Mouse HRP Conjugate	GE Healthcare	NA931V
Anti-Rabbit HRP Conjugate	GE Healthcare	NA9340V

2.3.4 Synthesis of SAM Analogs

Hey-SAM and Pob-SAM were synthesized as previously reported using reagents purchased from Sigma Aldrich and used without further purification.[68] Hey-SAM and Pob-SAM were purified by HPLC (Waters 600 Controller HPLC with an XBridge™

Prep C18 5µm OBD™ 19×150mm column), lyophilized, and stored in 0.01% trifluoroacetic acid before use.

2.3.5 Labeling of Cell Lysates with Synthetic SAM Analogs

Hek 293T cells were grown to ~40% confluence and cotransfected with PRMT5 WT/mutant and MEP50 WT plasmids using lipofectamine 2000 (Invitrogen). Cells were then treated with 20 µM Adox (Sigma Aldrich) for 48 hours to reduce global methylation levels. Cells were harvested when completely confluent, resuspended in methyltransferase reaction buffer (50 mM HEPES pH 8, 100 mM KCl, 15 mM $MgCl_2$, 10% glycerol) supplemented with 1mM PMSF (Sigma Adrich), 5 mM TCEP (Sigma Aldrich) and 1 tablet of protease inhibitor cocktail (Roche) per 25 ml buffer and lysed by sonication. Lysates were clarified by centrifugation at 16.1k RCF for 20 minutes followed by separation of the soluble lysate and quantification of its protein concentration. Equal total masses of protein were used for each condition of interest (typically 50-100 µg total protein for in-gel fluorescence experiments and 10mg total protein for proteomic experiments) and incubated with 100 µM cofactor (Hey-SAM or Pob-SAM) and 100 nM recombinant MTAN protein (to prevent product inhibition of methyltransferase activity) overnight. Following overnight incubation the reaction was quenched by protein precipiaion either through addition of 3:2:1 Methanol:Water:Chloroform followed by centrifugation for 10 minutes at 16.1k RCF or addition of 25x reaction volume of ice cold methanol and overnight precipitation at -80°C. Regardless of precipitation method, the precipitation protein was washed 2x with cold methanol followed by centrifugation to isolate a pellet of SAM analog labeled protein, which is allowed to dry for ~10 minutes before CuAAC.

2.3.6 CuAAC in Cell Lysates

Preparation of click cocktail: 1 mM $CuSO_4$ and 2 mM BTTP ligand (purchased Albert Einstein College of Medicine Chemical Synthesis Core Facility) were premixed for 60 minutes followed by addition of 2.5 mM Sodium Ascorbate (Sigma Aldrich) to reduce the Cu^{2+} to its active catalyst Cu^{+} state. 250 µM azide reagent (TAMRA-azide purchased from Life Technologies for in-gel fluorescence experiments and cleavable Diazo Biotin-Azide purchased from Click Chemistry Tools for biotin pulldown experiments) is then mixed with the active catalyst to yield our 4 component click cocktail.

Dried SAM analog labeled protein pellets were completely resuspended in click buffer (50 mM TEA, 150 mM NaCl, 2% SDS) and click cocktail added before shaking in the dark for 90 minutes. Reaction was quenched by protein precipitation as outlined above and protein pellets washed 2x with cold methanol and dried for ~10 minutes.

2.3.7 In-gel Fluorescence of SAM Analog Labeled Proteins

All steps prior to readout of fluorescent signal were performed with samples covered to prevent loss of fluorescence signal by photobleaching. Dried protein pellets were resuspended in loading buffer (40 mM Tris pH=6.8, 70 mM SDS, 10 mM EDTA, 10% glycerol, 10% β-ME) without dye to avoid interference with fluorescence signal and separated by SDS-PAGE. SDS-PAGE gels were fixed in 40% methanol, 10% acetic acid overnight to wash out free TAMRA dye and reduce background. After fixing overnight the gel was rinsed in ddH_2O to rehydrate and scanned for fluorescence signal using the TAMRA channel on a Typhoon TRIO variable mode imager (Amersham Bioscience). After fluorescence scanning the gel was stained with coomassie blue to confirm equal protein loading.

2.3.8 SILAC Labeling of Hek 293T Cells

SILAC labeling adapted from Ong et al.[53] Briefly: Hek293T cells were grown in SILAC DMEM (Hyclone) supplemented with either normal arginine and lysine (light) or $^{13}C6$ $^{15}N4$ arginine and $^{13}C6$ $^{15}N2$ lysine (heavy) purchased from Thermofisher. Cells were passaged at least three times before use in profiling experiments to ensure uniform isotopic labeling before use in experiments

2.3.9 Streptavidin Pulldown of Biotinylated Cellular Protein for MS or Western Blot Analysis

Streptavidin pulldown was carried out as previously reported.[69,70] High capacity streptavidin sepharose resin was purchased from GE Healthcare. All other chemical reagents purchased from Sigma Aldrich. Amicon Ultra 3kD Cutoff Centrifugal Filter Units (Millipore) were used for desalting of biotinylated protein prior to lyophilization. Samples used in western blot substrate validation were not subjected to iodoacetamide blocking and cysteine reduction and were not lyophilized prior to western blot analysis.

2.3.10 PRMT5 Substrate Profiling by MS

Desalted lyophilized proteins were sent to our collaborators the Haiteng Deng lab at Tsinghua University who performed protein digestion and quantitative MS analysis to determine peptide sequences and match them to known human proteins as previously described.[51] Raw data was received as total peak areas of peptides corresponding to human proteins with light and heavy peptides provided as separate peak areas.

2.3.11 Analysis of MS Data

Identified gene names from each replicate experiment were entered into a pivot table in micorsoft excel to identify all gene names present in all 3 experimental replicates. Those gene names present in all three replicates had mean heavy/light ratios determined, with a Log_2 Heavy/Light > 0 indicating enrichment. We performed a two-tailed t-test in excel to assign p-values for the significance of difference in means between the heavy sample

values in triplicates versus the light values. We used these enrichment and significance values to generate a volcano plot to visualize any outstanding hits demanding immediate follow-up. In the absence of any hits of this nature we instead performed several annotation steps to characterize our data set. The known functions of our enriched proteins were determined using both the Uniprot annotations and summary of each enriched protein and a PubMed search of the protein name to establish the breadth of studies concerning the protein of interest. The Phosphositeplus database was used to annotate any previously observed arginine methylation on enriched proteins. Finally, we used the gene set enrichment function in the human ConsensusPathDB platform (http://cpdb.molgen.mpg.de) to evaluate cellular pathways and processes that were overrepresented in our enriched protein data set.

2.3.12 Immunoprecipitation of BRD4 to Assess Arginine Methylation Levels

Hek 293T cells were treated with either 10μM DMSO, 5μM MS023 (Sigma Aldrich) or 10μM EPZ01566 (Sigma Aldrich) for 48 hours before harvesting. Harvested cells were lysed in immunoprecipitation buffer (20 mM Tris-HCl pH = 7.8, 100 mM NaCl, 25 mM $MgCl_2$, 10% glycerol, 0.5% Igepal 360) on ice for 20 minutes. Lysates were clarified by centrifugation at 16.1k RCF for 20 minutes and the protein concentration of the clarified lysates was quantified. 2 mg of total soluble protein per treatment condition of interest was then precleared with 10μL rabbit IgG (Cell Signaling) for 30 minutes followed by a 1 hour incubation 50 μL of Protein A/Protein G sepharose beads (Calbiochem) at 4°C for 1 hour with gentle shaking to remove proteins binding nonspecifically to IgG beads, which were then discarded while supernatant was retained. Cleared lysate was incubated with 5 μg anti-BRD4 antibody per mg soluble protein at 4°C for 1 hour with gentle shaking. 50 μL of Protein A/Protein G sepharose beads were added to lysates and

allowed to incubate for 90 minutes to precipitate antibody bound protein. The supernatant was then discarded and the beads washed 4x (5 minutes per wash at 4°C) with immunoprecipitation buffer. After washing, beads were incubated for 30 minutes on ice with 4x Laemmli SDS-PAGE loading buffer (Bio-Rad) with 10% β-ME added before boiling for 5 minutes to denature bound protein. After denaturation, proteins were separated by SDS-PAGE and probed for BRD4, SDMA, and MMA levels by western blot as outlined above.

2.3.13 Autoradiograpy to Validate *in vitro* Methylation of 4EBP1 by PRMT5 and PRMT1

Recombinant 4EBP1 was incubated overnight with SAM containing a tritiated S-methyl group, the SAH metabolizing enzyme MTAN, and PRMT5, PRMT1, or in the absence of PRMT (get these amounts tomorrow). These reaction mixtures were quenched with SDS buffer and separated by SDS-PAGE before confirming equal protein loading with coomassie blue staining. Gels were dried using a: and exposed to x-ray film (manufact) for 72 hours before developing on a (list machine).

2.3.14 m^7GTP Sepharose Pulldown

Hek293T cells were treated with either 10 μM EPZ015666, 5 μM MS023, 100 nM MLN0128 (a gift from Neal Rosen's group), or combinations of these inhibitors._Cells were harvested (1 T-150 flask at ~90% confluence), lysed in 1mL lysis buffer (20 mM Tris-HCL pH = 7.4, 100mM NaCl, 25mM $MgCl_2$, 0.5% Igepal CO-360), and cleared by centrifugation for 10 minutes at 13.2K RPM, to yield soluble lysate. Lysate was pre-cleared by incubation with 30 μL streptavidin agarose beads at 4°C for 10 min. Beads were removed by pelleting following 30 seconds centrifugation at 10K RPM. Protein concentration was quantified using the Biorad Pierce assay. Reserve ~5% of lysate was

reserved for use as an input control and equal amounts of total protein from each treatment were incubated for 1hr at 4°C with 30 μL m^7GTP-sepharose beads (Jena Bioscience). Pellet beads were pelleted by centrifugation for 30 seconds at 10K RPM and washed 4x with 0.5mL lysis buffer for 5 min at 4°C per wash. Beads were resuspended in lysis buffer containing 1mM GTP (Sigma Aldrich) and incubated for 1 hr at 4°C to remove GTP binding proteins that do not specifically recognize m^7GTP and pelleted by centrifugation for 30 seconds at 10K RPM and washed 4x with 0.5mL lysis buffer for 5 min at 4°C per wash once again. Beads were resuspended in 40 μL 4x ST Sample buffer (Biorad) and boiled for 5 mins followed protein separation by SDS-PAGE and western blot analysis.

2.4 Conclusion

We have successfully engineered the human type II arginine methyltransferase PRMT5 to accept the synthetic SAM analogs previously developed by the Luo group. We employed our engineered PRMT5 variant and the SAM analog Pob-SAM them to perform substrate profiling of PRMT5 in Hek293T cells using our BPPM technology combined with SILAC to perform quantitative proteomic analysis of candidate PRMT5 substrates. Our data set recapitulated several known PRMT5 substrates as well as revealing a number of novel candidate substrates of biological interest. RNA binding and processing proteins participiating in many different pathways were far and away the most significantly enriched type of protein in our profiling data. This does not come as a surprise as the best-characterized roles of PRMT5 are in the regulation of transcription through its activity toward histone tails and as a regulator of spliceosome assembly. We identified proteins belonging to both substrate types in our data set as well as a number of

hnRNPs involved in nuclear export of mature mRNAs and proteins involved in the regulation of translation, both ribosomal component proteins and essential regulators of translation initiation. We believe the most important role for PRMT5 implicated by our data set lies in the latter topic. Translation regulation is a major process involving multiple types of RNA (mRNA, tRNA, and rRNA) that PRMT5 has been tied to through its activity toward the ribosomal protein RPS10, but our data indicates it may play a far more significant role than has been previously appreciated.[31]

~~i)~~ Our future work on the role of PRMT5 in translation will focus on the translation initiation factors we have identified in our BPPM-SILAC data set. We intend to validate all of the enriched hits observed in our data set using both BPPM-western blot enrichment validation alongside *in vitro* methylation using recombinant substrate and PRMT5 or evaluating immunoprecipitated substrate for methylation using SDMA and MMA specific antibodies. After validating the translation initiation factors we found to be enriched, we will then evaluate the role of this methylation on translation initiation by mapping modification sites through mass spectrometry. We will then mutate the arginine residues we find to be modfied to lysine or alanine either target by target or in combination to examine the role of arginine methylation on the proper function of translation initiation factors. We will then investigate the functional results of arginine methylation deficient initiation factors on translation through polysome profiling or RNA crosslinking and immunoprecipitation experiments to measure changes in mRNA association to either ribosomes or translation initiation complexes. Finally, we hypothesize that PRMT5 may play a role in the regulation of translation under hypoxic conditions as eIF4E2 was highly enriched in our data set while eIF4E was not. PRMT5

Formatted: Indent: First line: 0.5", Line spacing: Double, No bullets or numbering

does not appear in a wealth of hypoxia literature but it was shown to be necessary for the HIF-1 mediated transcriptional hypoxia response in one study.[71] eIF4E2 has been shown to be necessary for specialized translation initiation under hypoxic conditions where it functions as an mRNA cap-binding protein in place of eIF4E.[60] The combination of strong enrichment of a specialized translation initiation factor in our PRMT5 BPPM-SILAC data set and previous association with hypoxia on the part of PRMT5 suggests a possible functional niche for PRMT5 in translation initiation under hypoxic conditions that is entirely unexplored.

2.5 References

1. Wei, H., Mundade, R., Lange, K. C. & Lu, T. Protein arginine methylation of non-histone proteins and its role in diseases. *Cell Cycle* (2014). doi:10.4161/cc.27353
2. Yang, Y. *et al.* PRMT9 is a Type II methyltransferase that methylates the splicing factor SAP145. *Nat. Commun.* (2015). doi:10.1038/ncomms7428
3. Zurita-Lopez, C. I., Sandberg, T., Kelly, R. & Clarke, S. G. Human protein arginine methyltransferase 7 (PRMT7) is a type III enzyme forming ω-NG-monomethylated arginine residues. *J. Biol. Chem.* (2012). doi:10.1074/jbc.M111.336271
4. Chen, D. *et al.* Regulation of transcription by a protein methyltransferase. *Science (80-.).* (1999). doi:10.1126/science.284.5423.2174
5. Wang, H. *et al.* Methylation of Histone H4 at Arginine 3 Facilitating Transcriptional Activation by Nuclear Hormone Receptor. *Science (80-.).* (2001). doi:10.1126/science.1060781
6. Guccione, E. *et al.* Methylation of histone H3R2 by PRMT6 and H3K4 by an MLL complex are mutually exclusive. *Nature* (2007). doi:10.1038/nature06166
7. Iberg, A. N. *et al.* Arginine methylation of the histone H3 tail impedes effector binding. *J. Biol. Chem.* (2008). doi:10.1074/jbc.C700192200
8. Yang, Y. & Bedford, M. T. Protein arginine methyltransferases and cancer. *Nature Reviews Cancer* (2013). doi:10.1038/nrc3409
9. Pollack, B. P. *et al.* The human homologue of the yeast proteins Skb1 and Hs17p interacts with Jak kinases and contains protein methyltransferase activity. *J. Biol. Chem.* (1999). doi:10.1074/jbc.274.44.31531
10. Branscombe, T. L. *et al.* PRMT5 (Janus Kinase-binding Protein 1) Catalyzes the Formation of Symmetric Dimethylarginine Residues in Proteins. *J. Biol. Chem.* (2001). doi:10.1074/jbc.M105412200
11. Fabbrizio, E. *et al.* Negative regulation of transcription by the type II arginine methyltransferase PRMT5. *EMBO Rep.* (2002). doi:10.1093/embo-reports/kvf136
12. Li, Z. *et al.* The Sm protein methyltransferase PRMT5 is not required for primordial germ cell specification in mice. *EMBO J.* (2015).

doi:10.15252/embj.201489319
13. Gkountela, S., Li, Z., Chin, C. J., Lee, S. A. & Clark, A. T. PRMT5 is Required for Human Embryonic Stem Cell Proliferation But Not Pluripotency. *Stem Cell Rev. Reports* (2014). doi:10.1007/s12015-013-9490-z
14. Friesen, W. J. *et al.* A novel WD repeat protein component of the methylosome binds Sm proteins. *J. Biol. Chem.* (2002). doi:10.1074/jbc.M109984200
15. Wang, M., Fuhrmann, J. & Thompson, P. R. Protein arginine methyltransferase 5 catalyzes substrate dimethylation in a distributive fashion. *Biochemistry* (2014). doi:10.1021/bi501279g
16. Burgos, E. S. *et al.* Histone H2A and H4 N-terminal tails are positioned by the MEP50 WD repeat protein for efficient methylation by the PRMT5 arginine methyltransferase. *J. Biol. Chem.* (2015). doi:10.1074/jbc.M115.636894
17. Pal, S. *et al.* mSin3A/histone deacetylase 2- and PRMT5-containing Brg1 complex is involved in transcriptional repression of the Myc target gene cad. *Mol. Cell. Biol.* (2003). doi:10.1128/MCB.23.21.7475
18. Pal, S., Vishwanath, S. N., Erdjument-Bromage, H., Tempst, P. & Sif, S. Human SWI/SNF-associated PRMT5 methylates histone H3 arginine 8 and negatively regulates expression of ST7 and NM23 tumor suppressor genes. *Mol. Cell. Biol.* (2004). doi:10.1128/MCB.24.21.9630-9645.2004
19. Migliori, V. *et al.* Symmetric dimethylation of H3R2 is a newly identified histone mark that supports euchromatin maintenance. *Nat. Struct. Mol. Biol.* (2012). doi:10.1038/nsmb.2209
20. Kwak, Y. T. *et al.* Methylation of SPT5 regulates its interaction with RNA polymerase II and transcriptional elongation properties. *Mol. Cell* (2003). doi:10.1016/S1097-2765(03)00101-1
21. Harris, D. P., Bandyopadhyay, S., Maxwell, T. J., Willard, B. & DiCorleto, P. E. Tumor necrosis factor (TNF)-α induction of CXCL10 in endothelial cells requires protein arginine methyltransferase 5 (PRMT5)-mediated nuclear factor (NF)-κB p65 Methylation. *J. Biol. Chem.* (2014). doi:10.1074/jbc.M114.547349
22. Wei, H. *et al.* PRMT5 dimethylates R30 of the p65 subunit to activate NF- B. *Proc. Natl. Acad. Sci.* (2013). doi:10.1073/pnas.1311784110
23. Yanling Zhao, D. *et al.* SMN and symmetric arginine dimethylation of RNA polymerase II C-terminal domain control termination. *Nature* (2016). doi:10.1038/nature16469
24. Hou, Z. *et al.* The LIM Protein AJUBA Recruits Protein Arginine Methyltransferase 5 To Mediate SNAIL-Dependent Transcriptional Repression. *Mol. Cell. Biol.* (2008). doi:10.1128/MCB.01435-07
25. Friesen, W. J. *et al.* The Methylosome, a 20S Complex Containing JBP1 and pICln, Produces Dimethylarginine-Modified Sm Proteins. *Mol. Cell. Biol.* (2001). doi:10.1128/MCB.21.24.8289-8300.2001
26. Chari, A. *et al.* An Assembly Chaperone Collaborates with the SMN Complex to Generate Spliceosomal SnRNPs. *Cell* (2008). doi:10.1016/j.cell.2008.09.020
27. Bezzi, M. *et al.* Regulation of constitutive and alternative splicing by PRMT5 reveals a role for Mdm4 pre-mRNA in sensing defects in the spliceosomal machinery. *Genes Dev.* (2013). doi:10.1101/gad.219899.113
28. Hsu, J. M. *et al.* Crosstalk between Arg 1175 methylation and Tyr 1173

phosphorylation negatively modulates EGFR-mediated ERK activation. *Nat. Cell Biol.* (2011). doi:10.1038/ncb2158
29. Andreu-Pérez, P. *et al.* Protein arginine methyltransferase 5 regulates ERK1/2 signal transduction amplitude and cell fate through CRAF. *Sci. Signal.* (2011). doi:10.1126/scisignal.2001936
30. Jansson, M. *et al.* Arginine methylation regulates the p53 response. *Nat. Cell Biol.* (2008). doi:10.1038/ncb1802
31. Ren, J. *et al.* Methylation of ribosomal protein S10 by protein-arginine methyltransferase 5 regulates ribosome biogenesis. *J. Biol. Chem.* (2010). doi:10.1074/jbc.M110.103911
32. Zhou, Z. *et al.* PRMT5 regulates Golgi apparatus structure through methylation of the golgin GM130. *Cell Res.* (2010). doi:10.1038/cr.2010.56
33. Nicholas, C. *et al.* PRMT5 Is Upregulated in Malignant and Metastatic Melanoma and Regulates Expression of MITF and p27Kip1. *PLoS One* (2013). doi:10.1371/journal.pone.0074710
34. Bao, X. *et al.* Overexpression of PRMT5 promotes tumor cell growth and is associated with poor disease prognosis in epithelial ovarian cancer. *J. Histochem. Cytochem.* (2013). doi:10.1369/0022155413475452
35. Gu, Z. *et al.* Protein arginine methyltransferase 5 is essential for growth of lung cancer cells. *Biochem. J.* (2012). doi:10.1042/BJ20120768
36. Han, X. *et al.* Expression of PRMT5 correlates with malignant grade in gliomas and plays a pivotal role in tumor growth in vitro. *J. Neurooncol.* (2014). doi:10.1007/s11060-014-1419-0
37. Yan, F. *et al.* Genetic validation of the protein arginine methyltransferase PRMT5 as a candidate therapeutic target in glioblastoma. *Cancer Res.* (2014). doi:10.1158/0008-5472.CAN-13-0884
38. Pal, S. *et al.* Low levels of miR-92b/96 induce PRMT5 translation and H3R8/H4R3 methylation in mantle cell lymphoma. *EMBO J.* (2007). doi:10.1038/sj.emboj.7601794
39. Wang, L., Pal, S. & Sif, S. Protein Arginine Methyltransferase 5 Suppresses the Transcription of the RB Family of Tumor Suppressors in Leukemia and Lymphoma Cells. *Mol. Cell. Biol.* (2008). doi:10.1128/MCB.00923-08
40. Ibrahim, R. *et al.* Expression of PRMT5 in lung adenocarcinoma and its significance in epithelial-mesenchymal transition. *Hum. Pathol.* (2014). doi:10.1016/j.humpath.2014.02.013
41. Shilo, K. *et al.* Cellular localization of protein arginine methyltransferase-5 correlates with grade of lung tumors. *Diagn. Pathol.* (2013). doi:10.1186/1746-1596-8-201
42. Liu, F. *et al.* JAK2V617F-Mediated Phosphorylation of PRMT5 Downregulates Its Methyltransferase Activity and Promotes Myeloproliferation. *Cancer Cell* (2011). doi:10.1016/j.ccr.2010.12.020
43. Aggarwal, P. *et al.* Nuclear cyclin D1/CDK4 kinase regulates CUL4 expression and triggers neoplastic growth via activation of the PRMT5 methyltransferase. *Cancer Cell* (2010). doi:10.1016/j.ccr.2010.08.012
44. Li, Y. *et al.* PRMT5 is required for lymphomagenesis triggered by multiple oncogenic drivers. *Cancer Discov.* (2015). doi:10.1158/2159-8290.CD-14-0625

45. Marjon, K. *et al.* MTAP Deletions in Cancer Create Vulnerability to Targeting of the MAT2A/PRMT5/RIOK1 Axis. *Cell Rep.* (2016). doi:10.1016/j.celrep.2016.03.043
46. Mavrakis, K. J. *et al.* Disordered methionine metabolism in MTAP/CDKN2A-deleted cancers leads to dependence on PRMT5. *Science (80-.).* (2016). doi:10.1126/science.aad5944
47. Kryukov, G. V. *et al.* MTAP deletion confers enhanced dependency on the PRMT5 arginine methyltransferase in cancer cells. *Science (80-.).* (2016). doi:10.1126/science.aad5214
48. Chan-Penebre, E. *et al.* A selective inhibitor of PRMT5 with in vivo and in vitro potency in MCL models. *Nat. Chem. Biol.* (2015). doi:10.1038/nchembio.1810
49. Antonysamy, S. *et al.* Crystal structure of the human PRMT5:MEP50 complex. *Proc. Natl. Acad. Sci.* (2012). doi:10.1073/pnas.1209814109
50. Wang, R., Zheng, W., Yu, H., Deng, H. & Luo, M. Labeling substrates of protein arginine methyltransferase with engineered enzymes and matched S-adenosyl-l-methionine analogues. *J. Am. Chem. Soc.* (2011). doi:10.1021/ja2006719
51. Guo, H. *et al.* Profiling substrates of protein arginine N-methyltransferase 3 with S-adenosyl-L-methionine analogues. *ACS Chem. Biol.* (2014). doi:10.1021/cb4008259
52. Hosohata, K. *et al.* Purification and identification of a novel complex which is involved in androgen receptor-dependent transcription. *Mol. Cell. Biol.* (2003). doi:10.1128/MCB.23.19.7019-7029.
53. Ong, S.-E. & Mann, M. A practical recipe for stable isotope labeling by amino acids in cell culture (SILAC). *Nat. Protoc.* (2007). doi:10.1038/nprot.2006.427
54. Meister, G. *et al.* Methylation of Sm proteins by a complex containing PRMT5 and the putative U snRNP assembly factor pICln. *Curr. Biol.* (2001). doi:10.1016/S0960-9822(01)00592-9
55. Rogers, G. W., Komar, A. A. & Merrick, W. C. eIF4A: the godfather of the DEAD box helicases. *Prog. Nucleic Acid Res. Mol. Biol.* (2002). doi:10.1016/S0079-6603(02)72073-4
56. Sonenberg, N. eIF4E, the mRNA cap-binding protein: from basic discovery to translational research. *Biochem. Cell Biol.* (2008). doi:10.1139/O08-034
57. Calnan, B. J., Tidor, B., Biancalana, S., Hudson, D. & Frankel, A. D. Arginine-mediated RNA recognition: The arginine fork. *Science (80-.).* (1991). doi:10.1126/science.252.5009.1167
58. Allers, J. & Shamoo, Y. Structure-based analysis of protein-RNA interactions using the program ENTANGLE. *J. Mol. Biol.* (2001). doi:10.1006/jmbi.2001.4857
59. Morita, M. *et al.* A Novel 4EHP-GIGYF2 Translational Repressor Complex Is Essential for Mammalian Development. *Mol. Cell. Biol.* (2012). doi:10.1128/MCB.00455-12
60. Uniacke, J. *et al.* An oxygen-regulated switch in the protein synthesis machinery. *Nature* (2012). doi:10.1038/nature11055
61. Musa, J. *et al.* Eukaryotic initiation factor 4E-binding protein 1 (4E-BP1): A master regulator of mRNA translation involved in tumorigenesis. *Oncogene* (2016). doi:10.1038/onc.2015.515
62. Gao, G., Dhar, S. & Bedford, M. T. PRMT5 regulates IRES-dependent translation

via methylation of hnRNP A1. *Nucleic Acids Res.* (2017). doi:10.1093/nar/gkw1367
63. Devaiah, B. N., Gegonne, A. & Singer, D. S. Bromodomain 4: a cellular Swiss army knife. *J. Leukoc. Biol.* (2016). doi:10.1189/jlb.2RI0616-250R
64. Brown, J. D. *et al.* BET bromodomain proteins regulate enhancer function during adipogenesis. *Proc. Natl. Acad. Sci.* (2018). doi:10.1073/pnas.1711155115
65. Lovén, J. *et al.* Selective inhibition of tumor oncogenes by disruption of super-enhancers. *Cell* (2013). doi:10.1016/j.cell.2013.03.036
66. Shi, J. & Vakoc, C. R. The Mechanisms behind the Therapeutic Activity of BET Bromodomain Inhibition. *Molecular Cell* (2014). doi:10.1016/j.molcel.2014.05.016
67. Eram, M. S. *et al.* A Potent, Selective, and Cell-Active Inhibitor of Human Type i Protein Arginine Methyltransferases. *ACS Chem. Biol.* (2016). doi:10.1021/acschembio.5b00839
68. Blum, G., Bothwell, I. R., Islam, K. & Luo, M. Profiling protein methylation with cofactor analog containing terminal alkyne functionality. *Curr. Protoc. Chem. Biol.* (2013). doi:10.1080/13691058.2015.1018949
69. Yount, J. S. *et al.* Palmitoylome profiling reveals S-palmitoylation-dependent antiviral activity of IFITM3. *Nat. Chem. Biol.* (2010). doi:10.1038/nchembio.405
70. Yang, Y. Y., Ascano, J. M. & Hang, H. C. Bioorthogonal chemical reporters for monitoring protein acetylation. *J. Am. Chem. Soc.* (2010). doi:10.1021/ja908871t
71. Lim, J.-H., Choi, Y.-J., Cho, C.-H. & Park, J.-W. Protein arginine methyltransferase 5 is an essential component of the hypoxia-inducible factor 1 signaling pathway. *Biochem. Biophys. Res. Commun.* (2012). doi:10.1016/j.bbrc.2012.01.006
72. Larsen SC, et al. Proteome-wide analysis of arginine monomethylation reveals widespread occurrence in human cells. *Sci Signal* (2016) 9, rs9
73. Musa, J., Orth, M. F., Dallmayer, M., Baldauf, M., Pardo, C., Rotblat, B., … Grünewald, T. G. P. (2016). Eukaryotic initiation factor 4E-binding protein 1 (4E-BP1): A master regulator of mRNA translation involved in tumorigenesis. *Oncogene.* https://doi.org/10.1038/onc.2015.515
74. Sengupta, S., Peterson, T. R., & Sabatini, D. M. (2010). Regulation of the mTOR Complex 1 Pathway by Nutrients, Growth Factors, and Stress. *Molecular Cell*. https://doi.org/10.1016/j.molcel.2010.09.026

Chapter 3: Substrate Profiling of the *S. cerevisiae* PRMT Hmt1

3.1 Introduction

Protein arginine methylation is conserved across eukaryotes, with *S. cerevisiae* possessing multiple type I, II, and III PRMTs as well as a unique type IV PRMT that generates a δ-N-monomethyl- arginine mark rather than the ω-N-methylarginine produced by all other PRMTs.[1,2] Yeast contain homologues to both the major mammalian type I PRMT, PRMT1, in Hmt1 and the major mammalian type II PRMT, PRMT5, in Hsl7.[3–6] Hmt1 shares approximately 50% sequence identity and 70% similarity with human PRMT1. Also like its mammalian homologue, Hmt1 has been demonstrated to generate the majority of methylarginine in yeast cells, with 80-90% of ADMA and 66% of MMA resulting from Hmt1 activity.[5] Like PRMT1, Hmt1 has been shown to methylate histones H2A, H2B, H3, and H4 *in vivo* and methylate H4R3me2a, although this particular modification appears to be transcriptionally repressive in yeast, it activates transcription in mammalian cells.[6,7] This represents an interesting case of highly conserved biochemistry resulting in divergent cellular function. The majority of confirmed Hmt1 substrates are heterogenous ribonucleoproteins (hnRNPs), an abundant group of RNA-binding proteins involved in RNA processing, splicing, and trafficking of RNA between the nucleus and cytosol. Among the most well characterized of these hnRNP substrates is Npl3, which is an mRNA binding protein important both for the transcriptional elongation and nuclear export of its binding partners. Hmt1 dependent methylation of Npl3 is required for proper nuclear export of Npl3 and its associated RNA molecules. Depletion of Hmt1 causes Npl3 to accumulate in the nucleus and subsequent Hmt1 overexpression restores its ability to traffic between the nucleus and cytosol.[8–12]

The regulation of the nuclear export of RNA is the most well understood cellular function of Hmt1 and in fact only around twenty Hmt1 substrates are known.[1,13] Although it appears to be responsible for the majority of arginine methylation in yeast, Hmt1 is not necessary for yeast cell survival and proliferation. Hmt1 deficient yeast cells display no gross phenotype under normal growth conditions. The only reported phenotypes of Hmt1 deficient cells are a dysfunctional heat shock response, increased resistance to inhibitors of ribosomal translation, and greater tolerance for high salt conditions.[10,14,15 16]

The current understanding of Hmt1 function appears to be highly contradictory. Hmt1 is known to be the major PRMT in yeast. Its activity accounts for the majority of arginine methylation in yeast cells under normal growth conditions yet it appears to be entirely dispensable for normal cell growth. Mammalian PRMT1 is known to methylate dozens, if not hundreds, of substrate proteins while Hmt1 has only 41 validated substrates.[1,17–23] The remarkable disparity between the known extent of Hmt1 mediated arginine methylation in yeast cells leads us to hypothesize that there are likely to be far more Hmt1 substrates in yeast cells than have been identified so far. Previous attempts have been made to identify the full scope of Hmt1 substrates using either proteomic shotgun mass spectrometry or affinity purification to identify novel Hmt1 binding proteins.[13,21,24–26] These attempts have largely failed to identify large numbers of novel substrates either because they are trying to identify protein-specific arginine methylation marks in the context of a total proteome, which is difficult to do with sensitivity, or because they are identifying high affinity binders of Hmt1, which may identify a number of proteins that associate with Hmt1 but are not modified by it. Furthermore, these

methods may fail to identify Hmt1 substrates that interact with Hmt1 only weakly and transiently.

Our BPPM technique allows us to enzymatically modify native PMT substrates and then enrich them from a pool of denatured cellular protein, which circumvents the difficulty of directly identifying methylation in a mix of total cellular protein as well as the requirement of interaction at the time of pull-down. Previous uses of BPPM to profile human type I PRMTs have identified significantly more candidate substrates than prior substrate screens of Hmt1.[19,27] BPPM has the ability to evade the shortcomings of more traditional screening techniques used to identify novel Hmt1 substrates in the past and a proven track record of identifying a large number of candidate substrates. We felt that the unique strengths of BPPM make it an ideal technique to uncover Hmt1's full substrate scope and reveal novel biological pathways in which it might play an important role. We were also enthusiastic about our first chance to apply our BPPM to the model organism *S. cerevisiae* which offers a new proving ground for the utility of our technique.

3.2 Results and Discussion

3.2.1 Establising an Hmt1 Mutant-Cofactor Pair *in vitro* Using the Model Substrate Npl3

Our BPPM technique relies on the combination of an active site mutant of the PRMT of interest and a synthetic cofactor the mutant can use to perform alkylation reactions of native substrates. Hmt1 is the yeast homolog of the mammalian protein PRMT1, so we performed both primary amino acid sequence and structural alignments of Hmt1 and PRMT1 which indicated Hmt1 M36 aligns with human PRMT1 M48, which

has been previously mutated to a glycine to perform BPPM profiling of PRMT1 in human cell lines (figure 33).[28 29 19]

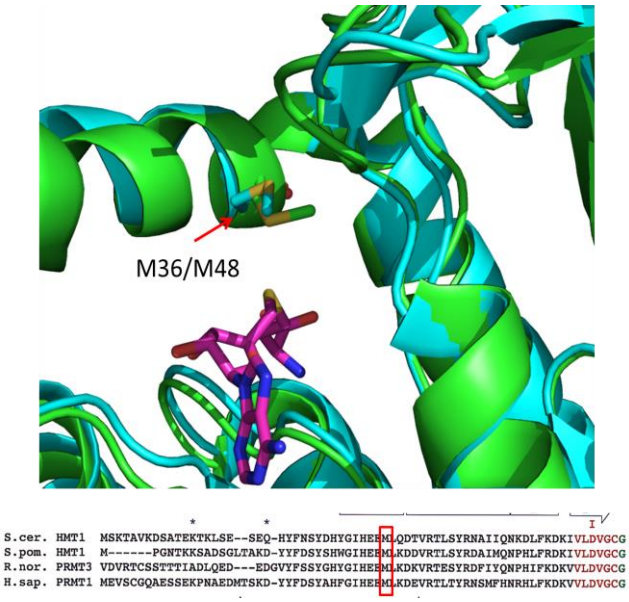

Figure 33: Sequence and structural alignment of S. cerevisiae Hmt1 and R. norvegicus PRMT1

A highly conserved methionine residue corresponding to amino acid 36 in Hmt1 and amino acid 48 in PRMT1 aligns in both the primary amino acid sequence and three-dimensional structure of the two proteins. Hmt1 Pdb ID: 1G6Q; PRMT1 Pdb ID: 1ORH

We received recombinant Hmt1 WT, M36G, the well-characterized catalytic dead mutant G68R,[9] and recombinant Npl3 protein along with yeast strains from the genetic background BY4741 containing all of the aforementioned mutations in the endogenous Hmt1 locus as well as an Hmt1 knockout strain (ΔHmt1) from our collaborator Michael Yu at SUNY Buffalo. With these materials in hand we wanted to assess the *in vitro* activity of our recombinant Hmt1 and the M36G mutant toward Npl3 with radiolabeled SAM using a scintillation assay. We were pleased to observe that Hmt1 M36G has far

lower activity toward SAM than Hmt1 WT (figure 34). We expect a lower affinity for SAM to improve the Hmt1 M36G's labeling efficiency in cell lysates where our synthetic cofactors must compete with endogenous SAM in higher concentrations and a greater propensity to use synthetic SAM analogs should result in more Hmt1-mediated labeling of cellular protein with trackable analogs and less with endogenous SAM, which we cannot track.

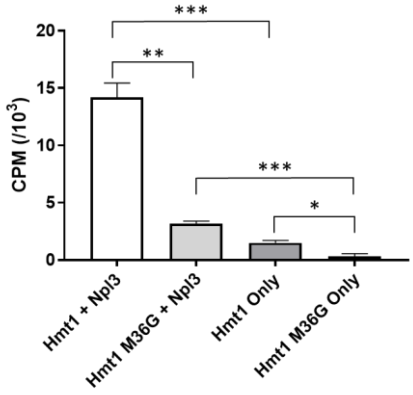

Figure 34: Scintillation Assay of Hmt1 WT and M36G labeling of Npl3

Hmt1 WT or M36G was incubated with its known substrate protein Npl3 (+Npl3) or with no substrate protein (Hmt1 only) overnight in the presence of tritiated SAM followed by activity measurement by scintillation.

Once we established that recombinant Hmt1 was active under reaction conditions that we had previously used we wished to determine whether Hmt1 M36G was capable of selectively modifying Npl3 using our synthetic cofactors Hey-SAM and Pob-SAM. We performed methylation reactions with recombinant Npl3 and either Hmt1 WT or M36G with either Hey-SAM or Pob-SAM and evaluated the degree of modification of Npl3 using in-gel fluorescence. We determined that Hmt1 M36G could use either Hey-SAM or Pob-SAM to modify Npl3 with the degree of modification from Pob-Sam so great that it

causes a noticeable mass shift (figure 35). This mass shift is likely caused by multiple labeling events on single Npl3 polypeptides, which contains 14 RGG methylation motifs, resulting in an observable mass shift from multiple 0.5 kD TAMRA dye molecules. Hmt1 WT cannot modify Npl3 using Hey-SAM to any appreciable extent but does appear to modify Npl3 using Pob-SAM. From this we concluded that Hmt1 M36G uses Hey-SAM selectively over Hmt1 WT while both M36G and WT can use Pob-SAM. This indicates that using Pob-Sam in the context of cell lysates would likely afford higher background than Hey-SAM as endogenous Hmt1 WT would be able to label cellular proteins with Pob-SAM even in the absence of an Hmt1 M36G mutant. This is highly undesirable, as other endogenous PRMTs, PKMTs, and non-protein methyltransferases might also be able to use Pob-SAM in a cellular context, resulting in broad non-specific labeling of cell lysates by Pob-SAM.

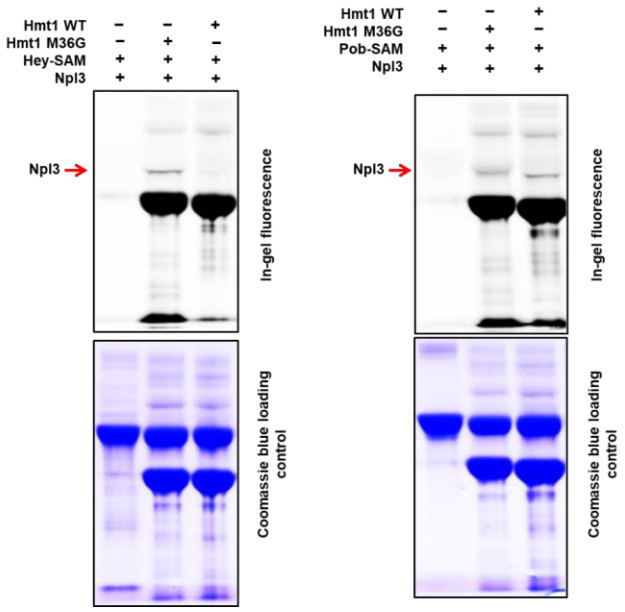

Figure 35: In-gel fluorescence of in vitro labeling of Npl3 by Hmt1 M36G

Reaction between either Hmt1 WT or M36G and Npl3 with Hey-SAM or Pob-SAM as a cofactor shows that Npl3 is selectively modified by Hmt1 M36G when Hey-SAM is used as a substrate. Hmt1 M36G and WT modify Npl3 comparably when Pob-SAM is used as a substrate. (Experiment performed by Dr. Chamara Senevirathne)

3.2.2 Selective Labeling of *S. cerevisiae* Cell Lysates Using a Mutant-Cofactor Pair

Once we determined that Hmt1 M36G was capable of selectively labeling Npl3 *in vitro* using Hey-SAM as a cofactor our next goal was to establish that Hmt1 M36G was broadly capable of labeling proteins in yeast cell lysate selectively over Hmt1 WT. To this end we grew yeast strains expressing Hmt1 WT, M36G, G68R, or ΔHmt1 overnight until they reached stationary phase to obtain as much material as possible. These cells were then lysed, the lysates incubated with Hey-SAM, subjected to CuAAC with TAMRA-azide and analyzed for fluorescence labeling. We observed several reproducible bands that appeared only in Hmt1 M36G expressing lysates, indicating that our Hmt1 M36G mutant is capable of selective labeling in the context of stationary phase yeast cell lysates (figure 36).

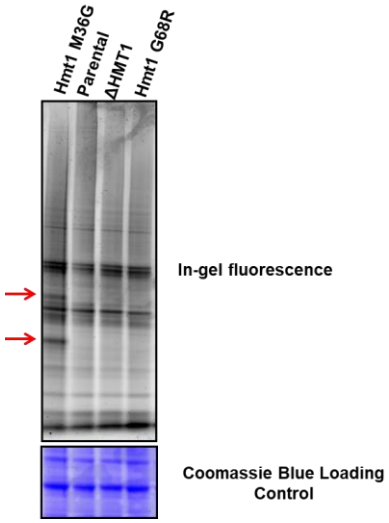

Figure 36: In-gel fluorescence of S. cerevisiae cell lysates harvested in stationary phase

Red arrows show distinct bands dependent on the expression of active Hmt1 M36G mutant.

It has been shown that yeast cells contain as much as seven-fold more ADMA and twice as much MMA during log-phase growth compared to stationary phase. [30] Due to this large disparity we determined that profiling Hmt1 substrates in yeast cells growing in log phase would give us a more complete picture of Hmt1's full substrate scope. We performed in-gel fluorescence experiments in yeast cell lysates harvested in mid log phase and determined that selective labeling of these lysates was comparable to that of stationary phase lysate and background signal was lower (figure 37). Our in-gel fluorescence labeling experiment in log-phase cell lysates demonstrated that our mutant-cofactor pair and labeling protocol is sufficient to provide selective labeling of yeast cells during the most biologically relevant period of growth. We felt comfortable using this

protocol in a large-scale mass spectrometry profiling experiment to identify novel Hmt1 substrates.

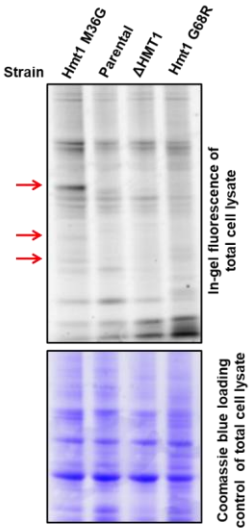

Figure 37: In-gel fluorescence labeling of S. cerevisiae cell lysates harvested during log-phase growth

Red arrows show Hmt1 M36G dependent labeling.

3.2.3 Large Scale Substrate Profiling of Hmt1 Using Tandem Mass Tag Mass Spectrometry

Our BPPM technique allows us to selectively label substrates of a PMT of interest in a cell lysate, but in addition to true targets our technique identifies many high abundance proteins and nonspecific binders to the beads we use in our pull-down technique. To circumvent the issue of these background proteins and prevent them from overwhelming our true signal, we employ quantitative MS techniques with a negative control group in addition to our positive control to identify nonspecific binders and enrich for true targets. In our profiling experiments of PRMT5 we used SILAC to differentiate

samples from each other and allow quantitative profiling with a negative control. SILAC relies on the addition of isotopically labeled supplemental amino acids to cell growth media which are then used in protein synthesis to generate proteins which have a distinct mass from the proteins of cells grown in normal media. Our protocol in human cells uses labeled lysine, which is an essential amino acid in human cells, and arginine, which is conditionally essential in human cells.[31 32] The yeast strain we used for all of our previous experiments is capable of synthesizing its own lysine and arginine so adapting our SILAC protocol to yeast would require us to generate our Hmt1 knockout and M36G mutants in a strain with a background that is auxotrophic for both lysine and arginine and repeat all of our prior in-gel fluorescence experiments to ensure that our results held in this new auxotrophic strain. Rather than doing this we chose to instead make use of a different technique for quantitative MS analysis called tandem mass tagging (TMT) which makes use of easily identifiable mass "barcodes" that are appended to peptides at the end of the processing for MS analysis (figure 38).[33]

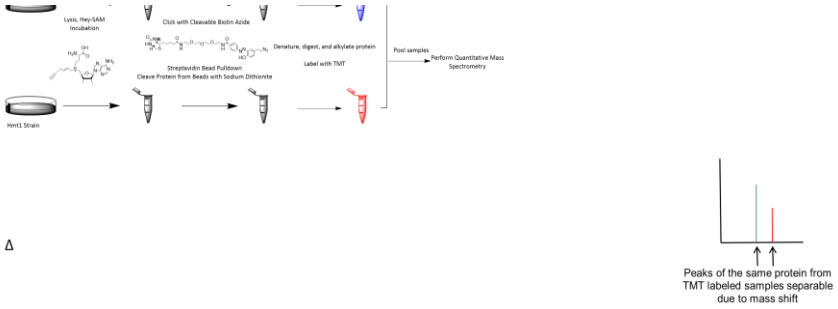

Figure 38: Workflow schematic for BPPM Hmt1 substrate profiling

Tandem mass tag technology is used for quantitative mass spectrometry analysis because the yeast strain used is capable of both lysine and arginine biosynthesis, making it an unsuitable system for SILAC.

TMT is easily adaptable to protein samples from any cell type or organism, unlike SILAC, which requires knowledge of the metabolism of the cells of interest to maximize the signal to noise ratio. To this end, we prepared triplicate samples of matched Hmt1 M36G and ΔHmt1 cell lysates of cells harvested in mid-log phase and treated with Hey-SAM. These Hey-SAM treated triplicates were analyzed by in-gel fluorescence to ensure that they showed selective labeling consistent with previous experiments prior to MS analysis (figure 39).

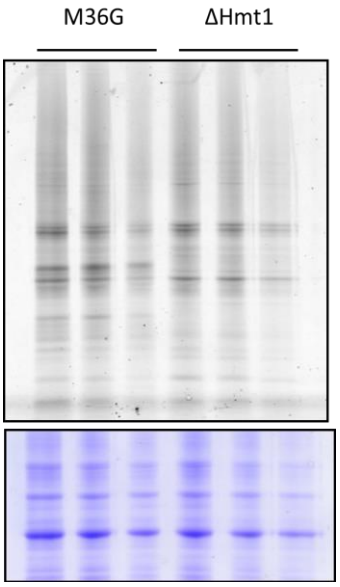

Figure 39: In-gel fluorescence analysis of triplicates of Hmt1 M36G and ΔHmt1 expressing cell lysates

These triplicate samples were used in TMT-MS substrate profiling.

We performed TMT MS analysis of our triplicate Hmt1 M36G ΔHmt1 sample pairs and found 872 proteins that appeared in all three of our samples, of which 540 were enriched in our Hmt1 M36G strain (figure 40). We created a curated list of all proteins with a M36G/ΔHmt1 ratio greater than 1 and a p-value ≥ 0.05 by annotating their known

biological functions and excluding those proteins with known roles in the yeast cell. The top 50 hits are included in a table below (table 4). We wished to crosscheck our list of candidate substrates against previously described Hmt1 substrates. We found that 21 of the 41 previously validated Hmt1 substrates were enriched in our Hmt1 M36G samples and no previously validated substrates were enriched in our ΔHmt1 negative control (table 5). We were encouraged by our data set's recapitulation of previous studies as it increases our confidence in the likely validity of our novel candidate substrates. Despite our confidence, we will need to directly validate each of our novel candidate substrates in order to demonstrate that they are bona fide Hmt1 substrates in a cellular context.

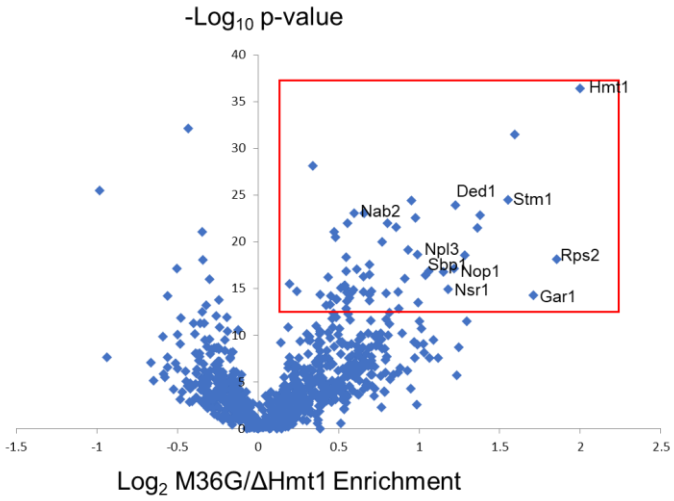

Figure 40: Volcano plot of proteins found in our TMT MS experiment.

Proteins within the red box correspond have a p-value of .05 or less and surpass the median enrichment threshold of .115. Previously identified Hmt1 substrates that fit these criteria are labeled.

Gene Name	Mean Enrichment	p-value
HMT1	3.994333333	0.000228092
THO1	3.02	0.000707529
PRO3	1.266666667	0.00153539
STM1	2.935333333	0.00357213

YPR172W	1.935333333	0.0036159
DED1	2.340666667	0.00406205
GCS1	1.579333333	0.00496972
NAB2	1.511666667	0.00497691
PUB1	2.598	0.00516484
LSM4	1.969333333	0.00551727
GLO2	1.747	0.00629327
RIB3	1.470666667	0.00629871
SEC13	1.81	0.00697714
YRA2	2.572	0.00714143
SOD1	1.389333333	0.00785324
MDE1	1.394333333	0.00892663
LSC1	1.705	0.0100002
RPS9A	1.908333333	0.0121853
NPL3	1.987666667	0.0136136
URA3	2.434333333	0.0140133
GRX3	1.459666667	0.0145614
RPS2	3.614333333	0.0153046
SSB1	1.613333333	0.0174766
NOP1	2.324666667	0.0193524
NFU1	1.530333333	0.0198464
YPT52	1.459333333	0.0206242
RPN13	2.085333333	0.0206843
SBP1	2.223	0.0208642
CCT6	1.615333333	0.0225505
TPM2	2.053333333	0.0229841
MDH3	1.575	0.0237148
RPS5	1.353	0.0240007
ABP1	1.878666667	0.0245945
ARO4	1.144	0.0281828
RTN1	1.451333333	0.0291816
GCV3	1.45	0.0294828
HOM3	1.428333333	0.0310553
RKI1	1.454666667	0.031159
NSR1	2.263333333	0.032241
GUK1	1.508666667	0.0328844
YIP4	1.630333333	0.0337919
TYS1	1.182	0.0338351
BNA1	1.572	0.0344996
DBP2	1.827333333	0.0346813
CKS1	1.463	0.0348167
GIS2	1.496666667	0.0348969
ERV2	1.736	0.035453
PNC1	1.306333333	0.0365763

TIF5	1.613	0.0369567

Table 4: 50 most highly enriched hits in TMT-BPPM triplicate

A full list of enriched proteins is included in appendix 2.

Substrate	In BPPM Data Set?	Enrichment	p-value
HMT1	Y	3.9943	0.000228
RPS2	Y	3.6143	0.015305
GAR1	Y	3.2663	0.037589
STM1	Y	2.9353	0.003572
DED1	Y	2.3407	0.004062
NOP1	Y	2.32467	0.019352
NSR1	Y	2.2633	0.032241
SBP1	Y	2.2233	0.020864
NPL3	Y	1.98767	0.013614
NAB2	Y	1.51167	0.004977
HRP1	Y	1.47533	0.211265
YRA1	Y	1.29967	0.114346
LHP1	Y	1.146	0.782739
IMD4	Y	1.135	0.372425
PAB1	Y	1.0787	0.507807
GUS1	Y	0.9717	0.844086
UGP1	Y	0.9557	0.855987
RRP43	Y	0.8863	0.832909
NUG1	Y	0.8773	0.771442
HTS1	Y	0.84	0.370894
PRP43	Y	0.783	0.507887
HHF1	N	N/A	N/A
HHF12	N	N/A	N/A
HRB1	N	N/A	N/A
SNF2	N	N/A	N/A
THO2	N	N/A	N/A
SCD6	N	N/A	N/A
RPD3	N	N/A	N/A
SNF2	N	N/A	N/A
BRR1	N	N/A	N/A
DIA4	N	N/A	N/A
MPP10	N	N/A	N/A
MRD1	N	N/A	N/A
RPA43	N	N/A	N/A
SPP381	N	N/A	N/A
UTP4	N	N/A	N/A
AIR2	N	N/A	N/A

GBP2	N	N/A	N/A
SNP1	N	N/A	N/A
CDC11	N	N/A	N/A
POB3	N	N/A	N/A

Table 5: Status of previously identified Hmt1 substrates in our MS data set

21 of the 41 previously described Hmt1 substrates were enriched in our data set. 9 of the 21 substrates enriched in the BPPM data set are among the 50 most highly enriched hits in the data set.

We next sought to gain some overall understanding of our enriched data set to gain a bird's eye view of important pathways and biological functions in which Hmt1 may play a role. We performed a pathway analysis on our set of 540 enriched proteins as well as an enrichment analysis for gene ontology (GO) terms using yeast-ConsensusPathDB.[34] We expected to find mRNA processing and export among the most heavily enriched pathways due to Hmt1's well-characterized role in the function of several hnRNPs.[11,35] To our surprise, the most enriched pathway was not mRNA export, but the constellation of pathways revolving around ribosome assembly, translation initiation, and translation elongation (figure 41). There have been ribosomal component proteins reported as Hmt1 substrates, but we expected to see a far greater effect on proteins involved in transcription and nuclear export. No studies have been conducted that show a role for Hmt1 in translation initiation.[15]

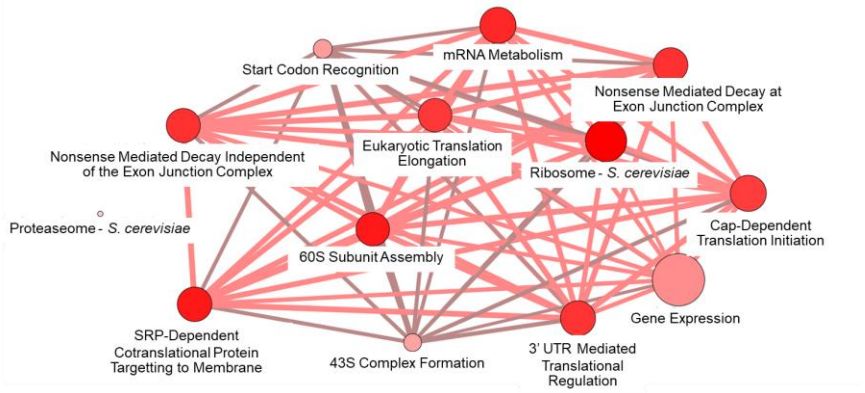

Figure 41: Connectivity map comprising analysis of major pathways enriched in Hmt1 substrate data set

The majority enriched pathways are related to ribosome assembly and translation.

The GO terms of highest significance in our gene enrichment analysis (once we excluded terms such as "metabolic process" or "cellular process" which we did not consider precise enough to be informative) were more closely aligned to our expectations and previous understanding of Hmt1 biology (table 6). We observed such GO terms as RNA binding, cytoplasmic transport, and RNA export from nucleus alongside ribosome biogenesis, which would seem to support the enriched groups we observed in our pathway analysis. The results of our gene enrichment analysis indicate that hnRNP function and RNA processing and localization are among the most enriched biological processes in our candidate substrate set, which recapitulates previous knowledge of the topic. One possible reason for the disparity between our pathway and gene enrichment analyses may be due to a difference in the sheer number of proteins involved in translation versus nuclear export; or the more detailed annotation of the former process compared to the latter.

GO Term	p-value	Total genes in Category	Genes in Data Set
RNA metabolic process	5.96E-08	1307	25
gene expression	8.05E-08	1615	38
RNA binding	0.0000131	557	25
cytoplasmic transport	0.000122	535	14
oxoacid metabolic process	0.000122	410	14
organonitrogen compound biosynthetic process	0.000122	367	14
metal ion binding	0.000244	809	13
ribosome biogenesis	0.000488	346	12
small molecule biosynthetic process	0.000488	321	12
nucleobase-containing compound transport	0.000977	150	11
protein complex subunit organization	0.00195	389	10
nuclear transport	0.00195	171	10
coenzyme metabolic process	0.00391	145	9
macromolecular complex assembly	0.00391	476	9
hydrolase activity, acting on acid anhydrides, in phosphorus-containing anhydrides	0.00391	417	9
actin cytoskeleton organization	0.00781	103	8
cytoskeleton organization	0.00781	227	8
macromolecule modification	0.00781	767	8
RNA export from nucleus	0.00781	90	8
DNA binding	0.00781	591	8

Table 6: Most highly enriched GO terms in Hmt1 candidate substrates

Our TMT mass spectrometry screen succeeded in recapitulating the majority of known Hmt1 substrates and functions in our analysis while also pointing to a major role for Hmt1in ribosome assembly and functional translation, a process in which it has been

implicated but not necessarily known to play an essential role. The broad trends of our data set point to RNA processing and translation as area of known Hmt1 function but far broader scope than has been previously reported. Our data implicates Hmt1 as a modifier of dozens of proteins involved in these processes rather than the several previously known. While we plan to work toward systemic analyses of these processes, particularly translation in collaboration with the Yu group, we first chose to focus on individual proteins which we thought might result in interesting phenotypes on their own.

3.2.4 Investigations of the Role of Hmt1 in DNA Replication and Repair

A small-scale pilot experiment that we performed prior to our large-scale triplicate showed Pol30 was the most highly enriched protein in our data set. This greatly interested us as Pol30 functions as the sliding clamp for meiotic DNA replication in *S. cerevisiae* and is therefore essential for proper S-phase DNA replication, cell growth, and a robust DNA damage response.[36] Since we had a ΔHmt1 yeast strand in hand alongside an Hmt1 WT strain with an identical genetic background we decided to compare the growth rate, cell cycle, progression, and sensitivity to DNA damage of the two strains. Any growth difference would indicate that Hmt1 plays an important role in these processes and suggest that Pol30 is a likely candidate protein through which Hmt1 effects this phenotype. We investigated the effect of Hmt1 on growth rate by monitoring yeast cell density over time in suspension culture and calculating doubling time of OD in log-phase growth. We observed no significant difference in growth rate or doubling time between Hmt1 WT, 36G, or ΔHmt1 strains (figure 42).

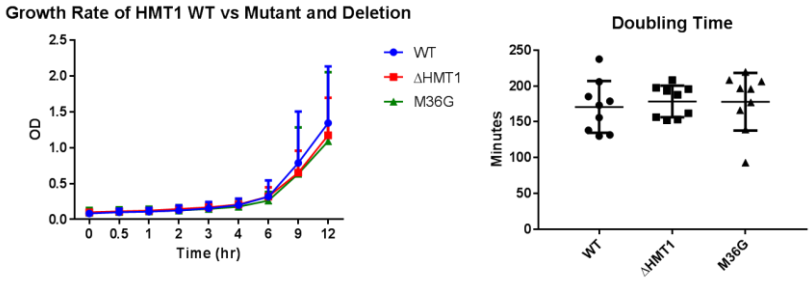

Figure 42: Growth rate and doubling time of yeast cells expressing Hmt1 WT, M36G, or ΔHmt1 were not significantly different

We then analyzed the cell cycle progression of our three yeast strains using flow cytometry to measure DNA content of asynchronous cells by propidium iodide staining. We observed a modest but statistically significant increase in cells in the proportion of Hmt1 M36G cells in G1 phase compared to WT. However, we observed no difference between WT and ΔHmt1 cell cycle occupancy (figure 43). This extremely modest cell cycle difference combined with the lack of observed difference in growth rates convinced us that Hmt1 is not important for cell growth and cell cycle progression under normal conditions and that any possible Hmt1 mediated methylation of Pol30 is either unimportant for normal cell growth or entirely redundant with the activity of other PRMTs.

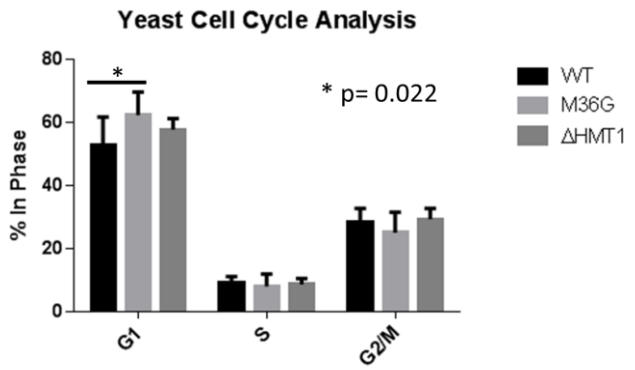

Figure 43: Cell cycle analysis of asynchronous cells with variable Hmt1 expression

We observed a modest increase in G1 occupancy of Hmt1 M36G compared to WT and no difference between any other treatments.

Since we observed no changes in cell growth under normal conditions in Hmt1knockout cells and Pol30 has been shown to play a role in DNA repair as well as normal replication we decided to examine the effect of Hmt1 on cell growth in the presence of DNA damaging agents.[37] We performed spot assays of Hmt1 WT and ΔHmt1 strains grown on standard yeast growth medium (ypd) plates with varying concentrations of the DNA damaging agents methyl methanesulfonate, camptothecin, and hydoxyurea. We observed no differences in sensitivity to any DNA damaging treatment between Hmt1 WT and ΔHmt1 strains (44).

The lack of differences in cell growth, cell cycle occupancy, and response to DNA damaging agents between Hmt1 WT and knockout cell lines reveals that Hmt1 is dispensable for cell growth under both normal and DNA damaging conditions. From this we can assume that Hmt1 mediated methylation of Pol30 is also dispensable for these functions. We cannot rule out the possibility that arginine methylation of Pol30 is

important for its function due to the potential redundant methylation by other PRMTs. However, we have determined that there is no Hmt1 dependent phenotype that could directly implicate its methylation of Pol30.

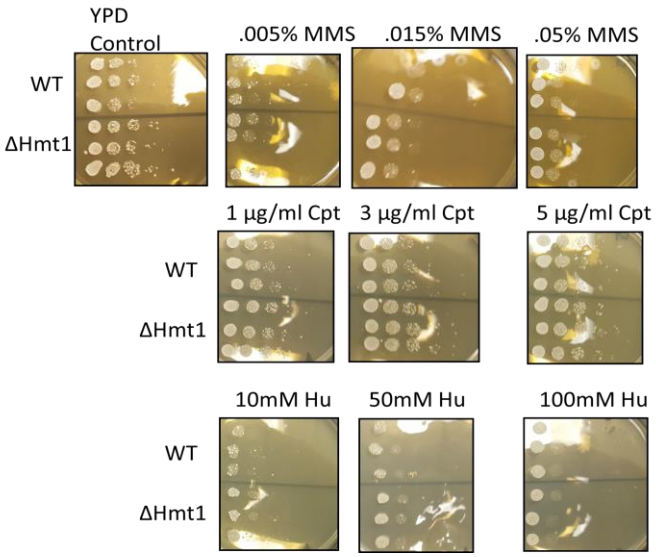

Figure 44: Assessing the role of Hmt1 on susceptibility to DNA damaging agents

We observed no difference in susceptibility between Hmt1 WT and ΔHmt1 to any of the three agents tested.

3.2.5 Investigating the Role of Hmt1 in Pyrimidine Nucleoside Biosynthesis

URA3 and URA6 were among the top hits in our TMT triplicate profiling experiment. They were interesting to us as they function in the same pathway; the biosynthesis of the pyrimidine nucleosides uridine triphosphate (UTP) and cytidine triphosphate (CTP) from glutamine or the salvage of free uracil to generate UTP and CTP (figure 45). Ura3 functions in the biosynthesis of UTP from glutamine by decarboxylating the nucleoside oritidine monophosphate to generate uridine

monophosphate (UMP). Ura6 functions directly downstream of Ura3 as a kinase that phosphorylates UMP to generate uridine diphosphate (UDP) which can then be phosphorylated once again to generate UTP, and CTP after further modification. Ura6 is also essential for the salvage of free uracil to regenerate UTP. Ura3 and Ura6 were particularly interesting to us as candidate Hmt1 substrates because their roles in nucleoside biosynthesis are essential for cell growth and survival. These roles are easy to probe by altering the available nutrients in yeast growth medium and comparing the growth rates of our Hmt1 WT and ΔHmt1 under conditions of nutrient deprivation. This allows facile analysis of the importance of Hmt1 in our pathway of interest and ensures that any substrate proteins we later confirm are methylated by Hmt1 can be easily shown to have a relevant phenotype stemming from this methylation.

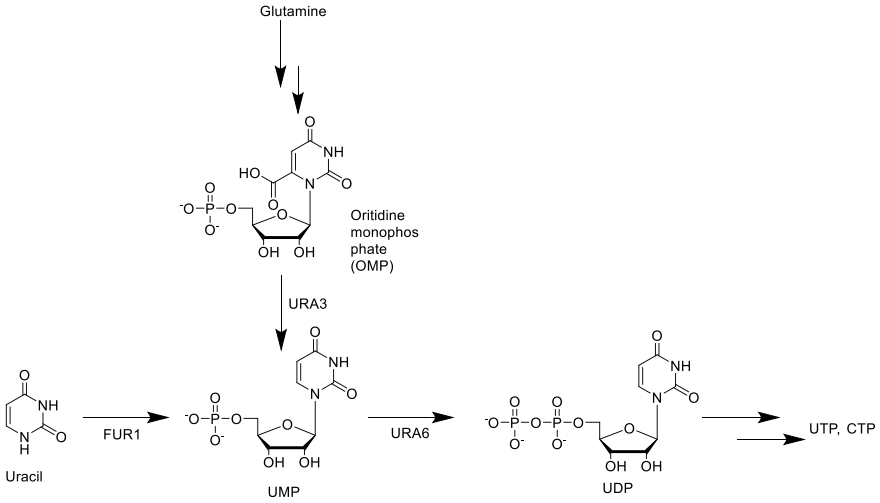

Figure 45: Schematic of the roles of Ura3 and Ura6 in pyrimidine nucleoside biosynthesis

Ura3 is necessary for conversion of oritidine monophosphate to uridine monophosphate while Ura6 is a kinase that converts uridine monophosphate to uridine diphosphate.

The BY4741 strain which serves as our WT parent strain does not express the Ura3 protein however both the Hmt1 M36G and ΔHmt1 strains we used for our profiling experiments have had Ura3 re-expressed as a positive marker for recombination into the Hmt1 locus.[38] The presence of Ura3 expression in both our Hmt1 substrate profiling sample and our negative control means that Ura3 could quite possibly be a bona fide Hmt1 substrate. However, the absence of Ura3 in our WT strain makes analysis of the role of Hmt1 activity on Ura3 function difficult. Since both our Hmt1 WT and ΔHmt1 strains express Ura6 we chose to focus our attention on investigating the possible role of Hmt1 function on Ura6 function. We reasoned that since Ura6 is a necessary enzyme in the process of generating UTP and CTP from uracil, cells with reduced Ura6 activity would be more sensitive to a reduced uracil supply than cells with normal Ura6 activity. Our hypothesis was that Hmt1 methylation likely increased Ura6 activity, so we would expect ΔHmt1 cells to be more sensitive to reduced uracil concentration in their growth medium than Hmt1 WT cells. We tested the role of Hmt1 in pyrimidine nucleoside biosynthesis and by extension Ura6 function by growing either Hmt1 WT or ΔHmt1 yeast strains on plates containing variable uracil concentrations and examining their relative growth rates with spot assays. We did not detect any major changes in growth rate between WT and ΔHmt1 to support our hypothesis (figure 46). We did observe a modest reduction in growth rate in Hmt1 WT compared to ΔHmt1 cells at 10 mg/L uracil, indicating that if there is any pyrimidine biosynthesis phenotype demonstrated by Hmt1 it is a reduction in the efficiency of pyrimidine biosynthesis rather than the increased biosynthetic efficiency we hypothesized. However, the effect we observed only at the lowest uracil concentration was very modest and it appears that our ΔHmt1

cells grow slightly quicker at all uracil concentrations tested, this modest decrease in growth rate may not have anything to do with uracil concentration. Our overall conclusion from our experiments is that we could not observe any phenotype in ΔHmt1 yeast relating to pyrimidine nucleoside biosynthesis pronounced enough to warrant further examination of yeast nutrient requirements within the pathway or biochemical characterization of candidate Hmt1 substrates within the pathway and their methylation sites. While it is entirely possible Hmt1 may methylate one or more proteins in the pyrimidine salvage and biosynthesis pathways, we think that it is unlikely that Hmt1 has a major biological role in the regulation of UTP and CTP biosynthesis.

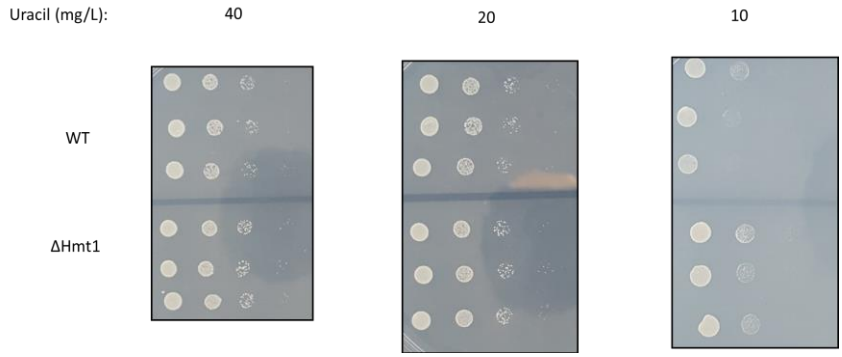

Figure 46: Spot assay comparing uracil dependence of Hmt1 WT and ΔHmt1 yeast

We observed what may be a modest reduction in growth rate of Hmt1 WT compared to ΔHmt1 at 10 mg/L uracil.

3.3 Methods

3.3.1 Yeast Strains and Growth Conditions

The WT yeast strain used in the preceding experiments is the S288C derived BY4741 strain. All Hmt1 mutant or deletion strains were derived from this background. All experiments were performed in haploid yeast. The ΔHmt1 strain has its Hmt1 locus

disrupted by insertion of a kanamycin resistance cassette. The Hmt1 M36G mutant strain was derived from the ΔHmt1 strain and generated by the addition of an Hmt1 M36G sequence flanked by a URA3 sequence into the endogenous Hmt1 locus. Yeast cells were grown in standard YPD media (MP Bio) unless stated otherwise. Suspension cultures were grown at 30°C and shaken at 225 rpm while plated cells were grown on YPD containing 2% agar.

3.3.2 Scintillation Assay for Recombinant Hmt1 Activity

The *in vitro* methylation reaction was performed as follows: 2.5 µg Hmt1 WT or M36G protein (expressed and purified from yeast by the Yu group) was incubated with 4 µg Npl3 protein (expressed and purified from yeast by the Yu group) and 0.75 µM C^3H_3 SAM (Perkin Elmer) in either the Yu group's MOPS assay buffer (50mM MOPS pH=7.2, 300mM NaCl, 2mM EDTA, 1mM DTT, .0005% BSA) or HEPES reaction buffer (50 mM HEPES, 1 mM TCEP, .005% Tween 20, .0005% BSA) in a 20 µL total volume at room temperature overnight. The reaction was quenched by blotting reaction mixture onto squares of P81cation-exchange filter paper (GE Healthcare, product discontinued) in 3x 6 µL aliquots. Filter paper was washed (4x 5 minutes) in bicarbonate to neutralize and remove excess SAM before cutting into individual squares, mixed with Ultima Gold scintillation solution (Perkin Elmer) and analalyzed with a Perkin Elmer Tri-Carb 2910 TR Liquid Scintillation Analyzer using the tritium channel giving results in counts per minute (CPM). Data were analyzed in graphpad prism and presented as mean ± standard error of the mean. Each result is a technical triplicate of three reads from a single methylation reaction.

3.3.3 Synthesis of SAM Analogs

Hey-SAM and Pob-SAM were synthesized as previously reported using reagents purchased from Sigma Aldrich and used without further purification.[39] Hey-SAM and Pob-SAM were purified by HPLC (Waters 600 Controller HPLC with an XBridge™ Prep C18 5µm OBD™ 19×150mm column), lyophilized, and stored in 0.01% trifluoroacetic acid before use.

3.3.4 Yeast Cell Culture and Lysis

Single colonies of either Hmt1 M36G or ΔHmt1 genotype were picked from YPD agar plates, suspended in YPD media (10 ml total culture volume for in-gel fluorescence and mass shift assays. For MS profiling experiments colonies were grown for 8 hours in 10ml YPD and this overnight culture was diluted into 500 ml YPD.) and grown either overnight (stationary phase experiments) or until reaching an OD 600 of 0.8-1.0 (log phase experiments). Cells were then pelleted by centrifugation and resuspended in 10x cell pellet volume methyltransferase reaction buffer (50 mM HEPES pH 8, 100 mM KCl, 15 mM $MgCl_2$, 10% glycerol) supplemented with 1mM PMSF (Sigma Adrich), 5 mM TCEP (Sigma Aldrich) and 1 tablet of protease inhibitor cocktail (Roche) per 25 ml buffer. Cells were lysed by addition of 1.5g acid washed sterile glass beads (Sigma Aldrich) per gram pelleted cells and 5 rounds of 1 minute of vortexing followed by 1 minute on ice. Lysates were separated from glass beads by piercing the bottom of containers and draining by low speed centrifugation. Lysates were then clarified by centrifugation at 16.1k RCF for 20 minutes followed by separation of the supernatant and quantification of its protein concentration.

3.3.5 Labeling of Cell Lysates with Synthetic SAM Analogs

Equal total masses of protein were used for each condition of interest (typically 50-100 µg total protein for in-gel fluorescence experiments and 10mg total protein for proteomic

experiments) and incubated with 100 µM cofactor (Hey-SAM or Pob-SAM) and 100 nM recombinant MTAN protein (to prevent product inhibition of methyltransferase activity) overnight. Following overnight incubation the reaction was quenched by protein precipiaion either through addition of 3:2:1 Methanol:Water:Chloroform followed by centrifugation for 10 minutes at 16.1k RCF or addition of 25x reaction volume of ice cold methanol and overnight precipitation at -80°C. Regardless of precipitation method, the precipitation protein was washed 2x with cold methanol followed by centrifugation to isolate a pellet of SAM analog labeled protein, which is allowed to dry for ~10 minutes before CuAAC.

3.3.6 CuAAC in Cell Lysates

Preparation of click cocktail: 1 mM $CuSO_4$ and 2 mM BTTP ligand (purchased Albert Einstein College of Medicine Chemical Synthesis Core Facility) were premixed for 60 minutes followed by addition of 2.5 mM Sodium Ascorbate (Sigma Aldrich) to reduce the Cu^{2+} to its active catalyst Cu^{+} state. 250 µM azide reagent (TAMRA-azide purchased from Life Technologies for in-gel fluorescence experiments and cleavable Diazo Biotin-Azide purchased from Click Chemistry Tools for biotin pulldown experiments) is then mixed with the active catalyst to yield our 4-component click cocktail.

Dried SAM analog labeled protein pellets were completely resuspended in click buffer (50 mM TEA, 150 mM NaCl, 2% SDS) and click cocktail added before shaking in the dark for 90 minutes. Reaction was quenched by protein precipitation as outlined above and protein pellets washed 2x with cold methanol and dried for ~10 minutes.

3.3.7 In-gel Fluorescence of SAM Analog Labeled Proteins

All steps prior to scanning the gel on the Typhoon imager were performed with samples covered to prevent loss of fluorescence signal through photobleaching. Dried protein

pellets were resuspended in loading buffer (40 mM Tris pH=6.8, 70 mM SDS, 10 mM EDTA, 10% glycerol, 10% β-ME) without dye to avoid interference with fluorescence signal and separated by SDS-PAGE. SDS-PAGE gels were fixed in 40% methanol, 10% acetic acid overnight to wash out free TAMRA dye and reduce background. After fixing overnight the gel was rinsed in ddH_2O to rehydrate and scanned for fluorescence signal using the TAMRA channel on a Typhoon TRIO variable mode imager (Amersham Bioscience). After fluorescence scanning the gel was stained with coomassie blue to confirm equal protein loading.

3.3.8 Detecting Npl3 Mass Shift after Peg-Azide Click Reaction by Western Blotting

20 μL of clicked reaction mixture was separated by SDS-PAGE, transferred to a nitrocellulose membrane and blocked in 5% BSA for 1 hour at room temperature before overnight incubation with primary antibody at a 1:1000 dilution at 4°C. Membranes were washed 3x with PBST before a 1 hour incubation with HRP-conjugated secondary antibodies (1:5000 dilution). Following by an additional 3x washes with PBST membranes were treated with Luminata™ Crescendo Western HRP Substrate (Millipore) and protein bands detected using a Fujifilm X-A2 digital camera with a KwikQuant Imager attachment. After protein band detection membranes were stained with Ponceau Red (Sigma Aldrich) to confirm equal protein loading between samples. The anti-Npl3 antibody used in this study was generated by the Yu group.

3.3.9 Streptavidin Pulldown of Biotinylated Cellular Protein for MS or Western Blot Analysis

Streptavidin pulldown was carried out as previously reported.[40,41] High capacity streptavidin sepharose resin was purchased from GE Healthcare. All other chemical reagents purchased from Sigma Aldrich. Amicon Ultra 3kD Cutoff Centrifugal Filter Units (Millipore) were used for desalting of biotinylated protein prior to lyophilization.

Samples used in western blot substrate validation were not subjected to iodoacetamide blocking and cysteine reduction and were not lyophilized prior to western blot analysis.

3.3.10 Hmt1 Substrate Profiling by MS

Desalted lyophilized proteins were sent to our collaborators the Haiteng Deng lab at Tsinghua University who performed protein digestion and quantitative MS analysis to determine peptide sequences and match them to known human proteins as previously described.[27] Raw data was received as total peak areas of peptides corresponding to human proteins with light and heavy peptides provided as separate peak areas.

3.3.11 Analysis of MS Data

Identified gene names from each replicate experiment were entered into a pivot table in micorsoft excel to identify all gene names present in all 3 experimental replicates. Those gene names present in all three replicates had mean Hmt1 M36G/ ΔHmt1 ratios determined, with a Log_2 Hmt1 M36G/ ΔHmt1 > 0 indicating enrichment. We performed a two-tailed t-test in excel to assign p-values for the significance of difference in means between the heavy sample values in triplicates versus the light values. We used these enrichment and significance values to generate a volcano plot to visualize any outstanding hits demanding immediate follow-up. In the absence of any hits of this nature we instead performed several annotation steps to characterize our data set. The known functions of our enriched proteins were determined using both the Uniprot annotations and summary of each enriched protein and a PubMed search of the protein name to establish the breadth of studies concerning the protein of interest. Finally, we used the gene set enrichment function in the yeast ConsensusPathDB platform (http://cpdb.molgen.mpg.de) to evaluate cellular pathways and processes that were

overrepresented in our enriched protein data set as well as the pathway mapping function to generate a pathway connectivity map.

3.3.12 Yeast Growth Rate and Doubling Time Assays

Single colonies of Hmt1 WT, M36G and ΔHmt1 yeast cells grown on YPD plates were picked, suspended in 5 ml YPD media and allowed to grow overnight. After overnight growth cell density was determined by OD 600 reading and cells were diluted to an OD of 0.1 in 5 ml fresh YPD and allowed to grow for 12 hours with OD measurements taken at 1, 2, 3, 4, 5, 6, 9, and 12 hours. Doubling time was calculated from the OD change between the 6- and 9-hour time points when cells had entered logarithmic phase growth based on OD. 3 colonies were picked from each strain. Standard deviation and significance from a two-tailed t-test were calculated in graphpad prism.

3.3.13 Cell Cycle Analysis

Single colonies of Hmt1 WT, M36G and ΔHmt1 yeast cells grown on YPD plates were picked, suspended in 5 ml YPD media and allowed to grow overnight. After overnight growth cell density was determined by OD 600 reading and cells were diluted to an OD 600 of 0.1 in 5 ml fresh YPD and allowed to grow to an OD 600 of 0.6-0.8. Cells were then separated from growth media by centrifugation and fixed in ice cold 70% ethanol (10^7 cells/ml). 300 µL of fixed cells were pelleted and ethanol was removed by vacuum before washing in 200 µL of 50 mM sodium citrate followed by pelleting and removal of wash. Cells were resuspended in 500 µL sodium citrate with 250 µg/ ml Rnase A (Sigma Aldrich) and incubated at 50°C for 90 minutes before digesting with the addition of 25 µL of 20mg/ml stock solution Proteinase K (Roche) and incubating at at 50°C for 60 minutes. 500 µL sodium citrate containing 16 µg/ml propidium iodide (Sigma Aldrich) was added to Rnase and proteinase treated cells and stained by shaking for 30 minutes at

room temperature while covered. For FACS analysis 150 µL stained cells was mixed with 150 µL sodium citrate and the DNA content of 10^5 cells in the sample measured by propidium iodide signal using a BD LSRFortessa cell analyzer (BD Biosciences). Flow data was analyzed and cell cycle occupancy of samples determined using FlowJo. Significance was analyzed in Graphpad Prism using a two-tailed t-test. Results represent 3 colonies of each yeast strain.

3.3.14 Yeast Spot Assays for Assessing Sensitivity to DNA Damage

Single colonies of Hmt1 WT and ΔHmt1 yeast cells grown on YPD plates were picked, suspended in 5 ml YPD media and allowed to grow overnight. After overnight growth cell density was determined by OD 600 reading and cells were diluted to an OD of 0.2 before 6 10-fold serial dilutions were performed and 5 µL of each dilution plated in triplicate on YPD plates containing variable concentrations of Hydroxyurea, MMS, or Camptothecin (all purchased from Sigma Aldrich; concentrations indicated in figure). After allowing dilute yeast cells to absorb into agar, plates were wrapped in cling film to prevent drying and allowed to grow at 30°C. Plates were photographed every 24 hours to assess relative growth rates.

3.3.15 Yeast Spot Assays for Assessing Sensitivity to Uracil Deprivation

Single colonies of Hmt1 WT and ΔHmt1 yeast cells grown on YPD plates were picked, suspended in 5 ml YPD media and allowed to grow overnight. After overnight growth cell density was determined by OD 600 reading and cells were diluted to an OD of 0.2 before 6 10-fold serial dilutions were performed and 5 µL of each dilution plated in triplicate on agar plates made with either complete synthetic media (Sigma Aldrich) or Yeast Nitrogen Base without amino acids (BD Biosciences) supplemented with Uracil-free drop out supplements (Sigma Aldrich) with variable Uracil (Sigma Aldrich)

concentrations added. After allowing dilute yeast cells to absorb into agar, plates were wrapped in cling film to prevent drying and allowed to grow at 30°C. Plates were photographed every 24 hours to assess relative growth rates.

3.4 Conclusion

We have successfully completed the engineering and substrate profiling of Hmt1. This marks our first application of BPPM technology in *S. Cerevisiae*. We have previously performed BPPM only in immortalized cell lines which may or may not faithfully recapitulate the biology of complete organisms. The advantage of working in yeast as a model organism for us is that our ability to validate targets in a cellular context allows us to make claims about yeast biology. We have previously developed techniques to perform our BPPM labeling in living human cells and extending this technique to living yeast cells would allow us to label Hmt1 substrates or the substrates of additional yeast PRMTs inside of a living organism. [42] Combining this live cell labeling with cell-compatible click chemistry and fluorescent labels would allow us to observe PRMT dynamics, activity, and localization inside a living organism in real time. This unprecedented live observation of PRMT activity would afford the opportunity to learn a great deal about PRMT activity under homeostatic and stress conditions and the turnover rate and dynamics of PRMT substrates under similar conditions.

Our profiling experiment captured the majority of previously known Hmt1 substrates as well as hundreds of new candidates. The number of targets identified makes it far and away the most extensive screen directly implicating targets of Hmt1 performed so far to our knowledge. We have identified candidate substrates that are members of protein families that have been previously shown to be arginine methylated in yeast such as THO1, hnRNPs, and ribosomal component proteins. Our future work now lies in fully

fleshing out and exploring the new targets and hypotheses we have generated from our screen. We must directly validate any proteins substrates of interest identified in the screen before we can make claims about their biology. We have not yet observed any novel or interesting phenotypes attributable to targets identified in our screen. Our plan to identify these phenotypes rests in our observation that many candidate Hmt1 substrates are ribosomal component proteins or proteins important for ribosomal assembly. We plan to identify any Hmt1 dependent methylation sites on these proteins and then perturb methylation sites we identify to assay potential changes in translation arising from the sum of many likely minor Hmt1-methylation changes in function.

3.5 References

1. Low, J. K. K. & Wilkins, M. R. Protein arginine methylation in Saccharomyces cerevisiae. *FEBS J.* **279**, 4423–4443 (2012).
2. Niewmierzycka, A. & Clarke, S. S-Adenosylmethionine-dependent Methylation in Saccharomyces cerevisiae. *J. Biol. Chem.* (1999). doi:10.1074/jbc.274.2.814
3. Tang, J. *et al.* PRMT1 is the predominant type I protein arginine methyltransferase in mammalian cells. *J. Biol. Chem.* (2000). doi:10.1074/jbc.275.11.7723
4. Stopa, N., Krebs, J. E. & Shechter, D. The PRMT5 arginine methyltransferase: Many roles in development, cancer and beyond. *Cellular and Molecular Life Sciences* (2015). doi:10.1007/s00018-015-1847-9
5. Gary, J. D., Lin, W. J., Yang, M. C., Herschman, H. R. & Clarke, S. The predominant protein-arginine methyltransferase from Saccharomyces cerevisiae. *J. Biol. Chem.* (1996). doi:10.1074/jbc.271.21.12585
6. Miranda, T. B. *et al.* Yeast Hsl7 (histone synthetic lethal 7) catalyses the in vitro formation of omega-N(G)-monomethylarginine in calf thymus histone H2A. *Biochem. J.* (2006). doi:10.1042/BJ20051771
7. Wang, H. *et al.* Methylation of Histone H4 at Arginine 3 Facilitating Transcriptional Activation by Nuclear Hormone Receptor. *Science (80-.).* (2001). doi:10.1126/science.1060781
8. Wong, C. M. *et al.* Yeast arginine methyltransferase Hmt1p regulates transcription elongation and termination by methylating Npl3p. *Nucleic Acids Res.* (2010).

doi:10.1093/nar/gkp1133

9. McBride, A. E., Weiss, V. H., Kim, H. K., Hogle, J. M. & Silver, P. A. Analysis of the yeast arginine methyltransferase Hmt1p/Rmt1p and its in vivo function. Cofactor binding and substrate interactions. *J. Biol. Chem.* (2000). doi:10.1074/jbc.275.5.3128

10. Yu, M. C. *et al.* Arginine methyltransferase affects interactions and recruitment of mRNA processing and export factors. *Genes Dev.* (2004). doi:10.1101/gad.1223204

11. Shen, E. C. *et al.* Arginine methylation facilitates the nuclear export of hnRNP proteins. *Genes Dev.* (1998). doi:10.1101/gad.12.5.679

12. Xu, C. & Henry, M. F. Nuclear export of hnRNP Hrp1p and nuclear export of hnRNP Npl3p are linked and influenced by the methylation state of Npl3p. *Mol. Cell. Biol.* (2004). doi:10.1128/MCB.24.24.10742-10756.2004

13. Plank, M. *et al.* Expanding the yeast protein arginine methylome. *Proteomics* (2015). doi:10.1002/pmic.201500032

14. Giaever, G. *et al.* Functional profiling of the Saccharomyces cerevisiae genome. *Nature* (2002). doi:10.1038/nature00935

15. Al-Hadid, Q., White, J. & Clarke, S. Ribosomal protein methyltransferases in the yeast Saccharomyces cerevisiae: Roles in ribosome biogenesis and translation. *Biochem. Biophys. Res. Commun.* (2016). doi:10.1016/j.bbrc.2016.01.107

16. Forment, J., Mulet, J. M., Vicente, O. & Serrano, R. The yeast SR protein kinase Sky1p modulates salt tolerance, membrane potential and the Trk1,2 potassium transporter. *Biochim. Biophys. Acta - Biomembr.* (2002). doi:10.1016/S0005-2736(02)00503-5

17. Yang, Y. & Bedford, M. T. Protein arginine methyltransferases and cancer. *Nature Reviews Cancer* (2013). doi:10.1038/nrc3409

18. Bedford, M. T. Arginine methylation at a glance. *J. Cell Sci.* (2007). doi:10.1242/jcs.019885

19. Wang, R., Zheng, W., Yu, H., Deng, H. & Luo, M. Labeling substrates of protein arginine methyltransferase with engineered enzymes and matched S-adenosyl-l-methionine analogues. *J. Am. Chem. Soc.* (2011). doi:10.1021/ja2006719

20. Low, J. K. K. *et al.* Protein substrates of the arginine methyltransferase Hmt1 identified by proteome arrays. *Proteomics* **16**, 465–476 (2016).

21. Jackson, C. A. *et al.* Proteomic analysis of interactors for yeast protein arginine methyltransferase Hmt1 reveals novel substrate and insights into additional biological roles. *Proteomics* (2012). doi:10.1002/pmic.201200132

22. Low, J. K. K., Hart-Smith, G., Erce, M. A. & Wilkins, M. R. Analysis of the proteome of Saccharomyces cerevisiae for methylarginine. *J. Proteome Res.* **12**, 3884–3899 (2013).

23. Lien, P. T. K. *et al.* Analysis of the physiological activities of Scd6 through its interaction with Hmt1. *PLoS One* **11**, 1–19 (2016).

24. Erce, M. A., Pang, C. N. I., Hart-Smith, G. & Wilkins, M. R. The methylproteome and the intracellular methylation network. *Proteomics* (2012). doi:10.1002/pmic.201100397

25. Erce, M. A., Abeygunawardena, D., Low, J. K. K., Hart-Smith, G. & Wilkins, M. R. Interactions Affected by Arginine Methylation in the Yeast Protein–Protein Interaction Network. *Mol. Cell. Proteomics* (2013). doi:10.1074/mcp.M113.031500

26. Milliman, E. J., Hu, Z. & Yu, M. C. Genomic insights of protein arginine methyltransferase Hmt1 binding reveals novel regulatory functions. *BMC Genomics* (2012). doi:10.1186/1471-2164-13-728

27. Guo, H. *et al.* Profiling substrates of protein arginine N-methyltransferase 3 with S-adenosyl-L-methionine analogues. *ACS Chem. Biol.* (2014). doi:10.1021/cb4008259

28. Weiss, V. H. *et al.* The structure and oligomerization of the yeast arginine methyltransferase, Hmt1. *Nat. Struct. Biol.* (2000). doi:10.1038/82028

29. Zhang, X. & Cheng, X. Structure of the predominant protein arginine methyltransferase PRMT1 and analysis of its binding to substrate peptides. *Structure* (2003). doi:10.1016/S0969-2126(03)00071-6

30. Lakowski, T. M. *et al.* Arginine methylation in yeast proteins during stationary-phase growth and heat shock. *Amino Acids* (2015). doi:10.1007/s00726-015-2047-5

31. Ong, S.-E. & Mann, M. A practical recipe for stable isotope labeling by amino acids in cell culture (SILAC). *Nat. Protoc.* (2007). doi:10.1038/nprot.2006.427

32. Young, V. R. Adult amino acid requirements the case for a major revision in current recommendations. *J. Nutr.* (1994). doi:1517S-1523S

33. Thompson, A. *et al.* Tandem mass tags: A novel quantification strategy for comparative analysis of complex protein mixtures by MS/MS. *Anal. Chem.* (2003). doi:10.1021/ac0262560

34. Herwig, R., Hardt, C., Lienhard, M. & Kamburov, A. Analyzing and interpreting genome data at the network level with ConsensusPathDB. *Nat. Protoc.* (2016). doi:10.1038/nprot.2016.117

35. Green, D. M. *et al.* Nab2p is required for poly(A) RNA export in Saccharomyces

cerevisiae and is regulated by arginine methylation via Hmt1p. *J. Biol. Chem.* (2002). doi:10.1074/jbc.M110053200

36. Bauer, G. A. & Burgers, P. M. Molecular cloning, structure and expression of the yeast proliferating cell nuclear antigen gene. *Nucleic Acids Res.* (1990).

37. Hoege, C., Pfander, B., Moldovan, G. L., Pyrowolakis, G. & Jentsch, S. RAD6-dependent DNA repair is linked to modification of PCNA by ubiquitin and SUMO. *Nature* (2002). doi:10.1038/nature00991

38. Brachmann, C. B. *et al.* Designer deletion strains derived from Saccharomyces cerevisiae S288C: A useful set of strains and plasmids for PCR-mediated gene disruption and other applications. *Yeast* (1998). doi:10.1002/(SICI)1097-0061(19980130)14:2<115::AID-YEA204>3.0.CO;2-2

39. Blum, G., Bothwell, I. R., Islam, K. & Luo, M. Profiling protein methylation with cofactor analog containing terminal alkyne functionality. *Curr. Protoc. Chem. Biol.* (2013). doi:10.1080/13691058.2015.1018949

40. Yount, J. S. *et al.* Palmitoylome profiling reveals S-palmitoylation-dependent antiviral activity of IFITM3. *Nat. Chem. Biol.* (2010). doi:10.1038/nchembio.405

41. Yang, Y. Y., Ascano, J. M. & Hang, H. C. Bioorthogonal chemical reporters for monitoring protein acetylation. *J. Am. Chem. Soc.* (2010). doi:10.1021/ja908871t

42. Wang, R. *et al.* Profiling genome-wide chromatin methylation with engineered posttranslation apparatus within living cells. *J. Am. Chem. Soc.* (2013). doi:10.1021/ja309412s

Chapter 4: Summary and Future Perspectives

4.1 Summary

This work describes the application of the BPPM platform for identifying novel methyltransferase substrates to the human type II arginine methyltransferase PRMT5 and the yeast type I arginine methyltransferase Hmt1 as well as subsequent efforts to validate targets identified in these profiling experiments and investigate their biological function. PRMT5, the major type II human PRMT, was engineered to accept synthetic SAM analogs relying on sequence and structural homology with previously engineered type I human PRMTs. Substrate profiling of human PRMT5 was performed using SILAC in Hek293T cells identifying hundreds of proteins selectively enriched in BPPM-active PRMT5 mutant containing cell lysates. Several of the top hits from this profiling experiment were validated using a BPPM biotin enrichment-western blot strategy, though some known targets could not be validated by this strategy. The translation initiation regulating protein 4EBP1 was chosen as a target of interest due to its known role as a regulator of translation initiation downstream of the mTOR signaling pathway.[1] 4EBP1 was validated as a PRMT5 substrate in the context of Hek293T cells using BPPM and validated as a substrate of PRMT5 and PRMT1 *in vitro* using native enzymes. However, attempts to demonstrate a role for arginine methylation in regulating 4EBP1 phosphorylation and mRNA cap binding complex association did not identify a clear PRMT-dependent phenotype. There are still obstacles in understanding the functional role of arginine methylation on 4E-BP1.

This work represents the first application of the BPPM platform to a type II PRMT and

PRMT5 and demonstrates that homology to a type I PRMT allows for the successful active site engineering of non-type I PRMTs. The validation of 4EBP1 as a PRMT5 substrate in cells using BPPM and *in vitro* using wildtype enzyme indicates that PRMT5 and PRMTs more broadly may play a role in the regulation of translation initiation in humans. The challenges faced in identifying a role for PRMT5 in the regulation of 4EBP1 function highlight the inherent difficulty of identifying and characterizing arginine methylation-dependent regulation of protein function.

Hmt1, the major arginine methyltransferase in *S. cerevisiae*, was engineered to accept synthetic SAM analogs in collaboration with the Yu group at SUNY Buffalo. BPPM substrate profiling of Hmt1 in yeast cell lysates was performed using TMT mass spectrometry. This substrate profiling experiment recapitulated the majority of previously identified Hmt1 substrates as well as identifying over 300 previously undescribed putative Hmt1 substrates including many proteins known to be involved in RNA binding and translation regulation. Roles for Hmt1 in the regulation of UTP metabolism, cell growth, and cell cycle progression were investigated using Hmt1-deficient yeast cells, though no phenotypes have been identified yet.

This work represents the first application of the BPPM platform to a non-mammalian system as well as the broadest substrate profiling of the Hmt1 enzyme reported to date. The identification of hundreds of candidate Hmt1 substrates indicates that it may play a broader role in *S. cerevisiae* biology than is currently understood, although the context in which it plays an important role is not yet clear.

4.2 Future Perspectives

PRMT biology is complex and often difficult to understand, therefore this work should be continued with three separate projects with unique applications: one project to further

characterize PRMT5 substrates with translational applications in oncology, one project using profiling Hmt1 to push the boundaries of the BPPM platform and enable substrate labeling in living systems, and one that combines the results of both PRMT5 and Hmt1 profiling experiments to investigate novel evolutionarily conserved functions of arginine methylation.

PRMT5 has become a desirable drug target in a number of cancers in the last several years because of the discovery that the common deletion of the tumor suppressor CDKN2A is often accompanied by a concomitant deletion of the MTAP gene, sensitizing cancer to PRMT5 inhibition.[2,3] This discovery greatly expanded the scope of cancer types considered candidates for treatment with PRMT5 inhibitors, but the mechanisms behind PRMT5 dependence are not always known and are likely to be highly variable considering the many tissues of origin of these cancers. BPPM analysis of PRMT5 substrates presents an opportunity to systematically study the source of PRMT5 dependence in cancers.

In order to identify essential PRMT5 targets in MTAP deficient cancers it would be necessary to perform paired BPPM experiments of MTAP deficient cancer cell lines and closely related cell lines of the same tumor type that contain functional MTAP (in the case where appropriate MTAP expressing cell lines do not exist MTAP could be re-expressed in cells). With this experimental design, proteins with depleted methylation in MTAP deficient cells compared to MTAP expressing cells are likely to be non-essential targets, while proteins that maintain relatively high methylation levels even in the absence of MTAP are likely to be essential PRMT5 targets in the cell lines where they are identified. These paired studies would be performed in a variety of cancer types

allowing essential PRMT5 targets in MTAP deficient cancers to be compared across many tumor types and tissues of origin to identify both recurrent PRMT5 targets that could be deemed broadly essential and cancer type-specific targets.

The results of these cancer type-specific BPPM studies could reveal new roles for PRMT5 in oncogenesis and tumor growth and survival, as well as new tissue-specific roles for PRMT5 based on the cell type of origin in the cancer cell lines investigated. The translational applications of these studies could be two-fold: identifying novel biomarkers to predict cancers vulnerable to PRMT5 inhibition and suggesting novel combination therapies to take further advantage of PRMT5 sensitivity by targeting tumor type-specific pathways that it regulates.

The second project would expand on our work performing substrate profiling of Hmt1 in *S. cerevisiae* cells. Our Hmt1 BPPM experiments were performed *ex vivo* in yeast cell lysates due to the technical difficulties and limitations outlined in the introduction chapter of this work. The inability to perform BPPM labeling in living cells severely limits the utility of the technique to address how methylation might change in response to cellular stress or changes in growth conditions. Adapting the previously published metabolic engineering work that has been performed in living human cell lines to living yeast cells would constitute the first example of BPPM in a living organism.[4] The ability to perform substrate labeling in living cells would allow the investigation of novel questions about methylation dynamics, the responsiveness of methylated protein turnover to stress, the effects of environmental changes on PRMT substrate choice.

The adaptation of the live cell BPPM platform to *S. cerevisiae* will likely prove challenging. Yeast genetics are more tractable than human cell genetics, making the

installation of engineered PRMT and MAT enzymes simple, but the effects of metabolic rewiring in yeast with the presence of an engineered MAT could be unpredictable and may require careful tuning of expression levels or an inducible promoter system. To perform PRMT substrate labeling in living cells and track dynamic methylation events or changes in the distribution of the methylome, it will be necessary to use azido-SAM analogs rather than alkynylated SAM analogs with azide click partners.[5] This step is necessary due to the cytotoxicity of Cu(I), which must be circumvented through copper-free click chemistry using strained cycloalkynes.[6] An appropriate MAT enzyme will therefore need to be validated as an azido-SAM generating enzyme or engineered to accept azido-methionine analogs as substrates. Following the engineering of a BPPM system capable of operating in living cells, substrate labeling would be performed under a variety of growth conditions such as rich media, starvation, and various nutrient deficiencies. Yeast cells subject to substrate labeling under these conditions would be subjected to copper-free click chemistry and the overall magnitude and distribution of arginine methylation would be analyzed using fluorescence microscopy. If broad changes in arginine methylation are observed, then substrate profiling using mass spectrometry could be performed to identify dynamic methylation events and investigate the role of PRMTs in adapting to changes in the growth environment of yeast cells.

The third project was inspired by our observation of translation initiation factors in our BPPM profiling experiments of both PRMT5 and Hmt1. While these are abundant proteins, the degree of enrichment occurred for these substrates and their presence t in both human and yeast data sets leads to the hypothesis that PRMTs play some role in the regulation of cap-dependent translation initiation. We have validated PRMT5 and

PRMT1-mediated methylation of human 4EBP1 and our collaborators have validated Hmt1-mediated methylation of eIF1A in yeast, both of which are hits in their respective BPPM experiments. Following up the role of translation initiation factor methylation with a two-pronged approach would be appropriate. In the case of PRMT5, initial studies of 4EBP1 did not reveal an effect on eIF4E association or overall translational output, but further studies of polysome content would reveal whether 4EBP1 methylation affects the ability of cells to recruit mRNA to the ribosome and assemble functional translation apparatus. The results of the PRMT5 BPPM profiling also hint at a role in the regulation of hypoxia specific translation. Appropriate follow-up experiments would be to explore the effect of PRMT5 perturbation on overall translation in cells grown in hypoxic conditions, as well as on hypoxia inducible transcripts and the association of mRNA to hypoxia specific translation initiation complexes. In the case of yeast, collaborators have shown that eIF1A methylation appears to affect translation initiation site fidelity, with methylation deficient mutants showing increased fidelity compared to the native protein. This indicates a possible role for methylation as a negative regulator of gene expression at the translational level in yeast. If this modification can be validated in human cells it will be interesting to see if it also serves a similar role.

Validated proteins in one species may have homologs validated in the other, and similar functional assays can be performed to determine whether a conserved methylation event plays the same role in both the yeast and human contexts. By pairing the study of arginine methylation of translation initiation factors in yeast and human cells it is possible to characterize the functional role of the same biochemical event across distantly related species. This allows for the identification of evolutionary conservation or

divergence of a modification's regulatory role in the fundamental cellular process of translation.

These three potential projects highlight the applications of this work to further multiple scientific disciplines, from translational biomedical research to chemical manipulation of proteins in living organisms to basic research in molecular biology and the evolutionary conservation of fundamental processes in cell biology.

4.3 References

1. Musa, J. *et al.* Eukaryotic initiation factor 4E-binding protein 1 (4E-BP1): A master regulator of mRNA translation involved in tumorigenesis. *Oncogene* (2016). doi:10.1038/onc.2015.515
2. Mavrakis, K. J. *et al.* Disordered methionine metabolism in MTAP/CDKN2A-deleted cancers leads to dependence on PRMT5. *Science (80-.).* (2016). doi:10.1126/science.aad5944
3. Kryukov, G. V. *et al.* MTAP deletion confers enhanced dependency on the PRMT5 arginine methyltransferase in cancer cells. *Science (80-.).* (2016). doi:10.1126/science.aad5214
4. Wang, R. *et al.* Profiling genome-wide chromatin methylation with engineered posttranslation apparatus within living cells. *J. Am. Chem. Soc.* (2013). doi:10.1021/ja309412s
5. Blum, G., Islam, K. & Luo, M. Using Azido Analogue of S-Adenosyl-L-methionine for Bioorthogonal Profiling of Protein Methylation (BPPM). *Curr Protoc Chem Biol.* (2013). doi:10.1002/9780470559277.ch120240.Using
6. Agard, N. J., Prescher, J. A. & Bertozzi, C. R. A strain-promoted [3 + 2] azide-alkyne cycloaddition for covalent modification of biomolecules in living systems. *J. Am. Chem. Soc.* (2004). doi:10.1021/ja044996f

Appendices

Appendix I: PRMT5 BPPM SILAC-MS Hits

Gene Name	Log_2 Enrichment	$-log_{10}$ p-value
MKI67	17.651	0.694893
ACTG2	17.55955	2.175381
KRT2	16.87507	0.088791
KRT14	15.39899	0.673053
HIST1H2AA	15.17637	1.266372
KRT16	15.14286	0.293271
WDR41	14.96327	0.629707
KRT17	14.83533	0.464979
KRT6B	14.82043	0.655406
GAPDHS	13.79015	1.481653
S100A9	13.17665	0.52774
KRT5	12.82421	0.305659
EDF1	12.61442	1.200517
BTN1A1	11.90357	0.695903
ACTL6A	11.80659	0.572926
ARFGEF1	11.7253	1.539239
RPA3	11.70194	1.227153
NYNRIN	11.42915	2.97957
GEMIN6	11.33089	1.132938
RTKN	11.13246	2.250931
CHTF8	11.02844	1.295128
NUFIP2	10.94958	2.620368
ACOT2	10.76986	0.320755
ASPM	10.7568	1.202072
ZNF768	10.73867	0.878393
HMGA2	10.64294	0.914136
ZNF593	10.5914	1.660853
NSFL1C	10.56652	1.028825
ARMCX3	10.53108	1.125574
DCTN4	10.48667	0.64294
NDNL2	10.39811	1.318402
ATXN2	10.33821	1.588395
S100A8	10.28566	0.450966
SMU1	10.24237	0.158469
YBX3	10.22107	1.166665
BRD4	10.18746	1.072945
TP53RK	10.12377	0.901915
TRMT112	10.00765	0.224796

YTHDC1	10.00329	1.293897
KHDRBS3	9.945067	0.62051
ATP5J2	9.872866	0.322285
FAM50A	9.846123	0.707522
UGP2	9.634557	0.284306
SP3	9.54787	1.032094
MACF1	9.486341	2.962881
WASL	9.472704	1.02803
SUGP2	9.44017	0.867206
SPEN	9.436669	0.922014
IFT74	9.415904	0.754673
MORF4L2	9.408421	1.06504
INCENP	9.384889	0.754004
TPR	9.379002	1.118527
PSMC1	9.336693	0.121026
ZCCHC3	9.287196	0.483941
ZC3H13	9.210816	1.050312
MARK2	9.201261	1.687937
CWC15	9.119274	1.396011
SCRIB	9.10348	0.770552
DDX23	9.01192	1.066155
CKAP4	9.005811	0.438519
EIF4E2	8.864542	0.566674
GTF2F1	8.770595	1.171133
CMBL	8.760959	0.387785
GTPBP6	8.676951	0.985336
MPST	8.62074	0.228377
ZHX1	8.53084	0.210768
ARPIN	8.523481	0.120948
AKAP8	8.50224	0.717316
ZNF622	8.472274	1.148804
MARK3	8.433888	1.226605
PHF10	8.402827	1.093088
LAMTOR5	8.356509	0.549987
FOXO3	8.330369	1.028332
SRSF11	8.304009	0.937131
MAGED2	8.24738	0.73089
TSR1	8.187076	0.445264
SART1	8.172285	0.912667
RRBP1	8.013735	0.520401
TCF20	7.956379	0.770263
NENF	7.93784	0.216957
TMEM214	7.924984	1.053265
WDR70	7.896211	1.428999
RBM6	7.864922	0.633616

TSR3	7.787561	0.664618
SNTB2	7.777238	0.013038
C1orf50	7.723067	0.487465
PELP1	7.695615	0.289022
HRNR	7.636319	0.074641
ZYX	7.505169	0.28104
TAF10	7.476775	0.103372
NUP43	7.458151	0.246174
SFXN1	7.416766	0.009048
RSAD1	7.265553	0.919117
RRP12	7.186642	0.067747
SRP19	7.147505	0.193704
MRPL13	7.139597	0.316679
DHX36	7.136504	0.807792
CCDC12	7.128085	0.117177
YBX1	7.096277	2.233343
CSNK2A1	7.086641	0.274291
TMOD3	7.064995	0.038808
HGH1	6.985558	0.380566
CUL1	6.980753	0.564828
METTL25	6.97761	0.231482
NXF1	6.977153	0.783254
THOP1	6.945333	0.167563
EIF4G2	6.906205	0.508011
ENOPH1	6.896447	0.261626
CHCHD1	6.886297	1.058737
SF3B2	6.87564	0.447955
GNPNAT1	6.859365	0.339204
PSMD3	6.824308	0.565055
HSPA14	6.800057	0.537442
PAPOLA	6.790689	0.173322
ACOT13	6.657306	0.192017
RALY	6.640928	0.965908
PRCP	6.593885	0.127831
NQO2	6.59122	0.181848
TXN2	6.573695	0.194661
CSTF1	6.57177	0.230393
SRSF3	6.487717	0.796869
ARL2	6.470796	0.010976
DCPS	6.460804	0.036381
FKBP8	6.408673	1.204257
VCPKMT	6.392928	0.044261
AHSA1	6.34666	0.127172
HLA-A	6.138103	0.479369
BABAM1	6.134094	0.029848

SGTB	6.066612	0.241078
TXNL1	6.005457	0.267031
HIST1H2AB	5.984882	1.044768
MAPRE1	5.981807	0.00874
POLR3A	5.965139	0.135409
EIF3H	5.897149	0.80867
NUP107	5.849858	0.274021
RBM10	5.774216	0.892337
ANLN	5.74004	0.5871
ACAT2	5.731368	0.332126
LAGE3	5.730481	0.024513
ASH2L	5.699965	1.132913
RBMXL1	5.682423	2.037886
HECTD1	5.553098	0.2835
TRA2B	5.552272	2.183362
C11orf58	5.540018	0.491568
EIF4H	5.520273	0.948707
YRDC	5.360258	1.048267
HIST1H4A	5.356079	1.655574
AIFM1	5.354598	0.092996
STT3A	5.277055	0.223053
CLUH	5.165508	0.48564
PNN	5.131424	0.496943
HNRNPAB	5.122656	1.168068
RBMX	5.122182	1.957514
DDOST	5.117743	0.016377
SUZ12	5.096	0.088373
INF2	5.069784	1.212623
CLASP2	5.065896	0.732416
C19orf43	4.93835	2.093035
CHCHD3	4.890266	0.022029
EIF2B3	4.887469	0.029349
ALDH5A1	4.843989	0.299825
WDR6	4.794246	0.510347
LYAR	4.791611	0.480873
PYGL	4.64175	0.048023
HNRNPA2B1	4.641473	1.564335
RFC5	4.638548	0.217234
NDUFV3	4.636079	1.880332
CFAP20	4.613281	0.117241
SRSF9	4.601355	0.82627
DUSP14	4.523862	1.021562
C11orf68	4.479621	0.993316
MMS19	4.428969	0.301916
MPLKIP	4.425394	1.526652

SMC4	4.3876	0.7164
WBSCR22	4.359549	2.069532
NUDCD2	4.275581	0.027908
TIMM9	4.252713	0.24787
NDUFAF4	4.244616	0.08916
HNRNPA0	4.230341	1.431234
TOP2B	4.141807	1.785959
TOE1	4.11678	0.181817
BYSL	4.098835	1.782502
UTP3	4.092331	2.382193
SRSF1	4.060349	1.291073
CECR5	3.957495	0.566595
RAB5C	3.947944	1.151676
RNF25	3.936051	0.686768
DDX5	3.92115	1.397106
PDS5A	3.907898	0.031935
RRP1B	3.880321	1.162455
SLIRP	3.880282	1.122903
HNRNPA1	3.847998	1.048009
DYNC1LI2	3.835123	1.616313
PDAP1	3.813841	1.258887
FAM98A	3.807451	1.824122
EIF4G1	3.638003	1.469214
G3BP1	3.630119	2.162462
FAM98B	3.617445	2.095385
EEFSEC	3.537379	1.529597
MSI1	3.511839	1.785694
PMVK	3.479842	0.383875
DDX17	3.464935	1.334579
SMARCD2	3.462381	1.916441
BCL7C	3.448921	0.9835
PDS5B	3.376671	1.456601
POLR1C	3.367367	0.26346
NCL	3.358215	1.515061
C1orf174	3.341781	2.678301
LEMD3	3.319298	2.091853
NELFA	3.288012	2.365812
PDHB	3.278942	0.271898
PFKL	3.253723	0.369036
PABPN1	3.234703	2.516196
NFATC2IP	3.182392	1.089707
ILF2	3.141549	3.947585
SFPQ	3.124438	2.205836
RPS21	3.10356	0.288428
BTF3	3.074871	1.6032

NTHL1	3.055278	0.590357
LMNA	3.054836	1.457323
ENPP1	3.054606	0.418363
ATXN2L	3.032121	0.832375
CAPRIN1	3.029736	0.6334
PSPC1	2.984288	1.532416
CHCHD2P9	2.984109	1.528299
CCDC137	2.97481	1.508706
RBM14	2.967603	0.15944
CPSF6	2.960742	1.980525
HNRNPUL1	2.911311	1.697246
ETF1	2.889837	1.798088
DDX3X	2.871576	2.223118
DNAJC10	2.840938	0.178417
RBM15	2.837103	0.45506
SNRPE	2.820566	1.139551
TRPT1	2.809706	0.64991
PDCD4	2.808569	2.161907
RRP1	2.769779	1.525185
MSI2	2.754643	1.464107
SNRPD3	2.726022	2.011214
DAZAP1	2.718799	3.560723
CHTOP	2.640205	1.618909
FUBP3	2.640013	2.047674
DDX47	2.632239	1.920488
TAF15	2.609834	1.541066
RAB5A	2.567199	0.931433
NOP2	2.543242	1.234992
RBM8A	2.361341	1.506006
MRE11A	2.355184	0.921765
SRRT	2.34159	1.485231
LARP4	2.340291	1.321719
TP53BP1	2.318913	1.148099
USP39	2.296404	1.265229
SMARCA5	2.290676	1.376904
SART3	2.284414	0.914694
SNRPB	2.265983	3.545681
FXR2	2.250123	2.756793
MECP2	2.246827	1.046342
PABPC1	2.227703	0.897987
POLR2C	2.125588	0.650227
TPT1	2.117852	0.041355
YLPM1	2.101151	0.82738
METTL14	2.094205	0.482959
PABPC4	2.091866	1.523331

MOGS	2.061347	1.99934
PRR3	2.013404	0.559549
GCFC2	1.978403	0.648648
EWSR1	1.97645	1.620135
NCBP2	1.95321	0.544437
ZNF326	1.937405	1.680466
GFER	1.935854	1.380271
DPP3	1.910345	0.359877
FOXK1	1.863804	0.828726
SERBP1	1.819757	2.584389
HNRNPU	1.805421	2.018827
MRPL16	1.80076	1.201485
CIRBP	1.79807	1.161831
UBAP2L	1.766307	1.417149
GIGYF2	1.744571	1.679804
ZGPAT	1.738504	0.801794
PRRC2A	1.734687	1.22667
U2AF1	1.730577	0.541062
DSP	1.723857	0.421507
SUPT16H	1.705906	1.434911
LARP4B	1.689809	2.066176
RBM39	1.681585	0.635355
SARNP	1.655462	0.919366
G3BP2	1.633449	1.821839
MRPL4	1.629259	1.720362
FMR1	1.557946	2.075086
KHDRBS1	1.505013	1.826843
HNRNPUL2-BSCL2	1.456405	0.725187
FUBP1	1.451453	2.562349
HNRNPH3	1.405501	2.881338
INO80	1.350698	0.666063
FAM120A	1.315161	0.750731
H2AFY	1.309991	1.099372
EIF3D	1.268439	1.392037
MTA1	1.22671	0.299712
CCT4	1.222217	1.222848
EIF4B	1.217805	1.317324
DDX21	1.190406	1.207147
KHSRP	1.180871	1.310195
MDC1	1.146356	0.63826
MRPL43	1.13892	1.860817
HNRNPL	1.133937	1.870628
GLRX3	1.125381	0.074128
DHX9	1.118683	1.587392

HNRNPC	1.115154	1.288507
UPF1	1.095106	0.682287
SUPT5H	1.094147	0.939962
MRPL15	1.07924	0.952951
NFXL1	1.03418	0.456007
HNRNPD	1.012604	1.545928
C5orf45	0.990438	1.313951
DYNC1LI1	0.976314	0.226983
CTPS1	0.94893	0.06437
MCM2	0.944794	1.53686
UBAP2	0.924709	0.979211
C7orf55-LUC7L2	0.915804	0.707123
IQGAP1	0.910777	0.839517
TRIP6	0.901727	1.372195
THRAP3	0.89107	1.02467
RPS14	0.883988	1.063405
RPL23	0.817894	1.061256
EIF4EBP1	0.805243	1.376125
HNRNPH1	0.802883	1.257741
C8orf33	0.783126	1.026971
PPAN	0.78165	0.331166
POLD1	0.777275	0.735769
CCDC9	0.772267	1.60873
SNRPD2	0.75954	1.578132
RBM3	0.73538	1.224312
SYNCRIP	0.700499	1.061595
GADD45GIP1	0.66963	1.158347
TUBB	0.648687	1.957877
NCAPD2	0.648052	0.340888
SNRPD1	0.559844	1.949357
DPYSL5	0.531211	0.665615
CCT7	0.523493	0.896811
VIM	0.505348	0.430834
LARP1	0.50399	1.292155
BRI3BP	0.480709	0.064087
HNRNPH2	0.461612	0.88549
SLC30A7	0.458737	0.222829
TUBB4B	0.448744	2.495756
RPS23	0.446308	1.253121
TUBB2B	0.442	1.394862
FOXRED1	0.407155	2.145276
TARDBP	0.398224	1.248116
MCM4	0.389433	0.810677
FKBP10	0.372197	0.882422

PSMC5	0.363433	0.077352
ATP5A1	0.354318	1.026843
XPO5	0.350176	0.200309
FXR1	0.343143	0.397235
IGF2BP1	0.334505	0.698363
WDR18	0.32308	0.059282
ALYREF	0.315048	0.446962
TUBB2A	0.281215	1.430495
RPL13a	0.27287	0.642404
TAGLN2	0.264089	1.521284
CSE1L	0.263779	0.289261
IPO5	0.259229	0.118177
SAFB	0.253843	0.286302
EDC3	0.244112	0.524908
RPL18	0.225785	1.152957
ETFA	0.224378	0.495316
PRRC2C	0.22047	0.391051
ANAPC7	0.218199	0.214449
FUS	0.202849	0.178222
FAF2	0.195806	0.002418
RANGAP1	0.189595	0.168233
FLNB	0.184664	0.205564
SF3B1	0.177863	0.210855
ZC3HAV1	0.175972	0.102846
MRPS25	0.16214	0.015333
MBD3	0.157186	0.16866
TUBB4A	0.148952	0.029863
AP3D1	0.138315	0.457393
HNRNPM	0.117402	0.035048
RPS5	0.11441	0.432
XRN2	0.099668	0.559405
LZIC	0.094498	0.311466
PRPF8	0.087753	0.019258
MSH2	0.083105	0.025994
VAT1	0.075214	0.606502
ATG4B	0.067664	0.046589
HSD17B12	0.064505	0.027268
BLVRA	0.061806	0.059434
FKBP5	0.061363	0.093129
XPO1	0.055679	0.291273
RBM27	0.051212	0.348127
PDCD6IP	0.050372	0.016422
RPS7	0.043972	0.079722
PSMD11	0.041034	0.220424
ACTR1A	0.035764	0.134331

RFC3	0.032758	0.184281
HNRNPF	0.032713	0.094107
LBR	0.023251	0.045617
COPB2	0.014745	0.167099
PRPSAP1	0.002564	0.135585
RPL17	0.001534	0.031687
EEF1D	0.000193	0.202578
FLNA	-0.00097	0.080152
SRP68	-0.00363	0.185683
SMC3	-0.00502	0.186294
METTL7A	-0.01832	0.235002
MTHFD1L	-0.02793	0.241551
KDELR1	-0.0417	0.309582
TMED10	-0.04757	0.329064
PUF60	-0.04798	0.004673
HSDL2	-0.05216	0.33078
NSUN2	-0.05672	0.334878
RPA1	-0.05923	0.375906
BCCIP	-0.06378	0.22655
HEXIM1	-0.06436	0.106456
HUWE1	-0.07251	0.769951
PGM1	-0.07254	0.088572
RGS10	-0.07486	0.091074
AP1G1	-0.08344	0.190093
TRIP13	-0.08548	0.189207
PRMT3	-0.08638	0.269814
IARS	-0.08921	0.297245
SUCLG2	-0.09185	0.175988
CARM1	-0.09235	0.282076
RAB1B	-0.09254	0.310031
DNAJC7	-0.09424	0.132225
LSM4	-0.09611	0.252431
PRR12	-0.0973	0.145141
PSMA6	-0.10364	0.499668
PDE12	-0.10379	0.319102
COPB1	-0.11884	0.327072
RPL27A	-0.12795	0.640995
FBXO22	-0.12883	0.813621
RPS26	-0.13247	0.694835
RPL15	-0.13662	1.242947
CLTC	-0.13856	0.335627
PSMD6	-0.14122	0.382742
NUP155	-0.14191	0.340033
RBM33	-0.15412	0.365433
C14orf166	-0.15461	0.534893

MATR3	-0.15506	0.310947
SUGT1	-0.15777	0.22711
AARS2	-0.16055	0.274924
PRMT5	-0.16285	0.545219
PTBP1	-0.16748	0.404004
HADHA	-0.16861	0.278307
HYOU1	-0.16942	0.145494
SNRNP200	-0.17106	0.269331
COMMD4	-0.17196	0.126263
LYRM7	-0.17198	0.390203
NASP	-0.1726	0.436059
HSPA8	-0.17836	0.642004
DHX15	-0.1837	0.425916
PSMD7	-0.18519	0.33901
PAPSS1	-0.18829	0.397738
ESYT1	-0.19012	0.487945
TMED9	-0.19233	0.368833
RCC1	-0.1927	0.923421
TIMM13	-0.19495	0.499244
AP1S1	-0.19583	0.443825
PLCG1	-0.19593	0.299785
RPRD1A	-0.19689	0.569093
RPN2	-0.20079	0.273775
HSPA4L	-0.20458	0.156651
PPP2CB	-0.20732	0.542174
U2AF2	-0.20831	0.801581
TPD52L2	-0.20942	0.650286
DPH2	-0.2098	0.37634
ACTN1	-0.21321	0.409441
NAP1L4	-0.21358	0.248613
SDHA	-0.21367	0.30315
TXNRD1	-0.21403	0.511565
TRDMT1	-0.21613	0.943382
SH3GLB1	-0.21659	0.548469
PRPF19	-0.21757	0.341014
HSP90AB1	-0.2187	0.420706
RPL37A	-0.22475	2.104951
EEF1B2	-0.22798	0.674204
LAMC1	-0.22881	0.380933
TLN1	-0.23283	0.65351
CKMT1A	-0.23313	0.401792
IPO4	-0.23811	0.68818
RPLP0	-0.23813	0.495721
EIF3F	-0.24036	0.18877
ACAA1	-0.24239	0.564561

DLAT	-0.24768	0.395187
MPG	-0.24812	0.53081
ST13	-0.24815	0.800046
DPYSL2	-0.24931	0.429482
RSL1D1	-0.25089	0.258217
AIP	-0.25175	0.647203
SPTAN1	-0.25175	0.276705
COPA	-0.25253	0.510803
LRPPRC	-0.25273	1.782167
GSPT1	-0.25307	1.365619
NUP50	-0.2537	0.388369
MYH9	-0.25557	0.721661
SMC1A	-0.25649	0.515724
NONO	-0.25747	0.86741
RRM1	-0.262	0.525019
TXNDC5	-0.26279	0.574065
METTL2B	-0.26501	1.184381
IMMT	-0.2669	0.46221
PFDN2	-0.27044	1.190158
FBL	-0.27512	2.447092
UMPS	-0.27689	0.571502
MGST3	-0.28103	0.527066
WDR77	-0.28315	1.010696
UGGT1	-0.28705	0.535165
RAB8A	-0.28722	1.200247
GLOD4	-0.28851	0.753412
PYCR2	-0.28869	0.613528
VDAC3	-0.29317	0.533528
HINT3	-0.29341	1.486656
VDAC1	-0.29695	0.538435
ALDH7A1	-0.29705	2.116487
ELAVL1	-0.29746	0.757267
DYNC1H1	-0.2987	0.483294
PDIA6	-0.29942	0.570063
CAND1	-0.3002	1.552943
TBCE	-0.30321	0.67092
DYNLL1	-0.30324	0.650044
FKBP4	-0.30341	0.939089
RAB1A	-0.30587	0.540995
MAP4	-0.30753	1.074846
EIF2S1	-0.31486	0.88298
PITRM1	-0.31645	0.45651
HINT1	-0.31696	1.112129
YWHAZ	-0.31846	1.523372
RPL18A	-0.3186	0.724478

UQCRFS1	-0.31868	1.311777
RPN1	-0.32064	0.585679
ALDH18A1	-0.32074	0.81435
PTRH2	-0.32199	0.620029
CAPN2	-0.32295	0.479153
COPZ1	-0.32442	0.931401
ATP2A2	-0.32768	0.783156
SLC25A5	-0.32905	0.431404
PPIB	-0.3302	1.905722
RAP1B	-0.33086	0.649272
SNAP23	-0.33111	0.620712
UBLCP1	-0.33234	1.005363
PROSC	-0.33253	0.42805
HSP90AA1	-0.33297	0.720778
HSP90B1	-0.33499	0.719609
PSMD12	-0.33535	0.497677
EFTUD2	-0.33561	0.578143
RAB2A	-0.33712	0.822629
RPS2	-0.33745	0.873477
PRKAR2A	-0.3379	0.314765
PPP2R1A	-0.34014	1.03053
PCBP1	-0.34152	0.638321
EPRS	-0.34155	0.615268
REEP6	-0.3437	0.60914
SURF4	-0.34554	1.145984
CHAC2	-0.34811	0.593176
DR1	-0.34927	0.680003
ANXA5	-0.35274	1.320322
USP7	-0.35319	0.65772
SEP15	-0.35486	0.65691
RARS	-0.35501	0.646738
ARF3	-0.3554	1.336754
FEN1	-0.35585	0.842476
PPIA	-0.35603	1.534996
TRAP1	-0.35636	0.81634
LARS	-0.35764	1.127558
HMGB2	-0.35769	1.358407
PURA	-0.35793	0.518842
TMEM33	-0.35884	0.712055
DIS3	-0.36122	0.685275
ACOT7	-0.36137	2.124272
DLST	-0.36232	0.601292
PARK7	-0.36282	1.9713
PSMB1	-0.36568	0.590613
PSMC6	-0.36593	1.36992

ACAD9	-0.36657	0.796037
PSMD1	-0.36803	0.550282
SAE1	-0.36867	0.857613
KIF5B	-0.37123	0.377884
RPL21	-0.37175	1.567712
RAB35	-0.37207	0.553318
UBE2O	-0.37234	0.565032
EIF1AY	-0.37257	1.654646
MCM3	-0.37497	1.584694
FTO	-0.37627	0.773621
TIPRL	-0.37652	0.289192
NSDHL	-0.37751	1.027021
HMGB1	-0.37867	1.210075
PGD	-0.37974	2.251441
SUMO2	-0.38062	1.736311
ATP2B1	-0.38128	0.511344
FASN	-0.38214	0.742554
DDX1	-0.38371	1.428721
RAB10	-0.38505	1.279258
PCYOX1	-0.38512	0.814919
DFFA	-0.38964	0.94014
ABHD10	-0.39017	1.165558
CAP1	-0.39062	0.831997
PSMC4	-0.39153	0.896112
SMYD5	-0.39275	0.998256
RPS16	-0.39345	1.212247
FN3KRP	-0.39427	1.0504
EEF1G	-0.39607	0.829859
DDX39B	-0.39626	1.335557
PSME2	-0.39812	1.652357
POLR2B	-0.39915	0.687739
AGTRAP	-0.39936	0.487608
COPG1	-0.40002	1.582283
AK2	-0.40093	0.856973
AIMP1	-0.40109	0.79047
TXN	-0.40124	1.129206
CCT6A	-0.40152	1.661652
RPL8	-0.40376	1.465297
RPL11	-0.40499	1.61378
CORO1B	-0.40518	2.265263
SLC25A13	-0.4055	0.806389
MDH1	-0.40557	2.190039
CRKL	-0.40582	0.630455
PARP1	-0.40666	1.754368
PCBP2	-0.40684	0.646117

GTPBP1	-0.40745	0.667424
YWHAQ	-0.40851	1.168364
CPNE3	-0.41445	0.855588
TIMM23B	-0.4145	1.211614
CYB5R3	-0.41711	0.430529
ARPC1B	-0.4189	0.705717
VDAC2	-0.41993	0.739516
EIF3L	-0.42027	0.603786
RPL24	-0.42216	1.061924
RPS3A	-0.42307	1.051178
CSDE1	-0.42349	0.469943
PIN1	-0.42376	2.09451
METTL15	-0.42451	0.90662
POLR2A	-0.42619	0.431603
CYB5B	-0.42765	0.727335
VRK1	-0.42929	1.028286
AS3MT	-0.42948	1.560044
ANP32E	-0.43086	0.945247
IDI1	-0.43298	0.523048
HCFC1	-0.43303	1.478298
NMD3	-0.43497	1.262603
UBC	-0.43544	0.916509
ASMTL	-0.43613	1.089317
PRDX6	-0.4362	0.596629
PRMT1	-0.43624	2.357952
ALDH2	-0.43687	0.906915
ISOC1	-0.43807	1.090379
MRPL14	-0.43925	0.841923
SUCLG1	-0.44007	0.549611
RPS4X	-0.4407	0.736119
HSD17B4	-0.44193	0.874248
RPS6	-0.44349	1.241083
LSM12	-0.44368	0.767366
PELO	-0.44376	1.980746
EIF4A1	-0.44464	2.185188
TRAPPC3	-0.4449	0.716977
WDR1	-0.44497	0.742892
GSTP1	-0.44764	2.321523
GAPDH	-0.44854	2.684147
FAH	-0.44945	0.817417
TARS	-0.44979	0.656717
RCC2	-0.45127	1.354487
HK1	-0.45184	0.926937
PFN1	-0.4534	1.701063
CORO1C	-0.45369	0.987617

GLRX5	-0.45409	2.335867
KPNB1	-0.45428	1.209069
BCAP31	-0.4555	0.71685
SCAMP3	-0.4556	0.800561
FARSB	-0.45589	0.876739
TRIM28	-0.45595	1.795932
SELO	-0.4562	0.927437
CPSF1	-0.45646	1.379331
PPP5C	-0.45696	0.992472
P4HB	-0.45706	1.329933
QARS	-0.45917	0.660665
RPS9	-0.4592	1.101383
MTCH2	-0.45943	0.588059
SEC61A1	-0.46115	1.524904
NAA40	-0.46211	0.746189
CACYBP	-0.46221	0.561493
C9orf64	-0.46308	0.653846
NDUFA7	-0.46392	1.209131
DNM1L	-0.46717	0.744603
RPL9	-0.46763	1.109978
MYO1B	-0.46945	1.107727
FARSA	-0.47063	1.24048
SSBP1	-0.47075	1.765841
XRCC5	-0.47103	0.795089
AHCY	-0.47253	2.440394
COPS4	-0.47316	0.963926
PSMA7	-0.47365	1.102987
TUBA1A	-0.47441	2.352414
MCM5	-0.47553	1.416492
NAA10	-0.4772	1.059083
CPOX	-0.47812	1.012292
RHOG	-0.47857	0.713667
RARS2	-0.47861	1.344163
LOC102724023	-0.48108	0.563949
C16orf13	-0.48134	2.333845
TPI1	-0.48619	1.878498
MMGT1	-0.48622	0.616475
PSMA5	-0.48837	1.40156
DDT	-0.48851	2.106511
ANXA2	-0.48924	1.610805
EEF1E1	-0.48975	0.609169
NDUFA5	-0.48985	0.954919
CAD	-0.49053	0.555358
VAPB	-0.49113	0.686263
ATP1A1	-0.49139	1.725908

MPDU1	-0.49153	0.761566
C1QBP	-0.49284	1.032707
BANF1	-0.49374	0.706764
PSMA4	-0.4961	1.826214
RAN	-0.49748	1.297495
RPS15A	-0.49973	1.15197
SRPRB	-0.5	1.226371
SEPHS2	-0.50112	1.300434
PCNA	-0.50262	0.765308
RPL14	-0.50415	0.582326
PKM	-0.50582	1.955515
RPLP1	-0.50606	1.139467
RPL34	-0.50691	1.197682
PSMB5	-0.50748	1.442017
RPL10A	-0.50896	1.378924
MRPS28	-0.50898	0.823999
DAK	-0.50921	0.709589
MOCS2	-0.51034	0.6258
SND1	-0.51188	1.409873
GNB2L1	-0.51381	0.811423
OAT	-0.51517	0.971454
COMT	-0.51866	0.439913
MRPL21	-0.52074	1.279483
ENO1	-0.52083	2.020231
IMPDH2	-0.52249	1.299927
HPRT1	-0.52415	1.288886
GRHPR	-0.52565	0.782865
RPS8	-0.52634	1.238384
DDX6	-0.52641	0.983286
MYL6	-0.52805	0.634485
UBA1	-0.52848	2.717867
CCT2	-0.52869	3.340913
TK1	-0.5295	1.037308
VCP	-0.53048	2.308579
HSPA9	-0.53146	2.923681
ATIC	-0.53244	1.559922
HSPH1	-0.53353	1.0203
ARPC4	-0.53353	1.531844
GAR1	-0.53367	0.983682
DDB1	-0.5343	1.806915
PGK1	-0.53559	1.035143
TRMT61A	-0.5401	0.82394
FUCA1	-0.54134	0.950584
GOT2	-0.54214	1.072809
ATP5O	-0.54358	0.95945

TMX1	-0.54396	0.609398
HINT2	-0.54483	1.373346
PSME3	-0.5461	0.88636
PNP	-0.54656	0.876037
LRRC47	-0.5474	1.211822
RPL22	-0.54764	1.158046
SOD2	-0.54773	1.476071
PRDX2	-0.5484	1.783644
RTCB	-0.54874	1.54494
TUBA4A	-0.54931	2.055173
EIF5A	-0.55041	1.379728
EIF3K	-0.5508	0.787003
XRCC6	-0.55099	0.991477
ETFB	-0.5512	1.022363
LDHB	-0.55215	2.020358
PTRHD1	-0.5522	0.626183
CFL1	-0.55503	2.340765
ALDH9A1	-0.55567	2.441859
CMPK1	-0.55699	1.164038
LDHA	-0.55859	1.871093
TXNDC17	-0.5597	1.170382
TCP1	-0.56089	1.456604
RPL7A	-0.56159	0.876409
USP5	-0.56337	0.561877
PSMA2	-0.56376	1.153577
FAHD1	-0.565	1.070852
PPA2	-0.5656	0.844199
POFUT1	-0.56696	1.842482
RPS17	-0.56775	1.089629
GANAB	-0.56925	1.929189
FKBP3	-0.56993	1.440454
CD81	-0.57204	1.357096
HDGF	-0.57284	3.235126
PYGB	-0.57289	0.434888
LCMT1	-0.5731	2.11397
RPL38	-0.57406	1.43088
FTL	-0.57484	0.493751
STRAP	-0.57682	1.053031
HSPA4	-0.57778	1.192789
PRDX3	-0.57807	2.158833
CBX3	-0.57847	1.622094
ZC3HAV1L	-0.57873	1.196263
ALDOA	-0.57911	1.458053
DLD	-0.57974	1.496239
RPL12	-0.57982	2.079439

SOD1	-0.57983	1.54356
AARS	-0.58073	1.17774
ANP32A	-0.58108	0.733758
AKT3	-0.58125	1.163801
PRMT6	-0.58405	1.147578
PSMA3	-0.58559	1.035536
OTUB1	-0.5863	1.016871
MYO6	-0.58667	1.01929
RPP30	-0.58798	0.966955
PSMC3	-0.58835	1.650288
MTA2	-0.59041	0.649207
REXO2	-0.59044	1.367301
SLC16A1	-0.59141	1.242947
PSAT1	-0.59153	0.779098
UQCRC1	-0.59422	1.108125
PSMD4	-0.59424	1.734933
RAB7A	-0.59487	1.01546
PEPD	-0.59526	0.821575
YWHAB	-0.59576	1.935306
ZFR	-0.5979	1.221374
ECH1	-0.59824	1.819115
MRPL32	-0.59826	3.613622
SLC25A3	-0.60039	0.825714
RUVBL1	-0.60062	1.381384
CDIPT	-0.60213	0.747615
HSPE1	-0.60231	0.808268
LACTB	-0.60327	0.96466
PIN4	-0.60328	1.946237
CCT8	-0.60419	2.080744
CLTA	-0.60496	0.589649
HSPD1	-0.6063	2.404076
ALDOC	-0.60635	1.040906
BUB3	-0.60683	1.28223
TOMM40	-0.60785	1.580484
SF3B3	-0.60843	1.425529
RPL5	-0.6085	1.288066
GGCT	-0.61137	0.639454
DRG1	-0.6125	1.672549
HSD17B10	-0.61571	1.527358
LYPLAL1	-0.61698	0.887058
UBA3	-0.6185	0.577231
PHGDH	-0.61921	1.635653
NAA15	-0.61927	0.876268
CA2	-0.61951	1.417582
CARHSP1	-0.61955	1.258765

NOMO1	-0.62031	0.739107
CALR	-0.62152	2.336739
NDUFS1	-0.62283	2.29491
ACLY	-0.62395	2.666062
G6PD	-0.62406	1.510227
DNPH1	-0.62425	1.277022
ATP6V1A	-0.62576	0.976268
PAICS	-0.62634	1.44705
LRRC59	-0.62793	0.645142
STOML2	-0.62808	1.496058
NUTF2	-0.6292	1.219147
HMBS	-0.62994	0.77749
YWHAE	-0.6305	0.888214
LYPLA1	-0.63058	0.790397
NPM3	-0.63132	1.425032
XPNPEP1	-0.63138	1.064103
PITHD1	-0.63322	0.913381
MDH2	-0.63375	1.541838
NDUFA2	-0.63413	0.90091
ISOC2	-0.63493	2.316675
GLO1	-0.63499	2.087907
RPL7	-0.63575	1.5646
LGMN	-0.63604	0.601972
HMOX2	-0.63608	1.046305
ACADM	-0.63646	1.517228
COTL1	-0.63747	0.570753
CALM2	-0.63865	0.917087
UQCRC2	-0.63879	1.759222
NME1	-0.64006	1.301711
NTPCR	-0.64065	1.553893
PDIA4	-0.64067	1.753812
GAMT	-0.64092	1.001001
WARS	-0.64129	2.539806
MTPN	-0.64307	2.605746
PHPT1	-0.64312	1.201245
TALDO1	-0.64411	1.227943
SERPINH1	-0.64441	0.655695
AKT1	-0.64591	1.090847
EEF2	-0.64599	1.836011
DCTN2	-0.64599	1.17453
BOLA2	-0.65287	1.099185
EIF6	-0.65297	0.89564
MRPS14	-0.65372	0.823532
RPL10	-0.65486	1.039036
SKP1	-0.65562	0.585297

YWHAH	-0.656	0.499629
AP1B1	-0.65603	0.652406
SHMT2	-0.65731	1.529468
METAP1	-0.65908	1.186793
TIMM17B	-0.66046	0.831447
CLNS1A	-0.66047	1.646989
RNPEP	-0.66078	0.916129
POLR2H	-0.66241	1.317283
MARC1	-0.66438	0.859022
EIF2S3	-0.66469	0.952043
RPL28	-0.66549	1.422186
COX5B	-0.66595	0.890214
RPS20	-0.66605	1.182043
CS	-0.66607	0.745145
SNRPA1	-0.66638	1.15074
APIP	-0.66655	2.361964
CANX	-0.66731	1.186242
ACO2	-0.66824	1.143081
H3F3B	-0.6701	1.772752
MTHFD1	-0.67013	1.883902
TOR1AIP2	-0.67069	4.441686
MCTS1	-0.6708	0.916712
GCLM	-0.67104	0.793739
SRM	-0.67158	1.148956
KPNA2	-0.67204	0.710738
HEXA	-0.67483	0.496836
ITGB1	-0.67624	1.097121
ADSL	-0.67799	1.030182
GART	-0.6782	0.685174
OLA1	-0.67876	1.471669
GPI	-0.67884	1.640278
RBBP7	-0.67911	1.947255
MCCC2	-0.68392	1.964296
TPM3	-0.68589	2.072543
ISCA2	-0.68684	1.351478
EIF3G	-0.68754	0.742141
MRPS11	-0.68766	0.703347
RPS28	-0.68794	1.491562
TRMT11	-0.68821	1.73849
UCK2	-0.69023	0.417726
GEMIN5	-0.69061	0.86511
YWHAG	-0.69284	1.329353
NUBP2	-0.69545	0.816536
CAPZA1	-0.69597	2.314571
GRSF1	-0.69695	0.804228

RPL6	-0.697	0.866812
AK1	-0.69853	0.724203
GOT1	-0.69994	1.185724
PPP1CA	-0.70045	1.085954
PSMB2	-0.70134	1.523849
MCM6	-0.70348	1.167157
CCT5	-0.70473	1.409873
AKR7A2	-0.70601	0.764036
FH	-0.71141	1.551218
RPS3	-0.71145	1.007041
TBCA	-0.71156	2.123908
MAT2B	-0.71194	1.255906
MAGOHB	-0.71283	1.658554
GSTCD	-0.71329	0.498293
CTSB	-0.71392	0.946773
COIL	-0.7147	0.706176
PRDX1	-0.71546	2.220658
DARS	-0.71617	1.7978
ERO1L	-0.71676	1.46529
PGP	-0.71837	1.229489
UCHL1	-0.71917	1.586447
PAFAH1B2	-0.72094	1.574134
EIF1AD	-0.7213	1.068043
PDIA5	-0.72294	0.815567
TROVE2	-0.72387	1.40219
ZC3H15	-0.72516	1.349114
CSTB	-0.72542	1.18569
GCN1L1	-0.72544	1.453635
CUTA	-0.72612	1.136578
TCEB2	-0.72706	1.731535
HSPA5	-0.72834	1.874995
MCM7	-0.73132	2.66663
APEX1	-0.73287	1.810014
GGH	-0.73444	1.943126
VBP1	-0.73454	0.856747
PRDX5	-0.73484	0.919431
PSMC2	-0.73488	2.089619
CDK1	-0.73826	1.72335
ARHGDIA	-0.74004	1.500963
TKT	-0.74075	2.166622
RPL4	-0.74098	1.494139
NPEPPS	-0.74524	2.311657
YARS	-0.74662	1.724377
ALDH1B1	-0.74781	1.55951
PPM1G	-0.74952	1.947625

VCL	-0.7499	1.085752
CFL2	-0.75181	1.608041
IARS2	-0.7522	0.792252
RAB14	-0.75338	1.136534
DHPS	-0.75341	2.250845
MAT2A	-0.75345	1.737325
TP53	-0.75372	0.755126
SEPT7	-0.75768	1.294444
QTRTD1	-0.75784	1.010934
PSMB3	-0.7583	0.939246
EIF2B1	-0.75906	1.022477
SPR	-0.75913	0.701384
SLC3A2	-0.76639	0.895895
UBE2N	-0.76659	1.638926
GSTO1	-0.76759	1.034917
PRDX4	-0.76858	2.250633
CHORDC1	-0.76874	0.747448
NANS	-0.77139	0.852729
BPNT1	-0.77198	0.773032
SSB	-0.77396	2.180805
ME2	-0.77509	2.029443
PCBD1	-0.77519	1.691202
GLUD1	-0.77523	1.602781
RFK	-0.77866	1.189887
LSM2	-0.77889	1.838947
CDC42	-0.77907	0.990445
CYCS	-0.77951	0.649428
CNPY2	-0.78249	1.179593
TES	-0.78462	0.985717
CLIC1	-0.7872	1.421187
PPIF	-0.78788	2.141733
NTMT1	-0.78878	1.222514
CKB	-0.79	2.023548
PFN2	-0.79216	2.41864
ABCE1	-0.79254	3.351135
ACAA2	-0.79281	1.706799
CCT3	-0.79655	3.097667
PFAS	-0.79706	1.415174
ESD	-0.79708	1.258391
TOMM34	-0.79751	2.534708
VARS	-0.79784	1.194212
NHP2L1	-0.79785	1.456937
PEBP1	-0.80114	1.816907
RPSA	-0.80208	1.360094
GRPEL1	-0.80333	2.435078

CNPY3	-0.80388	1.179131
SARS	-0.80513	1.384842
CTH	-0.80584	1.424919
FLAD1	-0.80617	1.736038
SCO1	-0.80697	1.130123
TMCO1	-0.80817	0.820775
PRKDC	-0.80819	1.453222
PRPF40A	-0.80823	1.013912
NPM1	-0.81043	2.656377
PSMD2	-0.81354	1.576834
RBBP4	-0.81422	1.70961
HSPA1A	-0.81433	1.406591
ADSS	-0.8149	1.466066
LTA4H	-0.81536	1.298019
PGRMC1	-0.81579	1.226674
SF3A3	-0.81708	0.751971
ACAT1	-0.82077	1.421124
NARS	-0.82116	0.875692
SEPT2	-0.82127	1.178437
ACTB	-0.82365	1.690826
DUT	-0.82605	1.165523
PREP	-0.82678	2.737882
GDI2	-0.8293	1.285286
CREG1	-0.83197	0.728153
EDARADD	-0.83338	0.990285
SDF2L1	-0.83831	0.823646
CLIC4	-0.83878	1.1974
CBR1	-0.84016	1.111342
RTCA	-0.84029	0.494436
TFRC	-0.8403	0.890018
IBA57	-0.84095	0.946461
PGLS	-0.8412	1.200531
NANP	-0.84552	1.352252
GSR	-0.84661	2.081021
GLS	-0.84701	2.501061
CPNE1	-0.84936	0.813067
PLOD2	-0.85354	0.787244
NUDT5	-0.85609	3.077868
SSR4	-0.85695	1.531871
CBS	-0.85715	3.260251
ACO1	-0.86418	0.97843
COA7	-0.86544	0.502425
METTL1	-0.86851	1.316635
NAMPT	-0.87003	0.968197
BOP1	-0.87009	0.67871

TPP2	-0.8703	0.74008
TRMT6	-0.87135	1.161663
NAA50	-0.8785	1.047761
USP14	-0.88019	1.264812
AGL	-0.88484	1.049667
ANXA6	-0.88944	2.605565
CTSC	-0.89188	0.818007
GLA	-0.89601	0.714456
ZC3H11A	-0.89688	1.165696
PGAM1	-0.89783	1.606365
PMPCB	-0.89975	1.529866
KDELC2	-0.90232	3.496629
PSMD14	-0.90311	0.687559
CAPNS1	-0.90556	1.213075
COASY	-0.90734	1.253689
PITPNB	-0.90867	0.875308
PRPSAP2	-0.91019	1.982675
NDUFA4	-0.91419	0.497161
APRT	-0.91802	1.191606
PPA1	-0.92105	0.736655
NDUFS3	-0.92303	0.78794
MTAP	-0.92402	1.689755
TSN	-0.9252	0.98277
PRMT7	-0.92747	0.774952
ASNS	-0.92839	1.713545
TUFM	-0.93471	1.252278
ATP5B	-0.93495	1.32951
UBA6	-0.93565	0.432598
GMPS	-0.93636	1.461062
ECHS1	-0.9364	2.333171
RPL19	-0.9393	1.724222
APOA1BP	-0.93939	2.493297
CDC37	-0.94349	2.403136
PTGES2	-0.94949	0.780441
LIN7A	-0.95341	0.601523
SCRN1	-0.95547	1.436496
GARS	-0.95556	1.401292
PPIH	-0.95816	1.773397
PCK2	-0.96039	0.843523
TBCB	-0.96058	0.903736
SERPINB1	-0.96227	0.952707
DDX19A	-0.96407	0.641082
UBE2K	-0.96561	1.12846
PWP2	-0.97064	0.512272
HEBP1	-0.97174	1.689331

GLB1	-0.97954	0.597015
PPAT	-0.97976	2.281271
L2HGDH	-0.98339	0.721131
UAP1	-0.9869	1.474458
GLUL	-0.98692	1.026054
PDXK	-0.98832	1.464555
BCAT1	-0.9889	1.383122
NUP37	-0.99124	1.54099
NME2	-0.99175	1.529231
UBR5	-0.99526	1.306943
TTLL12	-0.99869	0.867646
RPL29	-1.00106	1.376126
ETHE1	-1.00354	0.790195
OXCT1	-1.01623	1.029739
TXNDC12	-1.01931	3.9504
PCMT1	-1.02347	1.60736
PSMA1	-1.02975	1.087178
RNH1	-1.03118	1.582371
FAM49B	-1.03399	3.095847
C6orf211	-1.03572	1.118566
MRPL39	-1.03611	1.016337
MRPL2	-1.04888	1.319753
RANBP1	-1.05056	1.111856
COPE	-1.05854	1.318456
GRWD1	-1.06342	0.812141
SELENBP1	-1.06559	0.773857
BDH2	-1.06778	1.364046
DBN1	-1.06924	1.207554
KCTD12	-1.07074	1.007279
NME3	-1.08384	0.662422
EDC4	-1.08628	1.07076
ACP6	-1.0863	1.3321
HMGCS1	-1.09757	1.276319
LAP3	-1.11601	1.034686
NOP16	-1.12878	1.428438
MINA	-1.16514	0.465276
FSCN1	-1.1766	1.022175
UGDH	-1.19621	1.970268
GDI1	-1.20301	1.133644
METTL10	-1.21074	1.37764
EEF1A2	-1.22778	1.030448
ITGA5	-1.25942	1.182857
NXN	-1.26679	1.461643
SLC1A5	-1.27812	0.856646
ISYNA1	-1.28097	1.578441

NAPA	-1.28595	0.672279
NT5DC1	-1.2902	0.603445
EXOSC6	-1.29196	1.154283
MRPL28	-1.34686	0.818879
DENR	-1.35092	0.739652
UBE2L3	-1.35175	1.191132
IMPDH1	-1.38808	1.101686
ANP32B	-1.41168	2.060228
CAT	-1.41929	1.189168
NIFK	-1.43679	1.040749
NIP7	-1.45036	1.185976
CRABP2	-1.48186	1.486851
JUP	-1.56172	1.283856
AKR1A1	-1.576	1.049607
ECE2	-1.83617	0.683086
ANXA4	-1.87018	0.819468
KRT9	-3.16135	0.842453
ALB	-3.97069	1.071183
KRT10	-4.80695	1.108477
KRT1	-5.03842	1.18863
GLRX	-5.64626	2.03663

Appendix II: Hmt1 BPPM TMT-MS Data Set

Gene Name	Log_2 Enrichment	$-log_{10}$ p-value
HMT1	1.997955	36.4189
RPS2	1.85373	18.15178
GAR1	1.707672	14.24935
THO1	1.594549	31.50256
STM1	1.553524	24.47073
PUB1	1.377401	22.86943
YRA2	1.362891	21.46215
YMR315W	1.295135	11.47404
URA3	1.283527	18.5346
REP2	1	11.46805
URA6	1.244075	8.688659
YET1	1.233684	5.676048
DED1	1.226919	23.91255
NOP1	1.217024	17.13265
NSR1	1.178449	14.91591
SBP1	1.152508	16.80598
SER33	1.117473	7.562255
POF1	1.087237	9.498485
RPS20	1.064653	7.547737
RPN13	1.060278	16.84359
TPM2	1.037968	16.38572
YPT7	1.030218	8.115525
RPC19	1.028333	9.038968
YER134C	1.013879	10.68177
YBR062C	0.993493	13.45161
NPL3	0.991076	18.66027
RFS1	0.988412	9.001847
RPL42B	0.984772	2.534063
LSM4	0.977707	22.58276
TIF11	0.97257	7.546428
FMP41	0.967169	9.283573
YPR172W	0.952582	24.41784
ARF2	0.948102	4.267732
RPS9A	0.932313	19.14164
YCR090C	0.928276	6.195192
ABP1	0.909709	16.09162
PAA1	0.893492	10.23403
PHO88	0.882578	6.50008
SBA1	0.873682	12.85218
DBP2	0.86974	14.59905
RPS30B	0.869213	6.013015

SEC13	0.85599	21.56323
RPL37B	0.840497	5.750286
ERP2	0.818578	5.287274
PHO13	0.816941	12.39418
CGI121	0.815029	11.2348
SIS1	0.80763	9.97592
GLO2	0.80488	22.01124
RPL6B	0.798534	7.6824
SSU72	0.796044	11.7049
ERV2	0.795767	14.50347
RPL17A	0.792161	7.360493
YET3	0.79105	5.960169
TAE1	0.788547	8.552546
ARF1	0.78799	3.940176
RPL37A	0.783247	4.00829
PTC1	0.771181	8.567166
LSC1	0.769772	19.99991
NTF2	0.767796	2.281862
TMA22	0.765818	9.544462
HOR2	0.76327	9.477987
ERV25	0.76242	5.610971
ANB1	0.759866	10.19055
CBC2	0.735522	8.971754
ERG2	0.733499	10.07072
SFT2	0.73292	8.827055
RAD23	0.725668	9.86952
YBR096W	0.725378	6.666837
RPL27A	0.723923	4.242189
SSS1	0.722466	3.518616
YDR248C	0.708114	4.53059
RPL6A	0.707819	5.741904
RPS28B	0.706052	8.752089
YIP4	0.705167	14.71187
RPS7B	0.703987	7.729441
RPL13B	0.703396	7.245343
PRE3	0.702805	6.703378
HSP150	0.701919	11.54934
YDR476C	0.701919	5.779456
CCT6	0.691832	16.46844
TRR2	0.690939	13.70367
SSB1	0.690045	17.57543
TIF5	0.689746	14.32307
DDP1	0.689448	8.617099
AIM21	0.683771	10.18806
MXR1	0.683472	6.709074

RPS29A	0.67717	4.476665
CUE1	0.675665	6.962253
PRE2	0.673556	4.682363
RPL30	0.671142	4.603619
TIF6	0.67084	4.974964
YPT31	0.669027	8.024465
GCS1	0.659316	23.03668
YKT6	0.656268	7.333474
MDH3	0.655352	16.24981
RPL33A	0.653213	4.216714
BNA1	0.652601	14.62186
ERG11	0.652295	8.716007
APT1	0.650765	6.432114
ENT2	0.649539	7.043559
XPT1	0.642471	9.794896
RPN10	0.640929	6.937509
MOT2	0.639695	6.277713
SEC72	0.635987	9.959668
PUP1	0.628229	5.116975
ARL1	0.627607	7.678072
PET9	0.627296	9.518147
RPS27A	0.625426	8.260915
YOR131C	0.623867	8.645811
MET14	0.623555	3.640209
CRG1	0.622618	8.332739
ADE8	0.621681	5.947578
PRE1	0.620117	6.634782
RRB1	0.619804	7.938679
RPS29B	0.616985	3.698061
CPR3	0.614788	8.879013
UBC13	0.61416	7.813464
NFU1	0.613846	17.02318
CPR5	0.611959	6.446213
KTI12	0.606284	5.43511
RPC10	0.605968	5.863147
AHA1	0.601855	7.066397
RPS19A	0.599635	6.311183
SGT2	0.598365	5.812564
SAP30	0.598365	6.114938
NAB2	0.59614	23.0304
GUK1	0.593274	14.8301
TCB3	0.592317	5.80783
HCH1	0.590083	4.050806
SEC4	0.585924	5.729539
RPL24A	0.585604	7.81265

GIS2	0.581753	14.57213
RSE1	0.58111	9.067465
PRE5	0.578214	6.52038
RPB9	0.576603	6.821246
RPL21A	0.570463	11.64953
RPS7A	0.569167	4.545605
FLC2	0.56787	5.794898
YDL086W	0.56787	14.00731
RPS14B	0.561367	7.58008
HRP1	0.561041	6.751724
PRE7	0.560063	12.2893
RIB3	0.55647	22.00748
YLR126C	0.55647	8.881564
RIB1	0.556143	5.591129
FSH1	0.555816	5.97761
YPT1	0.553197	3.395785
CAP1	0.551557	13.63119
RPS13	0.549587	3.627865
CKS1	0.54893	14.58212
REB1	0.547943	6.04546
TIF35	0.547614	12.86161
GRX3	0.545639	18.36797
YPT52	0.545309	16.85623
COF1	0.54498	2.794802
RKI1	0.540689	15.06416
RTN1	0.537379	15.34891
GCV3	0.536053	15.30431
TIF34	0.535389	5.511917
RPS22A	0.534394	2.141678
RPS11B	0.533065	4.365035
SLC1	0.533065	2.055154
RPL20B	0.524732	6.442382
FPR2	0.522391	9.274193
REE1	0.521051	9.05826
YPL225W	0.520716	3.112715
YKL069W	0.518703	4.154019
RPL16A	0.518367	4.864189
FPR1	0.517024	3.802912
GEA2	0.515679	7.97272
SUI1	0.514669	0.537458
HOM3	0.514333	15.07864
RPL16B	0.510962	4.149964
TMA19	0.510624	4.471031
AAH1	0.509274	9.276766
RPL9A	0.507583	4.614451

YSA1	0.506568	10.72994
RPL19A	0.498421	5.106322
YAR1	0.496718	6.240147
SCS2	0.495695	10.08212
VPS1	0.49057	4.373539
IRC24	0.487486	13.83207
SAR1	0.4868	4.909266
RHO3	0.485427	13.87759
RPL7A	0.484396	11.93294
LOT6	0.481643	4.551323
PIS1	0.481299	3.125709
MDE1	0.479575	20.49312
SOD1	0.474393	21.04951
NAS6	0.472661	3.809108
RPN1	0.472314	4.778297
WTM1	0.471274	8.794524
RPE1	0.469191	12.3748
ERP1	0.465365	3.451211
PRX1	0.464668	6.924933
NIT3	0.462227	10.86899
RHO1	0.461878	11.78275
GSP2	0.459781	5.112153
YJL068C	0.456981	2.86302
HIS6	0.453474	14.16909
FRE1	0.450661	4.057301
PRE6	0.448549	6.707913
LAT1	0.448549	9.682321
AIM45	0.446433	13.29105
TMA20	0.44608	3.831686
YJR096W	0.442192	4.173493
MGM101	0.440775	3.88487
CIR1	0.438293	7.497679
RPS5	0.436162	16.19776
CBR1	0.435806	10.24964
BNA7	0.428678	8.349665
YMR178W	0.427249	6.679374
MRN1	0.427249	3.005586
TRR1	0.425459	4.796999
RPL2B	0.422592	13.23199
RPS9B	0.419719	3.381542
TRX2	0.419719	4.56687
HMF1	0.41828	2.969727
EMG1	0.414677	7.570215
ORM1	0.413594	3.792146
RPL18A	0.411426	4.925462

RPL32	0.403813	2.639096
MVD1	0.400538	5.424178
YCP4	0.39908	3.466524
PAN5	0.39835	7.452465
MMF1	0.39762	3.503274
UBC4	0.397255	3.135479
PMI40	0.396525	4.432068
SWH1	0.393233	2.580098
RFA3	0.391768	3.705364
YRB1	0.391034	3.64831
YKL033W-A	0.3892	9.211917
RPS16A	0.388832	3.726311
CPR1	0.387363	5.038858
SEC3	0.386995	0.006102
THS1	0.386995	6.672203
YLR179C	0.386627	10.39972
TSA2	0.385891	2.399486
CDC42	0.385523	6.105415
PNC1	0.385523	14.368
INM1	0.384787	8.303138
ARG7	0.38405	6.199245
PST2	0.382944	1.826555
GRX7	0.38036	5.047624
RPS1A	0.379621	10.14964
RPS24B	0.379621	4.851867
YRA1	0.378142	9.41779
YUH1	0.378142	3.385972
ASC1	0.377401	5.650114
NNT1	0.376661	3.117199
AIM7	0.37592	2.448679
RPL15A	0.375549	7.534793
GRX2	0.375549	3.482879
RPL36B	0.371094	0.947391
CAB4	0.371094	6.855218
RPS26A	0.368861	8.795906
ADI1	0.367371	0.542858
ERG6	0.366252	8.936119
DPM1	0.362517	6.889013
POR1	0.362517	10.96942
SEE1	0.362517	3.700138
TUP1	0.355392	7.116949
SOD2	0.355392	3.931942
ALG13	0.353511	1.545819
RPL23B	0.353135	5.286056
RPS8A	0.346342	4.876719

SRP54	0.343313	3.793123
PRO3	0.341037	28.13781
TUB3	0.339137	6.194288
SUR7	0.338377	3.614638
APD1	0.337616	3.390255
KGD1	0.331514	3.744057
YJL055W	0.330367	3.834583
TIF4631	0.326154	1.605974
BET3	0.325003	4.954748
RPL11A	0.325003	5.367657
ARC1	0.324619	9.421704
LYS12	0.324235	6.401626
DHH1	0.321928	5.499542
AHP1	0.320388	2.070371
YOR111W	0.318461	9.833845
YBL036C	0.318076	4.260614
PDB1	0.31769	4.51774
RPL43A	0.317304	2.923438
GPX2	0.315373	2.874244
HAM1	0.314213	2.646095
RPS1B	0.314213	4.816677
GVP36	0.312665	9.482071
RIB5	0.311503	1.816197
YPR148C	0.310728	7.968365
UBC1	0.31034	6.350196
RPN11	0.309564	2.498759
ERV29	0.303732	4.419734
FUR1	0.302173	10.15308
RPS0B	0.302173	5.5544
TRP1	0.301393	0.840875
RFA1	0.29944	2.831664
NCP1	0.299049	3.195602
CAF16	0.298658	5.29613
ALD4	0.296311	3.284421
OST3	0.294351	2.682501
YGL039W	0.290424	2.891197
RPS23B	0.289244	1.794596
TCP1	0.286881	6.442899
GSH2	0.281748	3.145117
PTK2	0.281352	5.910803
GLE2	0.280956	2.11476
SET5	0.279768	0.900446
SEC17	0.279372	3.695203
MEU1	0.276596	3.969607
GPD2	0.273814	5.967765

AML1	0.27262	4.019157
DUS3	0.269432	3.994507
CCT4	0.265437	4.579106
LPD1	0.265037	2.506448
RPS18B	0.264637	3.35311
HTA1	0.262233	3.608912
RNR2	0.262233	2.834833
LIA1	0.261029	9.339351
SIT4	0.260628	2.447298
IDH1	0.256608	2.516406
SUI2	0.256206	1.787328
ZPR1	0.253384	7.574014
PTC3	0.245698	6.635983
FET3	0.245293	5.112068
TMT1	0.244887	1.548064
ATP2	0.243263	4.421693
RPS17A	0.242857	2.264169
RPL31A	0.24245	2.541011
YIH1	0.241637	2.141038
TPI1	0.24123	6.484356
TYS1	0.24123	14.70633
RPL35A	0.240823	2.075964
SCL1	0.240823	4.521441
CKA2	0.235114	1.236592
RPL3	0.234706	4.032006
WRS1	0.233888	1.083522
ATP1	0.23307	6.754974
ERG8	0.232661	5.934581
PHO85	0.232251	2.602521
IDP1	0.229793	4.905569
BMH2	0.229383	3.164955
RPL8B	0.228152	3.791802
HXK1	0.228152	5.670307
YPR1	0.22404	5.211205
PDX3	0.223628	6.394975
RPS3	0.222805	5.320088
GPH1	0.22198	1.735475
GPM1	0.221568	4.693393
SSZ1	0.22033	3.405373
SPE3	0.22033	3.244563
MRH1	0.219504	1.36104
MRI1	0.217851	4.798323
IAH1	0.215782	2.220667
RPN9	0.214954	0.518948
TEF4	0.21205	5.600518

TSC10	0.21205	1.747102
MET12	0.209557	1.403622
PUP3	0.208725	2.789903
AAT2	0.204558	7.124043
TDA3	0.204141	2.317742
FCY1	0.202052	3.103866
YDL144C	0.202052	2.09458
HYR1	0.200797	2.065631
YNK1	0.198704	1.705463
LHP1	0.196607	1.06383
DUS1	0.196607	2.440154
EMP70	0.194928	3.64477
POM152	0.194507	4.382143
ADE5,7	0.194087	7.615123
ARO4	0.194087	15.50016
HOM6	0.191984	2.483684
YOR021C	0.189456	1.947017
WBP1	0.189034	0.226766
RPS0A	0.187768	6.933906
RPL25	0.187768	0.891201
ARA1	0.187768	6.469632
PDA1	0.187768	10.84352
RPN6	0.186923	3.236036
SEC53	0.185655	3.456569
CCS1	0.184809	2.780197
IMD4	0.182692	4.289612
LSG1	0.182692	2.981688
ADE1	0.181845	1.325366
APA1	0.181845	3.02246
SHB17	0.175471	3.994812
RPL8A	0.172061	4.613823
UTR4	0.171634	0.209741
SOL3	0.171634	1.229484
ADH5	0.17078	0.75607
MHT1	0.170352	2.198707
RPT6	0.168214	2.390064
RPS6A	0.168214	1.745687
RPS21A	0.167786	0.761174
RPP0	0.16693	2.560256
YBL055C	0.165215	2.165645
ADE12	0.163928	5.52535
BAT1	0.16264	1.611742
RNA14	0.16135	0.619869
PRS3	0.16006	1.474724
YMR226C	0.158768	2.291855

RPT1	0.158337	4.589815
PRO1	0.157475	0.797279
UBA4	0.157044	2.210619
RPL12A	0.156181	4.193658
TIF1	0.156181	4.182244
NIF3	0.156181	3.227499
RPL10	0.155749	1.609621
MDH1	0.154454	1.861716
VMA6	0.152724	3.329928
YMR099C	0.150993	0.254984
PPM1	0.148392	1.302082
HMG1	0.148392	3.894559
POL30	0.147958	2.338512
ADE2	0.146655	0.016565
PMC1	0.145351	1.837826
RHR2	0.14274	9.170998
GDA1	0.139251	1.794938
BNA6	0.138814	2.13448
ILV6	0.13444	2.189523
TUM1	0.130052	2.937936
GPI16	0.128733	1.819847
BMH1	0.126973	2.431624
ABZ2	0.126092	1.141205
LEU1	0.124769	1.547444
YER152C	0.123887	0.252991
KGD2	0.123887	1.816078
YME1	0.119467	1.223448
RPS21B	0.118581	1.148582
RPC40	0.118581	0.476508
PUP2	0.118581	1.116374
SAM1	0.118138	2.467342
MCK1	0.117695	0.017424
TRP5	0.116808	2.156067
CDC60	0.115477	1.352748
MTD1	0.115477	0.870779
RPL1A	0.114589	1.698227
HRI1	0.114145	1.02091
YNL010W	0.1137	1.332721
ASP1	0.112367	3.595901
TUB1	0.111922	1.385086
PAB1	0.109249	2.943013
PUS4	0.109249	2.434818
ABP140	0.108357	0.372912
BGL2	0.107465	2.531837
MAE1	0.100753	1.630926

ADK1	0.099856	1.623465
GET3	0.099856	2.727052
IPP1	0.097611	2.757889
AIM2	0.095812	0.916313
GAS1	0.094912	2.203905
TDH1	0.094461	0.560724
DED81	0.09356	2.164501
ILV2	0.093109	1.904793
PTC2	0.092658	2.342696
URA7	0.091305	1.710335
YDR161W	0.089498	0.635778
TRM44	0.089046	1.274755
IMD3	0.087237	2.334838
OLA1	0.085425	2.930127
CCT2	0.084064	1.507225
CLU1	0.082248	0.460616
PGM2	0.082248	2.3346
RNR4	0.08043	3.921195
HIS1	0.07952	1.084547
DPH5	0.079065	1.889561
TMN2	0.079065	0.086437
RNA1	0.077243	0.544433
CYS4	0.076331	1.941717
RPS15	0.075419	0.493738
OYE2	0.075419	3.049511
TSA1	0.074962	0.958137
PYK2	0.074505	1.187592
RPL14A	0.071305	0.016408
ARO3	0.069931	0.107999
SUA5	0.067639	0.75774
NAM7	0.06718	0.845764
DET1	0.06718	0.501993
TUB2	0.066721	0.443098
RPS4B	0.066261	0.83234
RPT2	0.064423	0.355089
IDH2	0.063963	0.99058
SXM1	0.063043	0.247511
KES1	0.0612	0.842446
YHB1	0.060278	0.627696
RTT10	0.058894	2.663582
SSO2	0.057046	0.981501
NCL1	0.055658	0.871941
RPL28	0.054733	0.953299
CDC21	0.054733	0.661343
CCT8	0.05288	0.781045

YFR006W	0.051952	1.013253
RAM2	0.051488	0.259579
RPN5	0.051488	0.226386
ARO2	0.051488	0.778405
GCN1	0.051488	0.43398
TUF1	0.051024	0.820226
EFB1	0.050095	1.05002
TEF1	0.048236	0.377107
SSB2	0.048236	1.291421
GDB1	0.046375	0.181746
CHO1	0.044977	3.519133
FAA1	0.044511	0.68138
KAR2	0.044511	0.807059
GLN1	0.044044	0.923012
GRE3	0.041243	0.886921
GRX1	0.040776	0.312015
GLC7	0.040308	0.843891
ERG10	0.039372	0.706214
PRS1	0.037968	0.476319
SAM2	0.037968	0.392724
CDC12	0.036093	0.331635
SAH1	0.036093	0.571589
YHI9	0.032806	0.156667
GRE2	0.031866	0.455939
SEC31	0.031866	0.21525
FOL1	0.029512	2.023385
FUN12	0.027154	0.439459
SFB3	0.027154	0.155339
YER156C	0.02621	0.224351
HSP104	0.025738	0.556699
TPA1	0.024792	0.249125
RPO31	0.023847	0.25167
DCS1	0.023374	0.39251
RPT5	0.019583	0.524242
ALA1	0.015783	0.353289
ADE13	0.014355	0.312043
UGA1	0.013403	0.430554
BAT2	0.012926	0.112346
ADE4	0.012926	0.51369
VMA2	0.012449	0.268389
FRA1	0.009586	0.307426
PHO3	0.009586	2.465702
ACS2	0.00863	0.638076
IST2	0.008152	0.342124
ADH1	0.00528	0.421404

ACT1	0.004801	0.102873
PFK2	0.004801	0.161496
RPL5	0.004322	0.731531
XRN1	0.001442	0.190708
MRT4	0.000481	0.047185
FRD1	-0.00048	0.232714
VMA1	-0.00048	0
CCT5	-0.00096	0.058976
SSA2	-0.00192	0.273945
GPD1	-0.00385	0.564387
NAP1	-0.00385	0.704646
SNF1	-0.00433	0.265341
DLD3	-0.00433	0.762427
ERG13	-0.00433	0.27014
QNS1	-0.00482	0.962417
ILV5	-0.00627	0.371573
VMA5	-0.00723	0.457401
TOS1	-0.0082	0.036087
PDC5	-0.0082	0.733751
KRS1	-0.01013	0.234973
SEC14	-0.01062	0.152063
ARB1	-0.01159	0.3196
GCD11	-0.01207	0.382164
GUA1	-0.01985	1.157508
ARI1	-0.02083	0.847569
SUP45	-0.02376	1.114145
ARC35	-0.02425	0.044903
RPL9B	-0.02523	1.414069
ARP2	-0.02523	0.841366
ARP3	-0.02572	0.375123
NOP2	-0.02572	0.839173
TDH2	-0.02621	0.321353
ACO1	-0.02767	1.293006
VTC4	-0.02915	0.413974
GAS3	-0.02964	0.873232
SES1	-0.03013	1.435545
GAS5	-0.03111	1.131158
HSP60	-0.03111	2.690313
PDC6	-0.03209	0.275384
ADO1	-0.03259	0.617445
MES1	-0.03308	0.517563
CAR2	-0.03455	0.703538
ASN1	-0.03505	1.524755
HEM2	-0.03702	1.480064
SAC6	-0.0385	0.642495

CYS3	-0.0385	0.837293
PGI1	-0.03899	0.735907
RVB1	-0.03998	0.150588
GUS1	-0.04147	0.736133
ASN2	-0.04345	1.680151
HXK2	-0.04345	1.349132
ERR2	-0.04444	1.041296
YHR020W	-0.04692	1.615023
PEP4	-0.04791	2.2907
TOM70	-0.04841	1.28733
SER1	-0.0499	1.109724
CWH41	-0.0504	1.295645
GCV2	-0.0524	1.053102
ZUO1	-0.0524	0.042556
THR1	-0.05339	1.431105
ACC1	-0.05489	1.756919
SUB2	-0.05489	2.200689
PDI1	-0.05589	0.379509
CHA1	-0.05689	1.324565
TAL1	-0.05889	2.554684
SER2	-0.0604	1.198692
THR4	-0.0619	1.196735
TRM3	-0.06291	2.532724
SSC1	-0.06492	1.313044
UGP1	-0.06542	0.675328
RPL4A	-0.06693	2.967052
PUS1	-0.06794	0.013432
TRP2	-0.06844	1.368283
IDI1	-0.06844	2.698123
KAP123	-0.06996	2.517841
RPS31	-0.07552	3.942975
PFK1	-0.07603	1.986759
SRP1	-0.07704	1.54025
RPA135	-0.07907	0.89722
TMA108	-0.07907	1.191207
NPT1	-0.07958	2.158772
PRT1	-0.08009	0.92124
YLR225C	-0.08009	1.785422
PHO5	-0.0806	2.202701
CCT3	-0.0806	2.167061
POL31	-0.08263	1.81691
CPR6	-0.08365	2.878286
GSH1	-0.08773	2.305828
SSA1	-0.08824	3.056247
GLN4	-0.08876	1.947473

YBR139W	-0.08978	1.434874
ADE17	-0.08978	1.73062
LAP2	-0.0908	1.679
SCP160	-0.09183	1.450002
YGR017W	-0.09183	1.13414
RPL34B	-0.09645	3.484933
HEM13	-0.09799	2.151139
SHM1	-0.09954	1.319319
MEF1	-0.09954	1.263354
YDL124W	-0.10057	5.799782
ADH3	-0.10366	2.42566
FAS1	-0.10521	3.154544
YGL185C	-0.10521	1.900372
QRI1	-0.10521	1.349938
DUG1	-0.10625	3.010795
GDH1	-0.10988	2.295538
QCR2	-0.11144	2.020812
UBP6	-0.11195	0.771967
NMD3	-0.11299	1.756776
YBR056W	-0.11351	2.065281
PHA2	-0.11404	4.233339
EHD3	-0.11404	0.819906
DCW1	-0.11456	1.574588
PMT2	-0.11456	5.197429
CCT7	-0.11508	1.101103
ARO9	-0.1156	1.370587
ABZ1	-0.1156	2.559254
YPR127W	-0.11664	1.925685
ARH1	-0.11716	1.469403
STI1	-0.11768	2.084813
UBA2	-0.12082	0.936294
ALD6	-0.12291	10.55446
EFT1	-0.12396	4.871236
DAK1	-0.12501	2.36007
NIP1	-0.12553	2.093117
DPS1	-0.12711	1.82883
ACO2	-0.12711	3.702633
ECM33	-0.12763	3.078866
LYS4	-0.13131	2.577589
YLL058W	-0.13131	2.602181
YCR015C	-0.13131	1.397614
PSA1	-0.13237	4.216909
RPO21	-0.13342	3.039714
LHS1	-0.13501	1.368378
SEC27	-0.13553	3.210948

SSE1	-0.13606	6.035862
GFA1	-0.13659	3.899331
UGA2	-0.13712	1.042378
PRC1	-0.13712	2.00381
PGM1	-0.13871	2.145271
TDA10	-0.14295	1.74252
RSP5	-0.14348	1.934259
PCM1	-0.14454	4.130247
PMU1	-0.14667	1.261373
ADH6	-0.1472	2.116061
TRP4	-0.14827	2.046526
RLI1	-0.1488	2.164637
BNA3	-0.15147	2.870659
ADE3	-0.15307	6.12153
FAS2	-0.15361	3.953129
CAB1	-0.15414	4.926786
PAN6	-0.15521	2.918239
ALD5	-0.15575	2.586301
PDC1	-0.15628	5.605094
MAP1	-0.15682	5.231032
FBA1	-0.15736	5.808111
FRS1	-0.15736	4.665673
PYC1	-0.15789	8.178993
CDC48	-0.16004	5.423951
THI6	-0.16112	0.390129
ALD2	-0.16165	4.820813
LYS1	-0.16327	4.067261
TRM2	-0.16327	3.143156
LYS20	-0.16381	3.367534
ARG1	-0.16488	5.372712
HOM2	-0.16488	3.682205
URH1	-0.16488	1.047134
ERG20	-0.1665	3.493574
ERG4	-0.16758	3.24713
FDC1	-0.16812	2.615255
VAC8	-0.1692	2.373627
ENO2	-0.16974	4.222176
SEC18	-0.16974	2.049003
GRS1	-0.17029	8.101168
PEP1	-0.17029	2.331991
ECM14	-0.17083	2.256298
SHM2	-0.17083	7.658422
RRP43	-0.17408	0.794024
SSH1	-0.17408	7.509827
TRM1	-0.17408	0.833892

RPN3	-0.17734	0.939415
CHC1	-0.17843	5.107589
YML082W	-0.1806	3.058882
NPY1	-0.18497	2.389612
NUG1	-0.1888	1.126967
TRP3	-0.19045	10.39093
MET22	-0.19319	11.94855
RVB2	-0.1976	1.474926
TDH3	-0.19815	4.869889
APE2	-0.1987	2.991536
GLY1	-0.19981	4.659904
KRE5	-0.20036	1.988269
HIS7	-0.20257	4.208992
ENO1	-0.20423	9.50224
LAP4	-0.20534	4.792624
SAM4	-0.20756	8.343937
CAR1	-0.20812	3.42043
COP1	-0.20812	3.915371
YNL247W	-0.20923	1.564851
PYC2	-0.20923	5.64769
TRM5	-0.20923	2.868717
BAR1	-0.2109	4.060586
MCM4	-0.21424	4.104391
YJR098C	-0.21703	0.953829
VMA13	-0.21703	3.507236
CRH1	-0.21759	3.948437
HSC82	-0.21815	6.047785
MET13	-0.22207	1.313321
NOG1	-0.22207	1.301888
VPH1	-0.22319	5.33653
LYS9	-0.22657	4.707904
TPS2	-0.22657	5.625015
YEF3	-0.22713	5.612014
LEU4	-0.2322	6.087702
PGK1	-0.23277	5.443939
PRO2	-0.23503	3.888079
TCB1	-0.23616	3.219334
ARO1	-0.23673	6.1693
ERG1	-0.239	10.82632
ADE16	-0.23957	4.315917
RTG2	-0.23957	2.125806
TPS1	-0.24013	7.212167
SFA1	-0.2407	4.094301
GLK1	-0.24127	5.361309
DYS1	-0.24355	8.465571

UBA1	-0.24355	13.77122
GLR1	-0.24412	5.66315
NEW1	-0.24469	3.7673
YOL098C	-0.24525	6.807627
VAS1	-0.24583	8.701362
FUM1	-0.2464	5.395261
PHO11	-0.24868	5.579955
YDR341C	-0.24868	7.200366
URA4	-0.25097	5.110335
MSN5	-0.25097	4.813374
TED1	-0.25097	1.357055
HTS1	-0.25154	4.307502
NTH1	-0.25154	2.39374
ZTA1	-0.25326	5.994931
ERG12	-0.25613	5.146392
FAA4	-0.259	8.664228
SPF1	-0.259	12.04897
RPB2	-0.25958	5.177626
HSP78	-0.25958	3.51009
RNR1	-0.26246	3.437503
OXP1	-0.26361	4.007262
YMR196W	-0.26419	3.785402
SEC23	-0.26592	6.243053
LYS2	-0.26766	6.815255
PMR1	-0.2723	1.576105
HFD1	-0.2723	3.126807
SEC21	-0.27404	8.628897
MRS6	-0.27637	2.084904
XKS1	-0.28045	2.920698
THI20	-0.28455	2.962428
EMW1	-0.28689	2.300189
MYO5	-0.28748	8.497994
HEF3	-0.29513	6.170721
ENB1	-0.29513	5.543055
AAP1	-0.29513	8.02273
SEC24	-0.29631	3.491148
CPA2	-0.29926	16.02039
KAE1	-0.29986	3.746978
URA2	-0.29986	9.568225
UBP14	-0.30876	4.831052
ELP2	-0.31115	3.78859
KTR1	-0.31175	3.903554
IML2	-0.31175	2.233932
URA8	-0.31234	2.873461
CRM1	-0.31413	2.184521

YBR053C	-0.31593	5.634637
GND1	-0.31833	8.77653
HIS5	-0.31833	4.539462
GDI1	-0.31953	4.118505
CDC19	-0.32073	13.22289
RKM4	-0.32433	2.478578
DBP5	-0.32554	2.447183
MSC7	-0.32554	3.268629
RPA190	-0.32976	4.467142
ZWF1	-0.32976	4.146261
SNQ2	-0.33158	9.513368
CPS1	-0.334	3.949785
EMI2	-0.334	11.24819
NMA111	-0.33521	6.188037
AMS1	-0.33703	5.048096
RKM1	-0.33703	4.33869
SEC26	-0.34008	6.910431
YNL134C	-0.34373	4.48094
ADE6	-0.34434	18.02232
HIS4	-0.34495	12.45771
SRM1	-0.34679	21.06475
GLT1	-0.34862	5.392915
PRP43	-0.35292	2.942329
RET2	-0.35414	4.114381
HEM12	-0.35661	4.836881
ARG4	-0.35722	11.24262
FKS1	-0.36339	7.701416
YMR027W	-0.36463	8.039178
APE3	-0.36773	7.25632
RPN7	-0.3752	8.021766
SUP35	-0.38145	6.348304
YPK1	-0.3827	5.919671
GSY1	-0.38396	3.35406
YGP1	-0.38773	8.063551
SEC61	-0.38899	4.787337
ILS1	-0.39214	10.12637
HXT3	-0.40036	11.29014
ILV3	-0.408	2.949398
SCW4	-0.4112	4.42559
RNY1	-0.42018	4.271969
COR1	-0.42211	4.83966
YJL171C	-0.42469	4.523003
YGR054W	-0.42533	2.840209
AIP1	-0.43505	32.11401
BDH1	-0.43766	4.532982

FRS2	-0.4468	5.029265
YKR018C	-0.44943	6.103255
PRD1	-0.46926	3.913777
MET6	-0.48063	11.84643
TKL1	-0.48331	9.042694
GCD6	-0.48331	3.144195
YOL057W	-0.50022	6.387426
PMA1	-0.5009	10.07195
ARO8	-0.50294	17.11306
CTR1	-0.51114	6.991829
KRE2	-0.52561	4.178502
STT3	-0.55993	7.612917
PDR5	-0.55993	14.23539
YPL260W	-0.56277	6.540835
CYC8	-0.5792	5.516431
EXG1	-0.58496	5.819458
ECM38	-0.58857	9.864971
CNM67	-0.64837	5.155578
HPM1	-0.66581	7.046265
NFS1	-0.93972	7.612215
URA1	-0.98279	25.47452